Investigating Novel Components and Mechanisms Involved in B Cell Receptor-Antigen Internalisation

Elizabeth Mary Natkanski

Division of Immune Cell Biology
National Institute for Medical Research
London

UCL

A thesis presented for the degree of Doctor of Philosophy, 2013

Declaration

I, Elizabeth Mary Natkanski, confirm that the work presented in this thesis is my own. Where information has been derived from other sources, I confirm that this has been indicated in the thesis.

Publications arising from this thesis

Elizabeth Natkanski, Wing-Yiu Lee, Bhakti Mistry, Antonio Casal, Justin E. Malloy, and Pavel Tolar. (2013). B cells use Mechanical Energy to Discriminate Antigen Affinities. *Science,* **340**, p 1587-1590

Abstract

The elimination of a wide variety of infections requires the production of high affinity antibodies specific for the invading pathogen. The generation of these high affinity antibodies depends on the ability of B cells to recognise and internalise antigens from the surface of antigen-presenting cells (APCs) in an affinity-dependent manner. B cells expressing high affinity B cell receptors (BCRs) internalise, process and present more antigen, obtain better T cell help, and are selectively expanded over lower affinity equivalents. However, the molecular mechanisms by which B cells extract antigens for presentation remain unclear.

Using a new fluid and flexible membrane substrate to mimic APCs, we show that B cells acquire antigen by dynamic myosin IIA-mediated contractions that pull out and invaginate the presenting membranes. Invaginations containing high affinity BCR-antigen microclusters were able to withstand the force of these contractions and recruit clathrin resulting in endocytosis. In contrast, low affinity BCR-antigen bonds quickly ruptured aborting internalisation.

Thus we conclude that coupling contractility to endocytosis permits B cells to discriminate between antigen affinities, which provides a mechanism for the selective advantage seen for high affinity B cell clones *in vivo*.

Disruptions in BCR-antigen internalisation has been linked to the growth of malignant B cells and the development of autoimmunity. Therefore, ultimately, our results could contribute to the effective design of future therapeutics for B cell diseases.

Acknowledgements

First of all, and most importantly, I should like to thank my supervisor Dr Pavel Tolar for giving me the opportunity to work on this project and for encouraging me to aim high and to be the best scientist I could be. I also would like to acknowledge my Thesis Committee: Dr Ben Seddon, Dr Victor Tybulewicz and Dr Tom Carter for taking the time during my PhD to critically examine my project and to give their invaluable advice.

Dr Wing-Yiu Lee has been an admirable fountain of knowledge from day one, and I will always be grateful for all the time he gave in helping me with the project. My thanks also go to all my friends, both within NIMR and out, for being there to support me and for their continual encouragement.

Thanks too, to my parents for all their support throughout my years of full time education. Their ideals of working hard, being thoughtful and having a dedication to seeing things through in many areas of their lives has always been an inspiration. Last, but by no means least, a big thank-you to Paul Eastwood, I couldn't have done it without you.

.

Table of contents

List of figures and tables

List of abbreviations

AFM	Atomic force microscopy
AP2	Activating protein 2
APC	Antigen-presenting cell
Arh-GAP	Rho GTPase-activating protein
Arh-GEF	Rho GTPase-guanine exchange factor
B1-8	B1-8$^{fl/fl}$Igκ-C$^{tm1Cgn/tm1Cgn}$
BAFF	B cell activating factor
BCR	B cell receptor
Bl6	C57 black 6
BSA	Bovine serum albumin
C-terminal	Carboxyl-terminal
C-type lectin	Calcium-binding lectin
CCL	Chemokine (C-C motif) ligand
CCP	Clathrin-coated pit
CCR	C-C chemokine receptor
CCS	Clathrin-coated structure
CD	Cluster of differentiation
CO_2	Carbon dioxide
CpG	Cytosine-phosphate-guanine
Cre	Cre recombinase
CXCL	Chemokine (C-X-C motif) ligand
CXCR	C-X-C chemokine receptor
Cy	Cyanine dye
DC	Dendritic cell
DiI/ DiD	Dialkylcarbocyanines
DNA	Deoxyribonucleic acid
dSTORM	Direct stochastic optical reconstruction microscopy
Erk	Extracellular signal-regulated kinases
et al	and others
Fab	Antigen binding fragment
FBS	Foetal bovine serum

Fc	Crystallisable fragment
FcγRIIb	Low affinity immunoglobulin gamma FC region receptor IIb
FDC	Follicular dendritic cell
Fl	Flox
FRAP	Fluorescence recovery after photobleaching
FRC	Fibroblastic reticular cell
FRET	Fluorescence resonance energy transfer
GFP	Green fluorescent protein
HBSS	Hank's buffered saline solution
HEK	Human embryonic kidney
HEL	Hen egg lysozyme
HEV	High endothelial venule
Ig	Immunoglobulin
IL	Interleukin
ITAM	Immunoreceptor tyrosine-based activation motif
kDa	Kilo dalton
LPS	Lipopolysaccharide
MHC Class II	Major histocompatibility complex class two
MyH9	Myosin heavy chain 9
Myl	Myosin light chain
Myo	Myosin
N-terminal	Amino-terminal
NP/NIP	Nitrophenyl hapten
Oligo	Oligonucleotides
Pax	Paried box protein
PBS	Phosphate buffered saline
PCR	Polymerase chain reaction
PI3 kinase	Phosphoinositide 3 kinase
PKC	Protein kinase C
PLAT-E	Platinum-E
PLB	Planar lipid bilayers
PMPLB	Plasma membrane planar lipid bilayers
PMS	Plasma membrane sheets

Rho	Ras homolog gene family member
RLC	Regulatory light chain
RNA	Ribonucleic acid
ROCK	Rho-associated coiled-coil containing protein kinase
SCS	subsacpsular sinus
shRNA	Short-hairpin ribonucleic acid
siRNA	Small-interfering ribonucleic acid
TCR	T cell receptor
TEL	Turkey egg lysozyme
Tfh	T follicular helper cell
TI	T cell-independent antigens
TIRF	Total internal reflection fluorescence
TLR	Toll-like receptor
YFP	Yellow fluorescent protein
α	Alpha
α-	Anti-
β	Beta
δ	Delta
κ	Kappa
μ	Micro
°C	Degrees Celsius
%	Percent
g	Gram
K_a	Affinity constant
m	Metre
mg	Milligram
ml	Millilitre
mM	Milimolar
mm	Millimetre
mN	Millinewton
ng	Nanogram
nM	Nanomolar
Nm	Nanometre

PFA	Paraformaldehyde
pN	Piconewton
rpm	Revolutions per minute
U	Units
x g	G-force
µg	Microgram
µl	Microlitre
µM	Micromolar
µm	Micrometre

Chapter 1 Introduction

1.1 The Immune System

The immune system is a complex network of specialised cells, tissues and molecular components designed to efficiently recognise, control and clear infections.

The immune system is comprised of innate and adaptive immune cells. Innate immune cells initially recognise patterns in the invading pathogens as “non-self” and initiate the immune reaction by the production of cytokines and chemokines, which activate other cellular members of the immune system and recruit them to the site of infection. Some innate cells such as macrophages and dendritic cells (DCs) are also able to present the peptides from the pathogen, or the pathogen itself in its native conformation, for recognition by T cells and B cells, respectively.

T and B cells constitute the adaptive immune system and are able to “adapt” their responses to be specific for the infectious agent following recognition of antigen by their highly specialised antigen receptors. Each and every B cell receptor (BCR) and T cell receptor (TCR) is unique due to somatic recombination and introduction of point mutations into the genes encoding both receptors during development. This greatly increases the chances of antigen recognition of unforeseen pathogens, which may have evolved to evade detection by the innate immune cells. B and T cell clones, which bind to the antigen with high affinity, are then selectively expanded to elicit antigen-specific mechanisms of pathogen elimination and differentiate into memory cells in preparation for any subsequent reinfection. How B cells are able to initiate these antigen-specific responses will be the focus of this study.

1.2 BCR-antigen internalisation – an overview

B cells begin their development in the bone marrow, and then migrate to the spleen to become fully mature naïve B cells primed for antigen encounter. B cells circulate in the blood and through secondary lymphoid organs in search of their cognate antigen. B cells bind to antigen in its native form and can recognise it both in solution and tethered to a cell of the innate immune system, which can act as an antigen-presenting cell (APC).

B cells bind to antigen through the variable region of the membrane immunoglobulin (Ig) component of the BCR (Lanzavecchia, 1987) (Figure 1). Binding of antigen to the BCR stimulates antigen-induced BCR signalling through the cytoplasmic domains of the Igα Igβ heterodimer, which is non-covalently associated with membrane Ig (Figure 1) (Hombach et al., 1990). This signalling, switches on the B cell nuclear activation programme and acts as the first signal required for B cell activation.

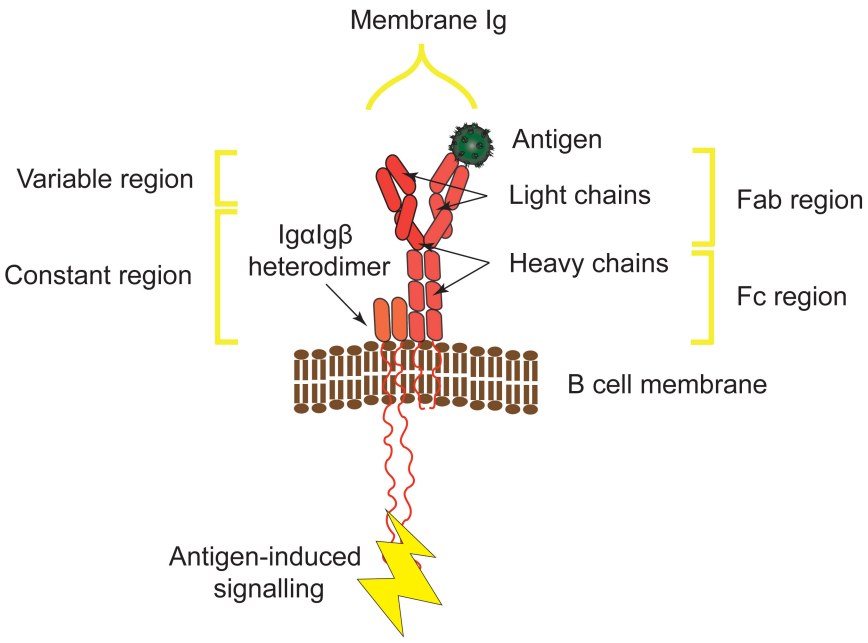

Figure 1: The BCR

As well as initiating signalling, antigen binding stimulates the BCR to enter the endocytic pathway and internalise the BCR-antigen complex (Figure 2). The BCR

traffics the antigen to intracellular degradative compartments where it is degraded into peptides and loaded onto major histocompatibility complex class two molecules (MHC Class II) (Davidson et al., 1991) (Figure 2). These MHC class II proteins are then presented on the B cell surface for recognition by cognate T cells (Lanzavecchia, 1985). Specific recognition between TCR and MHC Class II-peptide permits the release of T cell co-stimulatory factors such as interleukins (IL) and CD40 ligand (CD40L) (Figure 2), which give context-dependent stimulation and act as second signals required for full B cell activation and movement of the B cell into germinal centres (Han et al., 1995; Lane et al., 1992; Parker, 1993). B cells in the germinal centre are highly proliferative and go through rounds of somatic hypermutation on their BCRs to increase diversity of the antigen binding. B cells containing mutations improving their affinity for antigen are selectively expanded, released into the circulation, and differentiate into plasma cells to produce high affinity antibodies for pathogen elimination, or into memory cells in preparation for any subsequent reinfection (Rajewsky, 1996; Victora and Nussenzweig, 2012).

In addition to antigen processing and presentation, BCR-antigen internalisation also exposes antigen to endosomal toll-like receptors 7 and 9 (TLR7 and 9) (Figure 2), which are able to recognise RNA (Lau et al., 2005) and DNA (Bauer et al., 2001) sequences from viral and bacterial infections. Recognition of antigen by TLR7 or 9 can augment the B cell activation and aid pathogen recognition and clearance.

BCR-antigen internalisation also has role in regulating BCR signalling, (Chaturvedi et al., 2011). For example, internalisation has been associated with the termination of calcium and MAP kinase activity and the promotion of AKT stimulation. Therefore, disregulation of BCR internalisation and trafficking may contribute to the inappropriate BCR signalling, which has been observed in B cell lymphomas (Davis et al., 2010).

BCR-antigen internalisation is therefore the gateway for efficient B cell activation and stringent regulation of this process is vital in ensuring an efficient humoral response, while preventing pathology.

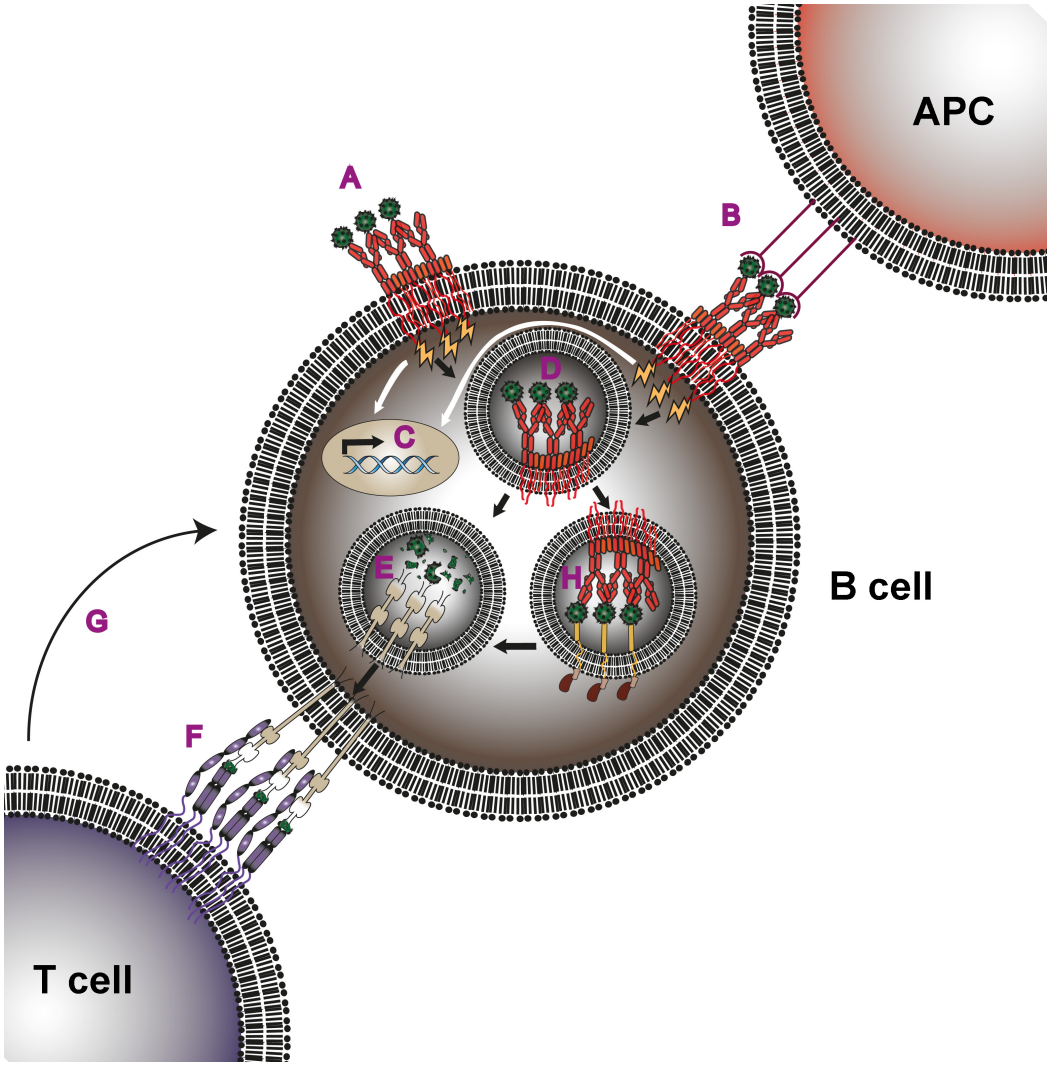

Figure 2: BCR-antigen internalisation

A) BCRs can recognise antigen in solution

B) BCRs can recognise antigen tethered to an APC

C) Antigen binding initiates BCR signalling and stimulates the B cell's nuclear activation programme (signal 1)

D) Antigen binding stimulates internalisation of BCR-antigen complexes

E) Internalised BCR-antigen complexes are trafficked to lysosomes, processed, and loaded onto MHC Class II molecules

F) Antigen loaded MHC Class II molecules are presented on the B cell surface for specific recognition by cognate T cells

G) Recognition of the antigen-loaded MHC Class II by T cells provides activation factors (signal 2)

H) Internalisation of antigen also permits antigen recognition by intracellular pathogen recognitions receptors such as TLRs

1.3 Antigen encounter

B cells primarily reside in the lymph nodes and the spleen. Considering the diverse range of the BCR repertoire, the chances of random contact between antigen and cognate B cell would be rare. Therefore secondary lymphoid organs are specifically structured to facilitate efficient antigen exposure to rare cognate B cells and to control cell-cell interactions (Batista and Harwood, 2009). In the lymph node, two areas can be identified based on their histological features: the cortex and the medulla. The cortex can be sub-divided into B cell follicles, which contains B cells, and the paracortex, also called the T cell zone, which contains T cells and DCs (Andrian and Mempel, 2003). The architecture of these regions is maintained by non-haematopoietic stromal cells such as fibroblastic reticular cells (FRCs) and follicular dendritic cells (FDCs). Apart from structural support, these cells also produce CXCL13 or CCL19, the defining chemokines that attract B and T cells to their respective zones (Andrian and Mempel, 2003; Gonzalez et al., 2011).

Lymph nodes are linked to both the lymphatic and circulatory systems and are strategically positioned around the body to ensure efficient trafficking and capture of lymphocytes arriving by blood and antigen draining from tissues (Batista and Harwood, 2009). B cells circulate around the body and enter the lymph nodes through the high endothelial venule (HEV). B cells then follow the CXCL13 gradient and reside in the follicle just below the subcapsular sinus (SCS), at the site of lymphatic antigen entry (Cyster, 2010). Whilst screening for antigen in the follicle, B cells are active and migrate at approximately 6 μm/ minute (Okada et al., 2005). B cells are able to recognise both soluble antigen, which can filter into the follicle, or antigen retained on the surface of an APC (discussed below). Following specific antigen binding, B cells upregulate CCR7 (receptor for CCL19) and move towards the T cell zone for T cell help and the initiation of the B cell response (Okada et al., 2005). If the B cell does not come into contact with specific antigen after approximately 24 hours it re-enters the circulation in search of the next lymph node and cognate antigen (Goodnow, 1997).

The white pulp of the spleen is similar in its structure to the lymph node with B cell follicles and the T cell zone. Surrounding the white pulp is the red pulp, which is rich in vasculature and functions to filter blood for cellular debris, foreign substances, and microorganisms. An area called the marginal zone, containing specialised marginal zone B cells, macrophages, and DCs, controls the entry of blood-borne antigen from the red pulp into the white pulp and exposure to the residing lymphocytes (Mebius and Kraal, 2005).

1.3.1 Soluble antigen encounter

Soluble antigen can arise through the protease-mediated cleavage of larger microorganisms (Catron et al., 2010) or secreted bacterial products (Roozendaal et al., 2009), or alternatively, from an injection or vaccination. These soluble antigens drain into the lymphatic vessels and are carried in the lymphatic fluid to the lymph node. The lymph node itself is protected from the unregulated flow of soluble antigens into the cortex by the SCS, which separates the afferent lymphatic vessel and the B cell follicle (Gretz et al., 2000). However, it has been shown that B cells are able to respond to these soluble antigens indicating the presence of a controlled mechanism permitting the antigens to cross this barrier.

Early electron microscopy images of the lymph node revealed small holes (0.1-1 μm) in the lining of the SCS (van Ewijk et al., 1988) indicating the possibility that soluble antigen could filter through these holes into the follicle (Figure 3A). In support of this theory *Pape et al 2007* intradermally injected hen egg lysozyme (HEL) antigen, tagged with green fluorescent protein (GFP), into the ears of recipient mice, which had previously been injected with HEL-specific MD4 B cells (Pape et al., 2007). Flash frozen cryosections of these lymph nodes demonstrated that MD4 B cells 150 μm away from the SCS and site of antigen entry, were able to acquire these antigens within minutes of injection. As B cells are unable to move more than approximately 6 μm/ minute without antigen, and are known to transiently decrease their mobility after specific antigen recognition (Okada et al., 2005), the authors suggest that antigen-positive B cells must have acquired antigen which diffused passively through the holes in the SCS.

More recently studies have shown that soluble antigens enter the B cell follicles through a conduit system (Figure 3A). Conduits are comprised of a core of collagen fibres surrounded by FRCs covering a basement membrane sheath. Conduits are abundant in the T cell zone, and in neonatal lymph nodes there are also ample levels in the B cell follicle, however during development, FDCs replace the majority of conduits in the B cell zone, leaving a much less dense network compared to the paracortex (Bajénoff and Germain, 2009). Using intravital imaging *Roozendaal et al 2009* demonstrated that small soluble fluorescently-labelled turkey egg lysozyme (TEL) antigen injected subcutaneously into recipient mice, entered the lymph node in a centripetal fashion, highlighting the presence of a follicular conduit network (Roozendaal et al., 2009). Observations of B cells acquiring this antigen, and electron microscopy images showing B cell pseudopods directly sampling the antigen-filled conduit core, demonstrated the use of these conduits in delivering antigen to B cells. The authors also revealed that if the TEL antigen was conjugated to a large fluorescent label (250 kDa), it was initially arrested at the SCS and then entered the lymph node with a delay. These findings mirror earlier studies showing that conduits have a size exclusion limit of 70 kDa (Gretz et al., 2000), and suggest that bigger antigens, require alternate mechanisms for entry into the follicle.

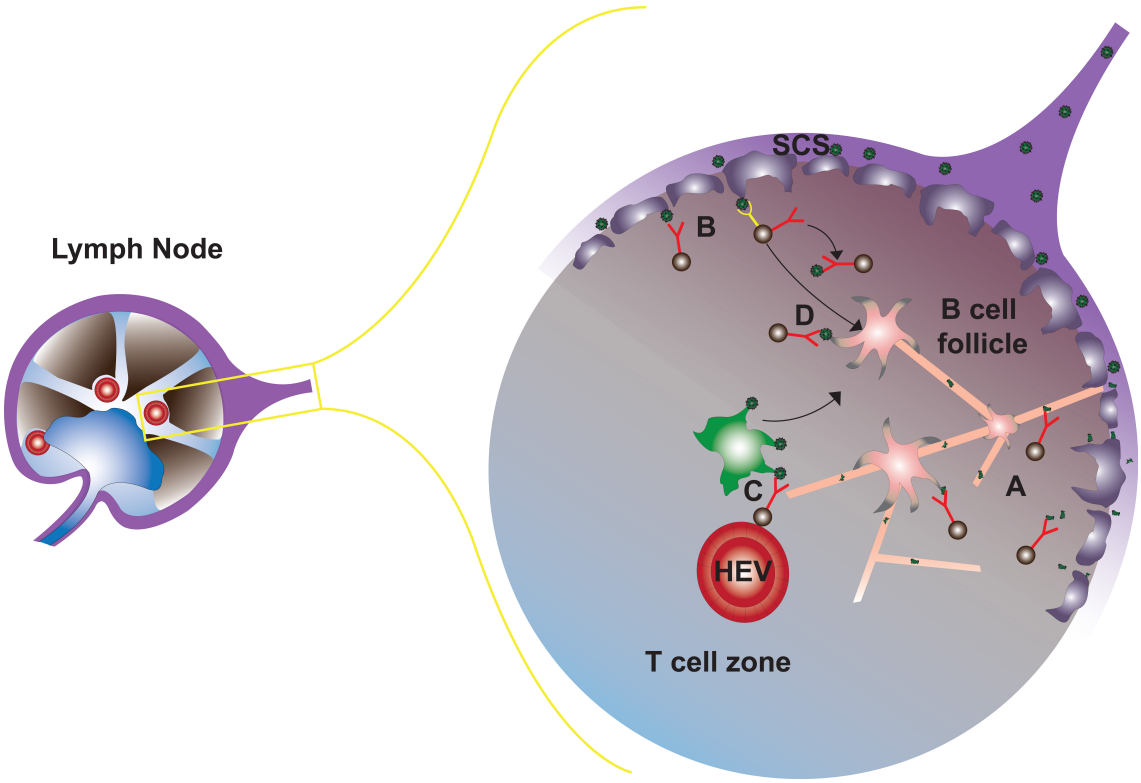

Figure 3: Antigen encounter in the lymph node

A) B cells can encounter soluble antigen that has diffused through gaps in the SCS, or filtered into the follicle through the network of conduits

B) Cognate or non-cognate B cells can bind to antigen transported over the SCS by SCS macrophages via their BCRs (red) or complement receptor (yellow), respectively. Non cognate B cells can then deposit the antigen on FDCs for later recognition

C) DCs can bind to antigen in the periphery and transport it into the lymph through the HEV. DCs can then present antigen to B cells as they exit the HEV

D) FDCs can retain antigen for a long time in the B cell follicle, and present it to B cells both before and during the germinal centre response

1.3.2 Membrane-bound antigen encounter

Although B cells can be activated by soluble antigen, the majority of antigen exposed to B cells during the immune response is bound to the surface membrane of APCs (Carrasco and Batista, 2006b). These APCs include macrophages, DCs and FDCs from the innate immune system.

In vitro and *in vivo* studies have shown that B cell activation following membrane-bound antigen encounter is more efficient than when exposed to a comparable soluble antigen (Batista et al., 2001; Huang et al., 2005; Qin et al., 1998; Wu et

al., 2008). This could be because of the expression of integrin receptors by the APC to facilitate long-lived and stable interactions with the cognate B cells (Allen and Cyster, 2008; Carrasco and Batista, 2006a; Carrasco et al., 2004). Or it could be because APCs concentrate and cluster antigen thereby increasing its avidity (Suzuki et al., 2009). APCs can also augment B cell activation through stimulation of the B cell co-receptors or through the secretion of soluble survival and activation factors (Allen and Cyster, 2008; Balázs et al., 2002; Depoil et al., 2007; Gonzalez et al., 2010a; Qin et al., 1998; Weber et al., 2008), as well as providing a platform for B-T cell interaction (Bergtold et al., 2005).

As well as increasing B cell signalling and activation, APCs can also act as antigen transporters to ensure B cells are able to see antigen that cannot diffuse passively into the lymph node, and they can support the continual improvement of the humoral response during affinity maturation in the germinal centres following infection.

1.3.3 The capture of antigen by antigen-presenting cells

Before B cells can become activated by APCs, APCs must first capture antigen and retain it on the surface of their cell membrane. B cells need to be able to recognise bacteria, viruses, fungi, and parasites, as well as environmental or synthetic chemicals. Although APCs don't need to recognise these antigens specifically, they do need to identify them as non-self so they can present them as pathogenic entities to the adaptive immune system. To be able to do this they have a selection of cell surface receptors to mediate this task. These include complement receptors and receptors which can recognise the Fc portions of soluble antibody, for example FcγRIIb receptors. These receptors recognise immune complexes, which are comprised of soluble antigen bound by natural or specific antibody and complement – complement are serum proteins which, when activated produce a protease cascade whose products bind to antigens and mark them for subsequent recognition by other components of the immune system (Bergtold et al., 2005; Carroll, 1998; Gonzalez et al., 2010a; Heesters et al., 2013; Qin et al., 1998). Another important receptor group, which can mediate antigen presentation on APCs, are C-type lectins. These receptors can bind to

carbohydrate moieties of infectious agents such as viruses and yeast (Gonzalez et al., 2010c; Taylor et al., 2004).

As BCRs recognise antigen in its native structure, APCs need to hold antigen in its native from. FcγRIIb and complement receptors have been shown able to internalise antigen into non-degradative endosomes and recycle them to their cell surface to allow stable and long-lived presentation of native antigen to B cells (Bergtold et al., 2005; Delamarre et al., 2005; Heesters et al., 2013).

1.3.4 The transport of antigen by antigen-presenting cells to B cells

As mentioned above, antigen can only diffuse into the lymph node if it is smaller than 70 kDa. Microorganisms such as viruses or bacteria are too big to filter into follicles, and small soluble protein antigens are thought to be quickly bound up into immune complexes by serum antibodies and complement. Therefore, APCs must transport these particulate antigens from the lymph into the follicle.

One set of APCs able to mediate transport of antigen into B cell follicles are macrophages, which line the SCS. These SCS macrophages were first identified using light and electron microscopy as monocyte-type cells which were able to transfer immune complexes, produced through subcutaneous injection of antigen into passively immunised mice, across their cell surface and along their cell processes, which penetrated the B cell follicle (Szakal et al., 1983). More recently, intravital imaging demonstrated that within minutes of subcutaneous injection of immune complexes, SCS macrophages are decorated with antigen, which can be directly presented to cognate B cells for specific recognition (Figure 3B), resulting in B cell activation and movement to the B-T cell border (Carrasco and Batista, 2007; Phan et al., 2007). Studies using vesicular stomatitis virus as antigen, demonstrated that the disruption of SCS macrophages following clodronate liposomes treatment, prevented the initiation of an adaptive immune response and caused an increase in systemic viral load (Junt et al., 2007).

Interestingly, non-cognate B cells have also been observed acquiring antigen from the SCS macrophages (Figure 3B). These B cells were able to bind to

antigen via their complement receptors and carry this antigen for deposition onto another family of APCs; FDCs, for later detection by cognate B cells (Heesters et al., 2013). The importance of non-cognate B cells transporting antigen was shown in both the spleen and lymph nodes of mice reconstituted with complement-receptor deficient B cells (Arnon et al., 2012; Cinamon et al., 2007; Ferguson et al., 2004; Phan et al., 2007). These mice had decreased antigen deposition on FDCs, which is required for germinal centre formation and maintenance, and therefore they also had a reduction in the subsequent humoral response. Although the ability of B cells to transport antigen has been known for a long time (Heinen et al., 1986), exactly how B cells are able to “give up” the antigen to FDCs is unknown, although reports suggest that the increased levels of complement receptor found on FDCs could outcompete the complement receptors on B cells (Carroll, 1998).

DCs are also important in bringing antigen into the follicle or spleen for presentation to B cells (Figure 3C). DCs can bind to pathogens in the peripheral tissues or in the blood stream and bring them into the follicle or spleen to stimulate a B cell response (Balázs et al., 2002; Berney et al., 1999; Chappell et al., 2012; Qi et al., 2006; Wykes et al., 1998). This is especially important if the infecting microorganisms are large and may not enter the lymphatic drainage (Balázs et al., 2002; Manolova et al., 2008). Intravital imaging of DCs pulsed with soluble antigen and transferred into recipient mice, showed that they homed to the lymph nodes and crowded around the HEVs, to maximise the chance of cognate B cell encounter as they entered the lymph node (Qi et al., 2006). In addition to presentation of intact antigen important for B cell recognition, DCs also process and present antigen on MHC Class II molecules, which is important for antigen recognition by cognate T cells (Bergtold et al., 2005; Delamarre et al., 2005). Expression of both processed and intact antigens facilitates cellular interactions between DCs, T cells and B cells and increases the efficiently of T cell help required for full B cell activation (Bergtold et al., 2005).

1.3.5 Antigen-presenting cells in maintaining the B cell follicle and supporting germinal centre function

Another important APC involved in stimulating effective B cell responses in the lymph node are FDCs (Figure 3D). As with the macrophages and DCs, cognate interactions of B cells with antigen presented on these APCs leads to B cell activation (Heesters et al., 2013; Suzuki et al., 2009). Through the continual recycling of antigen via complement and FcγRIIb receptors, FDCs have been shown able to hold the antigen on their cell surface weeks after infection (Fang et al., 1998; Heesters et al., 2013; Schwickert et al., 2007; Suzuki et al., 2009; Wu et al., 2008). This long-lived antigen retention is particularly important in orchestrating the somatic hypermutation and clonal selection of high affinity B cells during the germinal centre response (Allen and Cyster, 2008; Chan and Brink, 2012; Wu et al., 2008).

FDCs also have a role in maintaining the structural support of the B cell follicle and produce CXCL13 required to attract B cells to the follicle after entry into the lymph node (Cyster et al., 2000). Selective ablation of FDCs caused loss of structural integrity in the lymph node and the B cell follicles became disorganised bands of cells around the T cell zone (Wang et al., 2011).

Collectively, these studies reveal intricate mechanisms ensuring that B cells can respond to antigen irrelevant of size or site of infection (Manolova et al., 2008) and with appropriate co-stimulatory signals. Loss or reduction of the humoral response when activity of these APCs or their antigen-binding receptors are disrupted, demonstrates the vital role of membrane-presented antigen for the development of an efficient antibody response (Fang et al., 1998; Gonzalez et al., 2010b; Phan et al., 2007).

1.4 B cell development

Apart from B cell function in the periphery, BCR signalling is also instrumental during B cell development (Hardy and Hayakawa, 2001; Kurosaki et al., 2010; Mårtensson et al., 2010; Nagasawa, 2006; Wang and Clark, 2003). B cells

develop from common lymphoid progenitor cells and during this developmental process B cells interact with stromal cells, which give survival signals and developmental cues. The first B cell progenitor, the PrePro B cell (Figure 4), upregulates the cell surface marker B220. Following this, B cells move into the Pro B cell stage by upregulating the transcription factor Pax 5, which then stimulates Igα and CD19 surface expression, whilst the heavy chain locus of the BCR begins to rearrange (Nagata et al., 1997; Nutt et al., 1999; Wang and Clark, 2003). Rearrangement of the variable, diverse and joining genes in the heavy chain locus is mediated by the Rag1/2 recombinase, and then non-templated nucleotides are inserted into joints of the newly rearranged gene segments by deoxynucleotidyl transferase. Expression of a newly-rearranged signalling-competent Pre-BCR (Igμ paired with surrogate light chains) on the cell surface, is required for the transition from the Pro B cell stage into Pre B cell stage and is followed by proliferation (Gong and Nussenzweig, 1996; Kitamura et al., 1991; Pelanda et al., 2002) (Figure 4). Although it is possible that ligand-induced BCR signalling could mediate this proliferation stimulation, it has been widely suggested that this signal is BCR intrinsic and depends on the unique clustering properties of the surrogate light chains (Mårtensson et al., 2010; Ohnishi and Melchers, 2003). Light chains of the BCR are then rearranged producing an immature B cell.

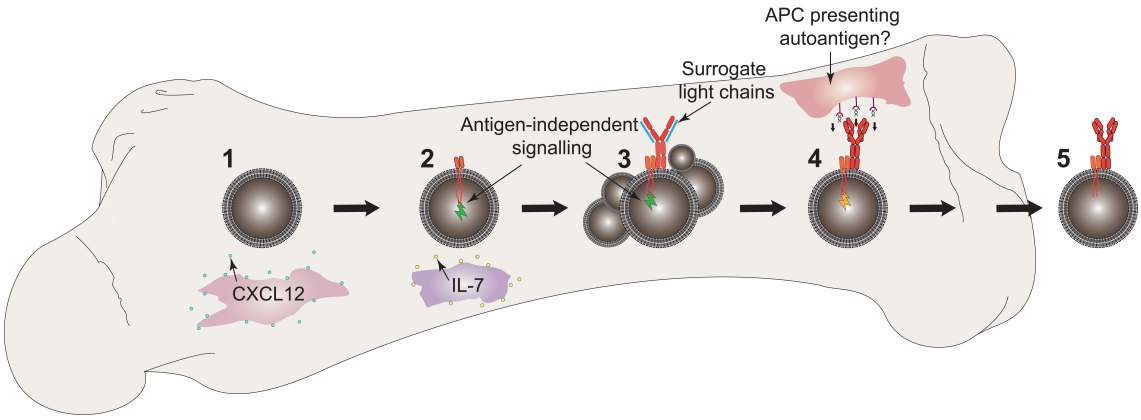

Figure 4: B cell development

Stage 1: PrePro B cells develop from common lymphoid progenitors in the bone marrow and interact with CXCL12 expressing stromal cells

Stage 2: Pro B cells interact with IL-7 expressing stromal cells and upregulate the Igαβ heterodimer, which signals for transcription and rearrangement of Igμ heavy chain

Stage 3: Pre B cells express Igμ heavy chain with surrogate light chains, which stimulates proliferation of the B cell and light chain rearrangement

Stage 4: Immature B cells express a fully assembled BCR, which stimulates B cell clonal deletion, BCR rearrangement, or release into the periphery

Stage 5: Mature B cells enter circulation

Immature B cells undergo negative selection, which depends on BCR-mediated recognition of autoantigens and is thought to prevent autoreactive B cells from entering the periphery. This was shown in MD4 mice whose B cells are specific for HEL and which were also engineered to express HEL tethered to stromal cells, as they had no peripheral B cells (Hartley et al., 1991). A similar phenotype was seen after the introduction of an anti-DNA BCR transgene into non-autoimmune mice (Chen et al., 1994). Separately, physical crosslinking of BCRs on immature B cells *in vitro* by αIgM antibodies, stimulated immature B cells to die (Norvell et al., 1995).

However, although these studies show the requirement for effective BCR signalling following autoantigen binding in sorting out the autoreactive B cells, we still don't know in what form the developing B cells recognise the autoantigens and whether some specialised APCs are involved. It is also unknown whether this developmental step requires BCR-antigen internalisation or whether cell-surface BCR crosslinking is sufficient. It has been shown that mutations in TLR-signalling pathways result in defects in negative selection, suggesting a possibility that antigen internalisation and trafficking to TLR-containing compartments may play an important role (Isnardi et al., 2008). Therefore, the role of antigen internalisation from APCs and APC-B cell interaction in B cell development is an interesting topic for future study.

1.5 BCR signalling

1.5.1 BCR signalling in the absence of antigen

Once B cells become mature and populate the periphery, they require constitutive BCR signalling even in the absence of antigen. This was shown by

the apoptotic loss of B cells following inducible Cre-mediated deletion of the heavy chain of the IgM, or deletion or mutation of Igα in peripheral B cells (Kraus et al., 2004; Lam et al., 1997). This loss of mature B cells was restored by constitutive PI3 kinase signalling, indicating that BCRs signal through this pathway to regulate B cell survival (Srinivasan et al., 2009).

The exact trigger for the survival signalling from the BCR is not well understood. It was originally hypothesised that these survival signals were initiated from the exposure of BCR to low levels of ligand or self antigen, or through spontaneous BCR tonic signalling (Kraus et al., 2004; Lam et al., 1997; Reth and Wienands, 1997). More recently, signalling in response to BAFF has been implicated. BAFF is a cytokine, which binds to its receptor (BAFFR) on the surface of follicular and marginal zone B cells. This binding induces BAFFR-mediated signalling, critical for B cell survival (Mackay et al., 2010). Inducible deletion of the BCR or the BCR-proximal signalling molecule Syk, led to unresponsiveness of B cells to BAFF and B cell death (Schweighoffer et al., 2013). These studies suggest that in this context the BCR can act as an adaptor protein in the BAFFR signalling pathway and functions following BAFFR-mediated phosphorylation of its Igα chain, by activating Syk and subsequently PI3 kinase (Schweighoffer et al., 2013).

1.5.2 Antigen-induced BCR signalling

The first biochemical steps after antigen binding to the BCR is phosphorylation of immunoreceptor tyrosine-based activation motifs (ITAM) found in the cytoplasmic domains of the IgαIgβ heterodimer by Src and Syk family tyrosine kinases (Dal Porto et al., 2004). Exactly how this is happens is a matter of debate. Three possible scenarios have been suggested recently.

Firstly, total internal reflection fluorescence (TIRF) imaging of labelled BCRs has shown that in the absence of antigen approximately 80% of BCRs are monomeric and freely diffuse on the plasma membrane (Tolar et al., 2005). This was demonstrated using fluorescence energy resonance transfer (FRET) analysis of BCR components labelled with FRET donor or acceptor proteins. In the absence

of antigen a very low FRET signal was observed between labelled components suggesting the majority of BCRs were not in close enough proximity to elicit a FRET signal. However, after antigen binding the FRET signal dramatically increased clearly illustrating the formation of oligomers, and then decreased suggesting 'opening' of the BCR cytoplasmic domain. This decrease in FRET did not reach levels seen without antigen, and coincided with the recruitment and activation of signalling molecules to the BCR (Tolar et al., 2005).

Targeted deletion of IgM segments identified the Cμ4 domain as the part responsible for mediating the change from monomer to oligomer. BCRs missing this portion were unable to oligomerise and could not signal in response to membrane-bound monovalent antigen, and constructs containing Cμ4 alone spontaneously clustered and signalled independently of antigen. These studies suggest that following antigen binding the BCR alters its conformation through the Cμ4 domain, facilitating oligomerisation. Once oligomerised, the cytoplasmic domain of the BCR opens permitting interactions with signalling molecules and initiating the activated-BCR signalling cascade. (Tolar et al., 2009b).

Secondly, it has been suggested that BCRs are inactive oligomers at rest (Schamel and Reth, 2000) and activated BCR signalling is prevented by auto-inhibition of the cytoplasmic domains. Binding of multivalent antigen then forces these oligomers apart into monomers, freeing the cytoplasmic domains to initiate signalling (Yang and Reth, 2010). Oligomerisation was recently demonstrated using confocal microscopy and bifluorescent complementation. Components of the BCR were tagged with either the N- or C- terminal of yellow fluorescent protein (YFP) and if the components came close enough together i.e. following dimerisation, a fluorescent signal was generated. In these studies a YFP signal was detected without antigen, suggesting oligomers were present on the cell surface. However it is difficult to understand the functionality of these oligomers as the bifluorescent interaction is irreversible, and therefore does not take into account the possibility of transient association due to the high number of BCRs found on the B cell surface. These studies also indicate that for BCRs to become fully activated, a multivalent antigen is needed to hold the BCRs apart, which

does not accommodate the results demonstrating BCR activation following stimulation with membrane-bound monovalent antigens (Tolar et al., 2009b). However, the percentage of total BCRs held in these oligomers was not assessed, and therefore could account for the 20% of immobile BCRs seen in other studies (Tolar et al., 2005; Treanor et al., 2010).

The third theory suggests that interactions between the Igβ chain and actin cytoskeleton allow the BCRs to diffuse freely in the membrane but in regions defined by cytoskeleton (Treanor et al., 2010). These actin-defined regions are thought to prevent the association of activating kinases or deactivating phosphatases, required for antigen-induced signalling. This was shown by the initiation of BCR signalling, comparable to that elicited by antigen binding, following cytoskeleton disruption (Treanor et al., 2010; 2011).

Within these defined regions BCRs were observed in nanoclusters containing approximately 30-150 IgD or 25-50 IgM molecules, using direct stochastic optical reconstruction microscopy (dSTORM) (Mattila et al., 2013). dSTORM allows the visualisation of BCRs at a much higher accuracy of 20 nm compared to 200 nm for TIRF and confocal microscopy (Pierce and Liu, 2010) used in the earlier studies. Whether these nanoclusters can mediate activated BCR signalling individually, or possibly could join with other nanoclusters to produce larger signalling-active microclusters, is not yet clear. Also it is not possible to conclude whether these nanoclusters are oligomers mediated by direct protein-protein interactions, or whether they are individual BCRs localised in close proximity (Mattila et al., 2013). One of the limitations of dSTORM is that it is carried out on fixed cells, which does not account for the dynamic nature of BCRs. Therefore the change in BCR organisation from resting and tonic, to antigen-bound and activated, is still open for debate.

1.5.3 Translocation to lipid rafts

Once the BCR has bound antigen, BCR-antigen complexes (whether oligomers, monomers or nanoclusters) decrease their rate of diffusion (Tolar et al., 2005; Treanor et al., 2011), group together to form microclusters, and translocate to

detergent-insoluble cholesterol-rich lipid rafts (Cheng et al., 1999; Sohn, 2006; Sohn et al., 2008). How the antigen-bound BCR moves to the lipid rafts is also unknown. The conformational change through the Cμ4 domain may alter the structure of the BCR so that dwelling in the lipid rafts is more energetically favourable (Tolar et al., 2009a), which could explain studies showing BCR-antigen translocation to lipid rafts independently of actin or canonical BCR signalling (Cheng et al., 2001). Alternatively, other studies suggest that this movement is dependent on actin activity stimulated by BCR binding to antigen. This insinuates some form of very early BCR signalling even before the BCR comes into contact with its established signalling mediators (Dal Porto et al., 2004; Treanor et al., 2011). Once in the lipid rafts, BCR microclusters can interact with Lyn, a Src family tyrosine kinase, which resides in the lipid rafts (Sohn et al., 2008). IgαIgβ ITAM phosphorylation by Lyn then recruits and activates Syk, which initiates the BCR signalling cascade (Bonnerot et al., 1995; Dal Porto et al., 2004; Ma et al., 2001). This antigen-induced signalling cascade stimulates many intracellular signalling pathways, which lead to a multitude of outcomes including B cell proliferation, survival, differentiation as well as internalisation and presentation of antigen. (Dal Porto et al., 2004; Kurosaki et al., 2010).

1.5.4 Synapse formation in response to membrane-bound antigen

The majority of antigen *in vivo* will be tethered to an APC, and *in vitro* studies have suggested that once B cells recognise membrane-bound antigen they form BCR-antigen microclusters arranged in an immunological synapse (Batista et al., 2001). To study the molecular requirements for this process, antigen tethered to planar lipid bilayers (PLB), has been used as a surrogate for APCs (Figure 5). PLB are very flat structures and together with TIRF microscopy allow high-resolution 2D imaging of molecular events occurring at the plasma membrane, which cannot be achieved *in vivo* (Pierce and Liu, 2010).

The formation of BCR-antigen microclusters, and the initiation of BCR signalling in response to PLB-bound antigen, stimulates F-actin dependent B cell spreading over the antigen-presenting surface (Figure 5A and B) (Fleire et al., 2006). As the

B cell spreads it continues to bind to antigen and form new BCR-antigen microclusters (Figure 5B), and then contracts bringing them into a central supramolecular activation cluster (Figure 5C), reminiscent of those found in T cell synapses (Fleire et al., 2006; Grakoui et al., 1999). The extent of B cell spreading, and therefore the final amount of antigen collected in the synapse, correlates with antigen affinity, and in order for B cell spreading to be initiated, a minimum affinity threshold must be attained (Fleire et al., 2006; Liu et al., 2010). This threshold can be lowered by increasing the avidity of the antigen (Tolar et al., 2009b), or by the presence of the integrin receptors LFA-1 and VLA-4, as well as through association with the BCR co-receptor CD19 (Arana et al., 2008; Carrasco and Batista, 2006a; Carrasco et al., 2004; Depoil et al., 2007; Lin et al., 2008). These findings confirm the roles for APC co-stimulatory factors mentioned earlier.

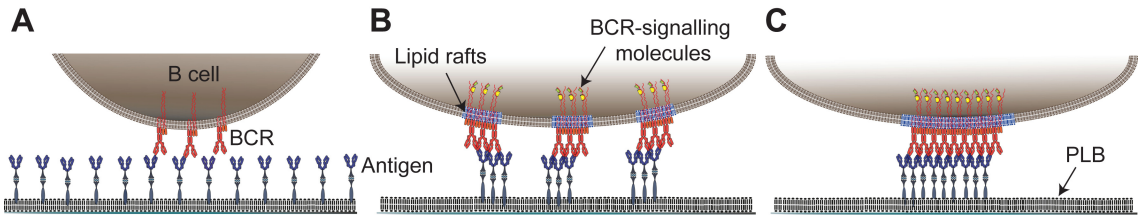

Figure 5: B cells form synapses with antigen-presenting surfaces

A) B cells bind to antigen via their BCRs

B) B cells spread over the antigen-presenting surface forming signalling-active BCR-antigen microclusters

C) B cells contract, bringing the BCR-antigen microclusters into a mature immunological synapse

Individual protein knockout studies in the DT40 chicken B cell line, showed signalling from Lyn and Syk, was required for B cells to adhere to the PLB, whereas synergistic activity between the more distal BCR signalling molecules, PLCγ and Vav, mediated spreading (Weber et al., 2008). Less is known about the process of contraction, and although it is understood to be F-actin dependent (Arana et al., 2008; Fleire et al., 2006; Lin et al., 2008), more recently, the involvement of the microtubule network has been implicated (Schnyder et al.,

2011). This was shown by the recruitment of the microtubule-motor Dynein to the contracting microclusters by a Grb2-Dok3-cbl complex.

1.6 BCR-antigen internalisation

While the formation of signalling active BCR microclusters immediately after antigen binding has been extensively observed *in vitro* in response to multivalent soluble antigen (Ma et al., 2001; Niiro et al., 2004) as well as both monovalent and multivalent PLB-bound antigen (Depoil et al., 2007; Fleire et al., 2006; Liu et al., 2010; Weber et al., 2008). How BCR-antigen microclusters are internalised remains unclear.

Studies have shown that BCR signalling is required for efficient antigen internalisation, suggesting a crosstalk between BCR signalling and endocytic machinery. For instance, antigen internalisation has been shown to be dependent on the signalling capacity of the BCR's IgαIgβ cytoplasmic domains. Using chimera constructs containing the cytoplasmic domains of either the Igα or the Igβ proteins, studies have shown that both chains contained residues that could individually mediate BCR internalisation (Bonnerot et al., 1995; Jang et al., 2010; Lankar et al., 1998). Point mutation studies have also shown that activity from both ITAM (Cassard et al., 1998; Gazumyan et al., 2006) and non-ITAM tyrosines within the IgαIgβ heterodimer (Hou et al., 2006; Patel and Neuberger, 1993) are required for this process.

Similarly, BCR proximal signalling molecules have been connected to this process. Antigen-stimulated Lyn knockout B cells were inhibited in their ability to internalise antigen, shown by retention of antigen on the cell surface (Chan et al., 1998; Ma et al., 2001). Downstream of Lyn, BCR signalling also activates regulators of the actin cytoskeleton, and a role for actin polymerisation in BCR-antigen internalisation has been proposed. For example, results from knockout and inhibitor studies on Bam32 (Niiro et al., 2004) and WASp (Becker-Herman et al., 2011) showed similarities in phenotype to Lyn knockout cells, and BCR-antigen internalisation is also reduced following disruption of Vav mediated

activation of Rac (Malhotra et al., 2009a; 2009b). Consistently with these studies, disruption of actin polymerisation itself also decreased BCR-antigen internalisation (Stoddart et al., 2005).

The primary endocytic mediator involved in BCR-antigen internalisation is thought to be clathrin. This was first shown by early electron microscopy studies, which demonstrated the endocytosis of antigen-bound BCRs through clathrin coated pits (Salisbury, 1980). More recently this has been supported by a correlation between BCR-antigen internalisation and lipid raft-associated clathrin phosphorylation, and a reduction in BCR-antigen internalisation after the inducible deletion of the clathrin heavy chain in DT40 cells. These studies use biochemical analysis to propose that antigen-induced BCR signalling stimulates phosphorylation of clathrin within the lipid raft scaffold initiating internalisation (Stoddart et al., 2002; 2005). Clathrin-mediated endocytosis is dependent on the recruitment and organisation of an array of specific adaptor proteins to the site of clathrin coated pit formation. Some of these adaptors are indispensible for clathrin action such as AP2, but others can vary depending on the cargo, cell type or environment (McMahon and Boucrot, 2011; Taylor et al., 2011). However, to date, the involvement of any cargo-specific adaptors required for BCR-antigen internalisation through clathrin-mediated endocytosis, remains unknown.

Although studies of BCR-antigen internalisation have identified roles for BCR signalling, lipid rafts, the actin cytoskeleton, and clathrin-mediated endocytosis, they have also indicated a significant level of redundancy in this process. Some studies suggest that lipid rafts act as a signalling platform only and antigen-bound BCRs are not internalised from these structures (Hou et al., 2006; Putnam et al., 2003). Also, deletion of clathrin, inhibition of actin activity or disruption of lipid raft heterogeneity, does not completely abolish BCR-antigen internalisation (Stoddart et al., 2005), suggesting alternative mechanisms can partially compensate for their loss. In addition, it is unknown whether the same components are required for internalisation of membrane-bound antigen as described for antigen in solution. In fact, the almost absolute requirement for actin activity for synapse formation in response to membrane-bound antigen (Fleire et al., 2006),

compared to a redundant role when faced with soluble antigen (Stoddart et al., 2005), suggests that the two internalisation processes may be different.

Therefore, although key players in BCR-antigen internalisation have been identified, their precise contribution and mechanism of action, and how they interlink together, requires further study.

1.7 Affinity-dependent antigen internalisation

B cells need to be able to internalise antigen in an affinity-dependent manner as affinity-dependent BCR-antigen internalisation allows the selective expansion of high affinity B cell clones. These B cells can then produce high affinity antibody, specific for the invading pathogen, marking it for elimination. This happens at two primary checkpoints of the B cell response. Firstly, at the point of antigen encounter in the B cell follicle to provide an immediate antibody response (Paus et al., 2006), and secondly during affinity maturation in the germinal centre to encourage the expansion of high affinity B cells and their differentiation into plasma cells and memory B cells (Chan and Brink, 2012; Rajewsky, 1996).

In vitro studies have shown that B cells can recognise and discriminate between a range of different antigen affinities (Batista and Neuberger, 1998). B cells respond with increasing efficiency to soluble monovalent antigen with affinities from $K_a > 10^6\ M^{-1}$ up until $K_a > 10^{10}\ M^{-1}$, where an affinity ceiling threshold is reached and the corresponding B cell response does not continue to grow irrelevant of any further increases in affinity (Batista and Neuberger, 1998). This increased B cell response to high antigen affinity was shown firstly at the level of BCR signalling by increased levels of calcium flux and phosphorylation of early BCR signalling mediators (Kouskoff et al., 1998), and secondly at the level of antigen presentation by higher levels of IL-2 production by cognate T cell specific hybridomas, which had been co-cultured with MD4 B cells and HEL antigens (Batista and Neuberger, 1998).

Similar dependence on affinity has been shown for membrane-tethered antigens. TIRF microscopy of antigen-loaded PLB revealed that cognate B cells had increased levels of spreading, microcluster formation, and subsequent antigen accumulation and synapse formation, when BCRs of high affinity were settled on the same antigen compared to the lower affinity equivalent BCR (Fleire et al., 2006; Liu et al., 2010). Taken together these studies suggest that high affinity monovalent antigen stimulates a greater level of signalling and BCR-antigen accumulation, which results in a higher level of antigen internalisation and presentation, and subsequent cognate T cell activation.

However, these measurements and studies only look at an individual reaction between a single Fab molecule of the BCR and a single epitope in the antigen. *In vivo*, considering the bivalent nature of the BCR, and the multivalency of antigen associated with the infections B cells must recognise, such as bacteria, viruses, fungi, and parasites, the majority of interactions between the BCR and the antigen will be multivalent. This means that B cell recognition of antigen is also affected by avidity (number of bonds between BCRs and antigen). High avidity antigen can be formed not only through the particulate nature of the antigen itself but also through complexing of antigen with natural antibodies or complement in the blood stream, or by clustering on the surface of APCs as mentioned earlier (Batista et al., 2001; Chan and Brink, 2012; Gonzalez et al., 2010a). *In vitro,* increasing the avidity of antigen raises its immunogenicity above the threshold required for maximum B cell stimulation, which prevents B cells from discriminating between antigen affinities in solution (Batista and Neuberger, 2000). However, *in vivo*, where antigens are primarily displayed on APCs, B cells respond to antigen in an affinity-dependent manner (Batista and Neuberger, 2000; Chan and Brink, 2012; Schwickert et al., 2011; Shih et al., 2002a; 2002b; Wan et al., 2013).

Observations of adoptively transferred B1-8 B cells with either a high or low BCR affinity for the nitrophenyl hapten (NP) into immunised recipient mice, showed that the rate of antigen internalisation and subsequent presentation correlated with affinity. This difference in internalisation rate didn't cause the observed affinity discrimination itself, as when low affinity B cells were transferred alone,

they were able to elicit a normal B cell response (Schwickert et al., 2011). Only when competition was introduced by transferring both high and low affinity B cells together, was there affinity discrimination and an almost exclusive expansion of high affinity clones which dominated the majority of the germinal centre response (Schwickert et al., 2011; Shih et al., 2002a). This was due to the increased levels of presented antigen on high affinity B cells, which monopolised T cell help at the B-T cell boarder and prevented lower affinity B cells from receiving the correct survival signals (Schwickert et al., 2011). Thus affinity discrimination at the B-T cell border selects BCRs with the relatively highest affinity to enter into the germinal centre (Schwickert et al., 2011). This relative selection mechanism, therefore, allows antigens of low affinity to still produce a successful immune response (Dal Porto et al., 1998; 2002), which is particularly important in the case of a primary infection, when the typical affinity of the BCR for a previously unseen pathogen is low (Chan and Brink, 2012).

Once in the germinal centre, B cells cycle between the light and dark zones. Within the dark zones B cells proliferate and activate somatic hypermutation. Somatic hypermutation introduces point mutations into the variable region of the BCR, diversifying the affinity for the stimulating antigen (Jacob et al., 1991; McKean et al., 1984). After one or more rounds of division B cells move to the light zone and test the fitness of the newly mutated BCR by binding to antigen displayed by light zone-resident FDCs (Allen and Cyster, 2008; Victora and Nussenzweig, 2012). B cells with a higher affinity are thought to internalise more of the antigen and present more to follicular helper T cells (Tfh) (Khalil et al., 2012; Victora et al., 2010). This T cell help has again been shown to be limiting and only those B cells with high enough affinity for the antigen receive T cell help, which stimulates not only their survival but also their movement back into the dark zone to continue another round of proliferation and somatic hypermutation (Victora et al., 2010). This mechanism ensures the continual selective expansion of high affinity B cells as the immune response progresses (Jacob et al., 1991; Rajewsky, 1996). In contrast, low affinity B cells internalise less antigen from FDCs, receive less help from Tfh, accumulate in the light zone, and die.

New studies by *Khalil et al 2012* have recently provided evidence showing that BCR signalling in the germinal centre reaction is inhibited by phosphatase activity, which may favour internalisation and presentation of the antigen to Tfh and possibly augments high affinity B cell expansion (Khalil et al., 2012).

Some antigens are highly stimulative to B cells and do not require T cell help to elicit antibody production; these are called T cell-independent (TI) antigens. TI antigens are usually large, polyvalent structures with repeating patterns such as carbohydrates from a bacterial capsid or virus. The polyvalent nature of these TI antigens allows extensive crosslinking of BCRs, which augments B cell signalling and intrinsically provides the stimulation needed for B cell activation and proliferation (Vos et al., 2000). These responses differ from T cell-dependent antigens as they do not form germinal centres, and function to quickly release soluble antibody against circulating pathogens (Shih et al., 2002b). Despite the lack of T cell help when faced with TI antigens, high affinity B cell clones are still able to outcompete low affinity clones. It is unclear how this competition happens, but it is possible that high affinity B cells internalise antigen more quickly, which in turn stimulates faster B cell proliferation, increases access to other stimulatory factors such as cytokines, and therefore facilitates the selective expansion of high affinity B cell clones.

The ability of B cells to internalise antigen in an affinity-dependent manner is vital during the immune response. This is important both at the point of initial antigen encounter, and to support the continual improvement of BCR affinity in germinal centres as the immune response progresses. Collectively, these studies show that the ability of B cells to discriminate between antigen affinities is due to the increased rate of antigen internalisation of high affinity B cells. However, the molecular mechanisms controlling this process are still unknown.

1.8 Defects in membrane-bound antigen internalisation can lead to autoimmunity or cancer

BCR-antigen internalisation is a tightly regulated process to ensure effective B cell function, and disturbances have been linked to B cell-mediated autoimmune diseases and cancer. These diseases can be a result of a range of either genetic factors, such as mutations in negative regulators of BCR signalling or they can be induced by the environment, for example by B cell responses to infection that cross-reacts with self-components. It is, therefore, important to consider how BCR-antigen internalisation prevents pathology, and how disturbances in this process can cause these diseases.

1.8.1 Autoimmunity

70% of newly developed immature B cells are autoreactive and have the potential to cause autoimmune pathologies by the production of autoantibodies specific for self-proteins, which then target self-cells for destruction (O'Neill et al., 2011; Plotz, 2003).

B cell interactions with APCs, in addition to their function in stimulating B cell activation, are also important in deleting these autoreactive B cells. Membrane-bound autoantigen is more efficient at this deletion than comparable soluble autoantigen. For example, during development, cognate B cells, which react with autoantigen expressed by stromal cells, are deleted and prevented from exiting the bone marrow, whereas their reaction to soluble autoantigen induces antigen-unresponsiveness (anergy) in the B cells, but they are still permitted to reach the periphery (Goodnow et al., 1988; Hartley et al., 1991). A similar deletion is seen after encounter with membrane-bound autoantigen in the periphery, which demonstrates an additional layer of control to ensure deletion of B cells specific for an autoantigen that is not present in the bone marrow (Russell et al., 1991; Taylor et al., 2012).

In the germinal centre, there is a risk that the newly mutated BCRs may cross-react with autoantigen and become autoimmune. Antigen presented by APCs in

the germinal centre can communicate to the B cell that the antigen is pathogenic and not self. This was shown by the rapid deletion of B cell clones in the germinal centre when soluble antigen, representing autoantigen, was added (Chan et al., 2012; Pulendran et al., 1995; Shokat and Goodnow, 1995).

Therefore, disruptions in the molecules that facilitate B cell-APC interaction, can lead to inappropriate activation of these B cells and the development of autoimmunity. For example, chronic expression of the integrins LFA-1 and VLA-4, which reduce the B cell activation threshold by facilitating adhesion between B cells and APCs, could promote B cell activation to low affinity autoantigens which should not normally stimulate a B cell response (Carrasco and Batista, 2006a; Carrasco et al., 2004). In addition, elevated expression of CD19, the BCR co-receptor shown to augment B cell activation in response to membrane-bound antigen (Depoil et al., 2007), has also been linked to an autoimmune phenotype by B cell hyper-responsiveness and autoantibody production (Hasler and Zouali, 2001). Conversely, loss of inhibitory factors, which prevent B cell response to autoantigens, can also cause autoimmunity. This was shown following the loss of CD22. CD22 is a receptor for α2,6 sialogglycoconjugates, which are commonly expressed on cell types which B cells are likely to encounter in an infection setting i.e. other lymphocytes and activated endothelium (Lanoue et al., 2002). The interaction between CD22 and α2,6 sialogglycoconjugates is thought to inhibit antigen-bound BCR signalling and reduce the expression of the B cell activation markers CD69 and CD86. As a result, B cells deficient in this BCR negative regulator, are prone to the production of autoantibodies and the initiation of autoimmune disease (O'Keefe et al., 1999; 1996).

Autoimmunity can also be caused by disturbances in BCR signalling, which normally controls antigen internalisation. Surprisingly, both Lyn knockout and Lyn gain of function mice are prone to autoimmune phenotypes characterised by hyper-responsive B cells and an increase in autoantibody production (Chan et al., 1997; Hibbs et al., 2002). It is difficult to ascertain how much of this phenotype is due to loss of internalisation as Lyn's role in B cell activation goes beyond stimulating internalisation. Lyn activity is required for phosphorylating both

positive and negative BCR regulators (Xu et al., 2005). Therefore when Lyn is lost, so is the activation of molecules, which inhibit B cell activation such as CD22, FcγRIIb, and SHIP-1 (Chan et al., 1998; O'Neill et al., 2011), and when Lyn is over expressed BCR activating molecules such as Syk are increased (Hibbs et al., 2002). These studies illustrate the complexity of BCR signalling and internalisation, and clearly demonstrate the difficulties in elucidating the exact mechanism and role of BCR-antigen internalisation *in vivo*.

One of the ways B cells prevent autoimmunity is through the process of anergy. Anergy is a non-reactive state of B cells, which occurs following recognition of autoantigen during development or in the periphery. Anergy can be initiated through chronic low-level stimulation of BCRs without T cell help (Cambier et al., 2007; O'Neill et al., 2011), but can also be controlled at the level of BCR-antigen internalisation. For example, when anergic B cells recognise DNA-containing autoantigens, they do not recruit TLR9 for amplification of the B cell response, but prevent antigen from meeting TLR9 before merging into late endosomes (O'Neill et al., 2009). However this altered trafficking in anergic B cells is reverted in autoimmune B cells, possibly by BCRs mistaking hypomethylated DNA from apoptotic cells for bacterial DNA (Leadbetter et al., 2002), or over active TLR9 signalling (Christensen, 2005). This results in the recruitment of TLR9 to internalised BCR-antigen complexes (Chaturvedi et al., 2008) and production of autoantibodies against self-DNA (Viglianti et al., 2003).

It has also been suggested that accelerated BCR-antigen internalisation from lipid rafts may help to maintain the unresponsiveness of anergic B cells. Studies showed that anergic B cells have a large intracellular pool of BCRs, present in a recycling endosomal compartment (Bléry et al., 2006). These anergic B cells had a faster rate of internalisation compared to naïve B cells, which prevented initiation of the signalling pathway leading to NFκB activation and subsequently B cell activation through the transcription of factors such as c-myc and bcl-XL. If lipid rafts were disrupted in these anergic cells by methyl-β-cyclodextrin, then BCRs quickly relocated to the cell surface and regained their responsiveness to antigen.

1.8.2 Cancer

In addition to antigen processing and engagement of antigen with intracellular TLRs, BCR-antigen internalisation also functions to alter BCR signalling to prevent the inappropriate survival of B cells, which could lead to cancer. Inhibition of BCR-antigen internalisation has been shown to maintain activate antigen-induced signalling complexes at the cell surface, which downregulates transcription factors controlling proapoptotic genes, and promotes B cell survival (Chaturvedi et al., 2011; Srinivasan et al., 2009).

This inhibition of internalisation together with the resulting hyper-responsive BCR signalling is seen in activated B cell like subtype of diffuse large B cell lymphoma cells (ABC DLBCL) (Davis et al., 2010). This is thought to be caused by mutations in the IgαIgβ ITAMs frequently found in ABL DLBCL biopsies. These mutations were shown to prevent the full activity of Lyn and inhibitory phosphatases, and inhibited BCR internalisation, causing a malignant phenotype.

These studies collectively show that although BCR-antigen internalisation is vital in the production of high affinity antibodies required for specific pathogen elimination, it is also important in preventing inappropriate B cell survival or B cell activation to autoantigens that could lead to the development of cancer or autoimmunity. By understanding how BCR-antigen internalisation works in normal physiology we hope to better understand how these processes are disregulated in disease. This knowledge could potentially be applied in the manipulation of BCR internalisation in order to treat B cell diseases.

1.9 Thesis Aims

It is well acknowledged that B cells require antigen internalisation in order to become activated and develop an efficient humoral response, as well as to prevent excessive BCR signalling. It is known that *in vivo* the primary source of antigen is tethered to APCs, and this presentation allows context-dependent antigen recognition by B cells, which augments and fine-tunes the B cell response. It is also known that this internalisation occurs in an affinity-dependent manner, which allows B cells to selectively expand high affinity B cell clones for the production of specific antibodies.

However, the mechanisms of B cell antigen extraction from APCs are still unknown. Studies using soluble antigen have identified specific components and pathways that are involved in BCR-antigen internalisation from solution, such as clathrin-mediated endocytosis, the actin cytoskeleton, lipid raft scaffolds and BCR signalling molecules. However, to date, there has not been a technique available to study the cellular and molecular mechanisms of BCR-antigen internalisation from an APC.

To address this question, we aimed to design and develop an antigen-presenting substrate from which B cells can internalise antigen, and using this substrate, we hoped to identify novel components and mechanisms involved in BCR-antigen internalisation.

Chapter 2 Materials and Methods

2.1 Mice

C57Bl/6 mice from an internal colony (called Bl6 throughout the thesis) were used for all experiments and as wild-type controls unless otherwise stated. B1-8$^{fl/fl}$ mice (a gift from K. Rajewsky (Sonoda et al., 1997)) were crossed with Igκ-deficient Igκ-C$^{tm1Cgn/tm1Cgn}$ mice (a gift from J. Langhorne) to produce the B1-8$^{fl/fl}$ Igκ-C$^{tm1Cgn/tm1Cgn}$ strain (called B1-8 throughout the thesis) and the strain was backcrossed onto C57Bl/6 background. The majority of B cells in these mice are specific for the nitrophenyl hapten (NP or NIP). MyH9$^{fl/fl}$ mice (purchased from Mutant Mouse Regional Resource Centers (Jacobelli et al., 2010)) were crossed with Mb1-Cre mice (a gift from V. Tybulewicz (Hobeika et al., 2006)) and the strain was backcrossed onto C57Bl/6 background (called Cre^{+}MyH9$^{fl/fl}$ throughout the thesis). These mice express Cre recombinase at the point of Igα expression in Pro B cells. Genotypes were confirmed using PCR analysis of DNA from ear snips. Mice were bred and treated in accordance with the guidelines set by the UK Home Office and UK NIMR Ethical Review Panel.

2.2 B cell purification and cell culture

Naïve B cells were obtained from splenocytes following red blood cell lysis (ACK buffer, Gibco) for all experiments except siRNA-mediated knockdown for which, a ficoll density gradient (GE Healthcare) was used. Naïve B cells were then negatively selected for using anti-CD43 microbeads on an autoMACs Pro separator (Miltenyi Biotec). Primary B cells and the Ramos human lymphoma cell line were cultured in RPMI 1640 media (Sigma) supplemented with 10% foetal bovine serum (FBS, Biosera), 1% MEM Non-Essential Amino Acids (Gibco), 2 mM L-glutamine (PAA Laboratories), 50 μM 2-mercaptoethanol (Gibco), 100 U/ml Penicillin and 100 μg/ml Streptomycin (Gibco). Adherent HEK293A, HEK293FT (both from Invitrogen), PLAT-E cells (a gift from V. Tybulewicz (Morita et al., 2000)) and bone marrow derived DCs were cultured in DMEM media (Gibco) supplemented with 10% FBS, 1% MEM Non-Essential Amino Acids, and

6 mM L-glutamine. 10 µg/ml blasticidin and 1 µg/ml puromycin (both InvivoGen) were added to PLAT-E media, 0.5 mg/ml Geneticin (Gibco) was added to HEK293FT media, and DCs differentiated from bone marrow cells using Flt3 ligand (a gift from G. Stockinger) for 7 days, were matured using 1 µg/ml LPS (Sigma) for 24 hours. Suspension HEK293A cells were maintained at 5 x 10^5 cells/ml, agitated at 120 rpm in Pro293S-CDM media (Lonza) supplemented with 1.5% FBS and 2 mM L-Glutamine. All cells were cultured in incubators humidified with 5% CO_2 at 37°C.

2.3 Antigens

BCR-specific antigen	Cellular target	Source
Goat F(ab')$_2$ α-mouse Igκ	Bl6 B cells	Southern biotec
Goat F(ab')$_2$ α-human IgM (µ chain specific)	Ramos cells	Southern Biotec
NP (4-Hydroxy-3-nitrophenylacetic acid active ester)- or NIP (4-Hydroxy-3-iodo-5-nitrophenylacetic active ester)- Osu	B1-8 B cells	Biosearch

Unless otherwise stated αIgκ and αIgM antigens were labelled with Cy5 or Cy3 using the Monoreactive dye kit (GE Healthcare) and biotinylated using EZ-link sulfo-NHS-LC-LC-Biotin (Thermo scientific).

To generate NIP-Qdot antigens, fluorescent Quantum dots (Qdot, Invitrogen) were haptenated with NIP-Osu in dimethylformamide (Sigma) for 3 hours and biotinylated. αIgM-Qdots were produced by mixing Qdots conjugated to streptavidin 1:1 with biotinylated αIgM.

NP or NIP antigens were produced from the haptenation of AlexaFluor647-labelled goat F(ab')$_2$ (Jackson Immunoresearch) with NP- or NIP-Osu and biotinylated. To load cognate immune complexes onto DCs for recognition by B1-8 B cells, NP/NIP antigen was mixed 1:1 with anti-biotin IgG1 antibodies (Sigma) for 30 minutes on ice. For AFM experiments, DCs were loaded with immune-

complexes consisting of αNP antibodies (Serotec) and NIP antigens for 1 hour on ice.

For 3D localisation of antigen particles, biotinylated-αIgκ was loaded onto PMS and then a small number of antigen molecules were labelled with a low concentration of streptavidin-conjugated Qdots.

2.4 Antibodies

Antibody	Clone	Source	Final concentration
α-mouse CD19 FITC	1D3	BD biosciences	1 μg/ml
α-human GAPDH-Alexa647	14C10	Cell Signaling	1:500 dilution
α-mouse CD45R/B220	RA3-6B2	BD biosciences	1 μg/ml
α- clathrin heavy chain	23	BD Transduction Laboratories	0.25 μg/ml
α-Dynamin2	Polyclonal	Abcam	1 μg/ml
α-β-actin	AC-74	Sigma	1:5000 dilution
α-AP2 μ1	EP2695Y	Epitomics	1:1000 dilution
α-mouse IgM μ chain specific-FITC	Catalog number: 115-097-020	Jackson Immunoresearch	5 μg/ml
α-mouse CD93 (AA4.1)-APC	AA4.1	eBioscience	2 μg/ml
α-mouse CD23-PE	B3B4	eBioscience	5 μg/ml
α-mouse/human CD45R/B220 PerCP-Cy5.5	RA3-6B2	Biolegend	1 μg/ml
α-mouse CD8a-brilliant violet 570	53-6.7	Biolegend	0.5 μg/ml
α-mouse CD4-efluor 450	RM4-5	eBioscience	1μg/ml
α-mouse CD19-APC	6D5	Biolegend	2 μg/ml
α-mouse CD2 (LFA-2)-PE	RM2-5	BD Biosciences	2.5 μg/ml
α-mouse IgD efluor 450	11-26	eBioscience	1 μg/ml

α-mouse IgD-PE	11-26	eBioscience	0.5 μg/ml
α-mouse TCR-β-APC	H57-597	eBioscience	1 μg/ml
α-mouse CD5 (Ly-1)-PE	53-7.3	eBioscience	2 μg/ml
α-mouse CD23-APC	B3B4	Invitrogen	1:100 dilution
α-human/mouse CD45/R (B220)-efluor 450	RA3-6B2	eBioscience	1 μg/ml
α-mouse/human CD45R (B220)-PE	RA3-6B2	ebioscience	1 μg/ml

2.5 Inhibitors

Inhibitors were incubated with B cells in Hank's buffered saline solution (HBSS) supplemented with 0.01% bovine serum albumin (BSA, Sigma). Dynasore was incubated with HBSS containing no BSA. All inhibitors were preincubated with B cells for 15 minutes at 37°C before addition to antigen-loaded PMS or soluble antigen. Solvent in the appropriate buffer was used as control.

Inhibitor	**Target**	**Source**	**Final concentration**
PP2	Lyn	Invitrogen	20 μM
LFM-A13	Btk	Caymann Chemical	50 μM
Bisindolylmaleimide	PKC	Caymann Chemical	20 μM
PD184352	Erk1/2	Selleckchem	2 μM
SMIFH2	Formin	Sigma	10 μM
NSC-23766	Rac1	Biovision	100 μM
Dynasore	Dynamin2	T Kirchhausen	80 μM
Blebbistatin	Myosin IIA	Caymann Chemical	50 μM
Y-27632	Rock1	Sigma	50 μM

2.6 Planar lipid bilayers (PLB)

DOPS (1,2-Dioleoyl-*sn*-Glycero-3-[Phospho-L-Serine] (Sodium Salt)) or DOPE-biotin (1,2-Dioleoyl-*sn*-Glycero-3-phosphoethanolamine-N-(Cap Biotinyl) (Sodium Salt)), were mixed at a molar ratio of 1:10 with DOPC lipid (1,2-dihexanoyl-*sn*-glycero-3-phosphocholine) (All from Avanti) in choloform. The lipids were dried overnight using argon and resuspended in degassed phosphate buffered saline (PBS). The lipids were then sonicated to produce unilamellar vesicles, clarified by ultracentrifugation at 36 000 rpm for 16 hours, and prepared in a 0.1 mM lipid solution in PBS. Glass coverslips were cleaned in sulfuric acid and hydrogen peroxide at a ratio of 3:1 and attached to Labtek imaging chambers (Nunc). Lipid bilayers were formed by fusing the unilaminar vesicles onto the clean coverslips.

For PLB in Figure 6, PLB formed from DOPE-biotin and DOPC were incubated with 5 μg/ml streptavidin (Southern Biotec) in PBS, washed, and incubated with NIP-Qdot antigens.

For PLB in all subsequent experiments, PLB from DOPS and DOPC were incubated with 24 nM biotinylated annexin V (BioVision) in HBSS. After washing, PLB were incubated with 5 μg/ml streptavidin, washed again, and incubated with indicated antigens. When not explicitly stated, PLB were loaded with antigens at 1 μg/ml, resulting typically in 50 antigen molecules per μm^2. In some cases, the concentration of antigen was titrated to achieve the density specified in the experiments. The calculation of antigen density on the substrates was performed as previously described (Tolar et al., 2009b). Briefly, antigen was diluted to a concentration that allowed resolution of single antigen molecules. The average fluorescence intensity of the single antigen molecules was used to convert fluorescence intensity of experimental antigen concentrations to number of antigen molecules per μm^2.

2.7 Plasma membrane sheets (PMS)

Suspension HEK293A cells were seeded onto poly-L-lysine (Sigma)-coated Labtek imaging chambers (Nunc) and cultured overnight to 100% confluency. Cells were then washed in PBS and sonicated with a probe sonicator placed 5 mm above the cells for 20 seconds at room temperature. This shears off the cells, leaving the ventral plasma membrane attached to the coverslip with its cytoplasmic side exposed. PMS were blocked with PBS supplemented with 1% BSA and then incubated in HBSS 0.1% BSA with 24 nM biotinylated annexin V. After washing, PMS were incubated with 5 µg/ml streptavidin, washed again, and incubated with indicated antigens as on the PLB.

2.8 Plasma membrane planar lipid bilayers (PMPLB) – Wing-Liu Lee

Suspension HEK293A cells were lysed in 5 mM $NaH_2PO_4/NaHPO_4$, pH 8 at 10 x 10^6 cells/ ml for 30 minutes on ice, and then homogenised using Dounce tissue-grinder pestle (Sigma). Nuclei were removed by centrifugation at 500 x g at 4°C for 10 minutes and plasma membranes were isolated by centrifugation at 20 000 x g at 4°C for 30 minutes. The membrane pellet was resuspended in a buffer containing 500 µM $NaH_2PO_4/NaHPO_4$, 100 µM $MgSO_4$, pH 8, on ice for 1 hour. Membrane vesicles were then purified by centrifugation at 100 000 x g at 4°C. The vesicle pellet was resuspended in the same buffer and used immediately. PMPLB were formed by fusing the vesicles onto glass coverslips. Antigen was attached via biotinylated annexin V and streptavidin and its density was quantified as on the PLB and PMS.

2.9 Imaging

All microscopy analysis and live-cell imaging was carried out on an Olympus IX81 microscope, with an Andor iXon EMCCD Camera and 100x objective (Olympus). Live-cell imaging was done at 37°C on a heated stage with an objective heater.

TIRF or epifluorescence timelapse images were acquired with time resolution of 2-5 seconds for 20 minutes, and corrected for photo-bleaching. The TIRF angle was setup as shallow as possible to extend the depth of field further away from the coverslip. All images were aligned, background-subtracted and corrected for spectral bleedthrough and photobleaching. Images were analysed using ImageJ and Matlab (Mathworks). All Matlab algorithms were written by Pavel Tolar.

Reconstructed images showing antigen internalisation from PMS, PLB and DCs were generated from z-stacks by first deconvoluting the stacks, and then using maximal projection of the middle of the cell along the y axis (PLB and PMS) or z axis (DCs).

2.10 Atomic force microscopy (AFM) force spectroscopy – Pavel Tolar

AFM was performed using a setup integrating AFM and optical imaging (JPK instruments). To carry out force spectroscopy with PMS, PLB, PMPLB and DCs, gold-coated Biolever cantilevers (nominal spring constant 6 mN/m, Olympus) were exposed to UV light for 30 minutes and then conjugated to DOTP (Pierce)-activated streptavidin. The cantilevers were then washed and used immediately. Spring constant was measured for each tip using the JPK software and varied between 5.2 and 6.0 mN/m. PMS, PLB, PMPLB and DCs, were loaded with antigens, washed, and attached to poly-L-lysine coated coverslips. AFM force spectroscopy was carried out on PMS, PLB or PM-PLB visualised using DiI or DiD (Invitrogen), and on the dorsal surfaces of the DCs' lamellopodia, visualised by brightfield imaging. Negligible binding was observed in samples lacking the biotinylated annexin V or antigen. Data were processed using the JPK analysis software.

2.11 Internalisation assays

2.11.1 Soluble antigen internalisation using flow cytometry

Internalisation of soluble antigens was measured using flow cytometry. Cells were incubated with biotinylated antigens for 30 minutes on ice, washed, and stimulated to internalise for indicated times at 37°C. Control cells were kept on ice. Then, cells were fixed with 2% paraformaldehyde (PFA, Alfa Aesar) and stained with 1 μg/ml of fluorescently labelled streptavidin (Jackson Immunoresearch) to visualise any antigen remaining on the cell surface. Antigen internalisation was calculated by subtracting the streptavidin fluorescence of the heated sample from the cold sample and dividing by the fluorescence of the cold sample. Data was analysed using FlowJo.

2.11.2 Soluble antigen internalisation using microscopy

To quantify internalisation of soluble NP/NIP antigens, B1-8 B cells were attached to poly-L-lysine-coated coverslips, incubated with NP/NIP antigens for 20 minutes, fixed with 2% PFA and stained with 1 μg/ml Cy3-labelled streptavidin (Jackson Immunoreserach). To determine the intensity of the internalised antigen in each cell, background from regions outside the cells was subtracted. Z-stack images of antigen and streptavidin on cells were processed through a 3D bandpass filter and thresholded to create 3D masks. The antigen mask was applied to the original antigen stack. Next, the streptavidin mask was used to exclude antigen present on the cell surface and therefore not internalised. The resulting antigen fluorescence was integrated. The percentage of internalisation was expressed as the intensity of internalised antigen minus the antigen colocalised with streptavidin divided by total antigen intensity. Data was analysed using Matlab.

2.11.3 Membrane-bound antigen internalisation

Internalisation from PMS, PMPLB and PLB was quantified from z-stack images, similarly as for the NP/NIP soluble antigens, but integrating antigen fluorescence only from image planes above the substrate. Specifically, background was subtracted using regions of interest outside of presenting membranes. Z-stack

images of antigen were processed through a 3D bandpass filter and thresholded to create a 3D mask. The antigen mask was applied to the original unfiltered antigen stack to include endosomal antigen and exclude scattered fluorescence background. Internalised antigen fluorescence was then calculated by integrating antigen fluorescence in the masked antigen images in stacks above the substrate. In experiments with primary cells, we found that all antigen above the substrate was inaccessible to cell-impermeable secondary 1 μg/ml fluorescently labelled streptavidin staining and was therefore considered internalised. In experiments with Ramos B cells, we found that some antigen above the substrate was accessible to this staining. Therefore, secondary streptavidin staining was used to exclude the streptavidin-colocalised antigen from the analysis as described for soluble antigens. The percentage of internalisation was expressed as the intensity of internalised antigen divided by total antigen intensity, which included the internalised antigen and the antigen left on the substrate underneath the cell. The percentage of internalised antigen colocalised with DiI-stained lipid, was expressed as the intensity of internalised antigen, minus antigen not colocalised with DiI, divided by total antigen intensity. Data was analysed using Matlab.

2.12 Fluorescence recovery after photobleaching (FRAP)

FRAP imaging was performed using TIRF microscopy at 37°C. Substrates were labelled with DiI or loaded with antigen, imaged for 10 seconds, and then a circular region of 13 μm in diameter was bleached at maximum laser power for 1 minute using the field diaphragm. Substrates were then imaged every 10 seconds for an additional 10 minutes. Fluorescence recovery was analysed using ImageJ by measuring fluorescently-labelled antigen or DiI intensity in the FRAP region throughout the experiment. The intensity in the FRAP region was normalised to fluorescence in a non-bleached control region.

2.13 3D particle localisation – Pavel Tolar

DiI-labelled PMS were loaded with Qdot-antigen. Imaging was performed in epifluorescence mode. 3D localisation of the Qdots was performed using a cylindrical lens (f = 1 m) inserted into the infinity space of the emission path (Huang et al., 2008). Gaussian fitting was used to extract the elipticity of the fluorescent spots. To convert the data to vertical distances, we acquired calibration images of Qdots attached to coverslips, while stepping up the microscope z-stage in 10 nm increments. Positional accuracy was estimated from timelapse images of stationary Qdots on coverslips and was ~40 nm. Vertical position of the Qdots in B cell synapses were expressed as their vertical distance from the mean position of Qdots present on the coverslip outside of synapses.

2.14 Analysis of membrane invaginations

Membrane invaginations were detected by staining the lipids in the PMS with DiI or DiD. The invaginations were equally detectable in epifluorescence illumination and in TIRF. For 3D particle localisation, the membrane dyes were excited in epifluorescence mode. For timelapse TIRF imaging, we used p-polarised laser, which produces evanescent field that is mostly vertically polarised and therefore preferentially excites DiI dyes in vertically oriented membranes (Sund et al., 1999).

Membrane invaginations were tracked in space and time from timelapse images of DiI or DiD stained PMS using previously developed tracking algorithms (Tolar et al., 2009b). Briefly, image sequences were aligned and normalised to the image of the PMS prior to cell spreading, and then processed using a bandpass filter. Fluorescent spots were tracked and their lifetime was calculated from the length of the tracks using Matlab.

Intensity of antigen associated with the invaginations was calculated as the mean intensity in 5 by 5 pixel regions centred on the track coordinates, including 1

frame before the start and 1 frame after the end of the track. Antigen intensities were normalised to the average antigen intensity on the PMS before cell spreading.

2.15 Protein knock-down using siRNA

2 x 10^6 Ramos cells, or 3 x 10^6 primary B cells stimulated with 1 μg/ml of CpG (Sigma) for 24 hours, were nucleofected (Amaxa Nucleofector II) with 3 μM siRNA oligonucleotides (oligos, Ambion) using the Amaxa Mouse B Cell Nucleofector Kit or the Amaxa Cell Line Nucleofector Kit V (Lonza), respectively. Following nucleofection primary B cells were cultured with 200 ng/ml BAFF (PeproTech). Efficiency of knock-down was assessed 96 hours after nucleofection by western blot or flow cytometry.

siRNA target	siRNA oligo ID	Catalog number
Negative control No.1	-	AM4635
GAPDH	-	4404025
CD19	S63587	4390815
Clathrin heavy chain	S475	4390825
AP2M1	S3114	4392421
Dynamin2	S4212	4390825

2.16 Western blot

Ramos or primary B cells were lysed with RIPA buffer containing 1% NP-40 (Sigma), 0.5% sodium deoxycholate (Sigma), 0.1% SDS (Sigma), protease inhibitor cocktail diluted 1:100 (Sigma) for 20 min on ice. Samples were then spun at 13 000 rpm 4°C, and proteins were separated using 10% SDS-PAGE (Invitrogen) in reducing conditions. Proteins were transferred to nitrocellulose membranes (Millipore), blocked in 5% milk in Tris Buffered Saline with 0.1% Tween20, and probed in the same buffer with primary antibodies against proteins of interest, followed by secondary antibodies conjugated to hydrogen peroxidase.

2.17 Lentiviral production and infection

Recombinant lentiviruses were produced by lipofectamine 2000 (Invitrogen)-mediated co-transfection of HEK293FT cells with the VSVg and δ8.9 helper plasmids, together with the TRC RNAi Consortium's shRNA-containing pLKO.1 plasmids (Sigma). Empty pLKO.1 was used as control. Lentivirus-containing media were harvested 72 hours following transfection and centrifuged with Ramos cells in the presence of 8 μg/ml polybrene (Sigma) for 90 minutes at 1350 x g. 24 hours after spinfection, infected cells were selected using 3 μg/ml puromycin.

shRNA Clones (Sigma)

Target	Clones
Dynmain2	TRCN0000006649
AP2M1	TRCN0000060238 TRCN0000060239 TRCN0000060241 TRCN0000060242
RHOA	TRCN0000047710 TRCN0000047708 TRCN0000047711 TRCN0000047712
ROCK1	TRCN0000002159 TRCN0000121092 TRCN0000121093 TRCN0000121094
HIP1R	TRCN0000117222 TRCN0000117223 TRCN0000117225 TRCN0000117226
ARH-GAP4	TRCN0000047189 TRCN0000047190 TRCN0000047191 TRCN0000047192
ARH-GAP15	TRCN0000047253 TRCN0000047254 TRCN0000047255 TRCN0000047256
ARH-GAP17	TRCN0000047448 TRCN0000047450 TRCN0000047451 TRCN0000047452
ARH-GAP26	TRCN0000029754 TRCN0000029755 TRCN0000029756 TRCN0000029758

ARH-GAP27	TRCN0000048354 TRCN0000048355 TRCN0000048356 TRCN0000048357
ARH-GAP30	TRCN0000149213 TRCN0000179792 TRCN0000183676 TRCN0000183499
ARH-GEF1	TRCN0000033564 TRCN0000033566 TRCN0000033567 TRCN0000033568
ARH-GEF2	TRCN0000003173 TRCN0000003174 TRCN0000003176 TRCN0000010764
ARH-GEF6	TRCN0000007400 TRCN0000007401 TRCN0000007403 TRCN0000007404
ARH-GEF18	TRCN0000047533 TRCN0000047535 TRCN0000047536 TRCN0000047537
MYL12B	TRCN0000053654 TRCN0000053655 TRCN0000053656 TRCN0000053657
MYL6	TRCN0000054138 TRCN0000054139 TRCN0000054140 TRCN0000054142
MYH9	TRCN0000029465 TRCN0000029466 TRCN0000029467 TRCN0000029468
MYO1E	TRCN0000152890 TRCN0000150353 TRCN0000151296 TRCN0000152421
MYO1C	TRCN0000122924 TRCN0000122926 TRCN0000122927 TRCN0000122928

2.18 Retroviral production and infection

Retrovirus was produced by lipofectamine 2000-mediated transfection of PLAT-E cells (Morita et al., 2000) with pMSCV containing one of the following constructs: clathrin light chain-GFP (Ehrlich et al., 2004), LifeAct (Riedl et al., 2008) (a gift from J. Burkhardt), or myosin IIA regulatory light chain (RLC) 12B (MYL12B)-

GFP (MYL12B was amplified and inserted into pMSCV with GFP, in our lab, by Bhakti Mistry). Primary Bl6 B cells, pre-stimulated with 1 µg/ml CpG (Sigma) for 24 hours, were spinfected with retrovirus-containing supernatants in the presence of 20 µg/ml polybrene for 90 minutes at 1350 x g. 24-48 hours after spinfection, infected cells were added to antigen-loaded PMS and imaged.

2.19 Analysis of clathrin light chain-GFP, myosin IIA RLC-GFP, and LifeAct activity

The intensity of myosin IIA RLC-GFP or LifeAct associated with the invaginations was calculated as the mean intensity in 5 by 5 pixel regions centred on the track coordinates, including 3 frames before the start and 1 to 2 frames after the end of the track. Myosin IIA RLC-GFP and LifeAct intensities were normalised to the average intensity in the synapse in the same frame.

To calculate the colocalisation of invaginations with CCSs, the positions of CCSs were tracked and colocalisation for each time point in each invagination lifetime was considered positive if there was a CCS within 2 pixels of the invagination coordinates. Control colocalisation in each cell was performed using CCSs shifted by 5 pixels in a random direction, maintaining boundary conditions within in the cell.

2.20 B cell phenotyping of $Cre^{+}MyH9^{fl/fl}$ mice – in collaboration with Harold Hartweger

B cells were flushed from the femur and tibia of rear left leg using 10 ml of DMEM and 2% FBS. B cells were removed from the peritoneal cavity by injecting 5 ml of PMS supplemented with 5 mM ethylenediaminetetraacetic acid, massaging the abdomen, and removing the fluid. B cells from the spleen and lymph nodes were mashed through a 70 µm strainer. All cells were washed in DMEM 2% FBS and then red blood cells were lysed using ACK buffer. The remaining cells were washed again, and stained for the cell surface

markers described in Chapter 5 Table 1 for 20 minutes on ice in PBS. Absolute cell numbers were ascertained using FlowJo. Alive cells were identified as negative for the Live/Dead stain (Invitrogen).

Chapter 3 Plasma membrane sheets are a new artificial substrate that can mimic antigen-presenting cells when studying BCR-antigen internalisation

3.1 Introduction

B cells are exposed to antigen primarily in the secondary lymphoid organs. B cells can respond to antigen in solution following antigen filtration into the B cell follicles (Pape et al., 2007; Roozendaal et al., 2009), but the majority of antigen encountered by B cells *in vivo* will be retained on the surface of an APC (Batista and Harwood, 2009; Cyster, 2010).

Intravital imaging has captured the interaction of B cells with antigen-loaded APCs in the lymph node throughout the immune response (Phan et al., 2007; Qi et al., 2006; Schwickert et al., 2007; Suzuki et al., 2009) and both *in vivo* and *in vitro* studies have confirmed that antigen acquisition from these APCs is a prerequisite to B cell activation, differentiation and antibody production (Batista et al., 2001; Carrasco and Batista, 2007; Chappell et al., 2012; Junt et al., 2007; Moseman et al., 2012; Phan et al., 2007; Qi et al., 2006; Schwickert et al., 2007; Suzuki et al., 2009; Wang et al., 2011).

To delineate the molecular mechanisms involved in B cell recognition of membrane-bound antigen, PLB have been used *in vitro* as a surrogate for APCs. Live-cell TIRF images of B cells interacting with antigen-loaded PLB has revealed that B cells initially spread over the antigen-presenting surface collecting BCR-antigen microclusters, and then contract to bring them into the centre of the synapse (Depoil et al., 2007; Fleire et al., 2006). This process has been shown to be dependent on the structure of the BCR (Tolar et al., 2009b), BCR and CD19 signalling (Depoil et al., 2007; Schnyder et al., 2011; Weber et al., 2008), the actin cytoskeleton (Liu et al., 2012; Mattila et al., 2013; Treanor et al., 2011), and also on the affinity, multivalency, and concentration of the antigen (Fleire et al.,

2006; Tolar et al., 2009b). However the mechanisms and components required for the subsequent antigen acquisition and internalisation are still unknown.

Here we aimed to develop an antigen-presenting substrate, which can support B cell internalisation of membrane-bound antigen *in vitro*. We hoped that visualisation of this process using TIRF microscopy would allow us to investigate the dynamics of BCR-antigen internalisation, and support the use of a membrane-surrogate in future investigations into the molecular components governing this process.

3.2 Results

3.2.1 B cells are unable to internalise antigen tethered to planar lipid bilayers

To visualise internalisation of membrane-bound antigen by B cells, we initially used PLB as a surrogate for APCs. PLB were formed following the fusion of unilamellar vesicles on glass coverslips. We attached NIP-Qdot antigen to biotin-containing lipids within the PLB using a streptavidin linker (Figure 6A). To the antigen-loaded PLB we then added primary splenic B1-8 B cells that express a BCR specific for the NIP hapten (Sonoda et al., 1997). Live cell imaging using TIRF microscopy showed B1-8 B cell spreading over the antigen-loaded PLB and the production of antigen microclusters, which was followed by contraction of the B1-8 B cells pulling the antigen into the centre of the synapse (Figure 6B, Movie 1). Loss of fluorescence from the TIRF field would be indicative of internalisation, since movement of antigen up into the B1-8 B cell would remove it from the evanescent field exciting the Qdots. However, no loss of antigen fluorescence from the synapse was seen during the imaging, suggesting the B1-8 B cells were arrested at the point of synapse formation and internalisation didn't take place. This was confirmed using epifluorescent z-stack images taken every 300 nm throughout the B1-8 B cell interacting with PLB. Side view reconstruction of these images showed that antigen is not extracted from the PLB by the B cell, but is retained in the synapse (Figure 6C).

The incapability of B1-8 B cells to internalise antigen wasn't due to the type of B cells chosen, or the antigen produced, as Ramos B cells were also unable to extract antigen from the PLB (Figure 6C), and flow cytometry showed B1-8 B cells were able to internalise the NIP-Qdot antigen from solution (Figure 6D). In an attempt to optimise this system we increased the affinity between the BCR and antigen by using MuMT-MD4 B cells, which have a BCR with over 1000 times higher affinity for HEL antigen than the B1-8 BCR has for NIP ($K_A \sim 5 \times 10^{10}$ M^{-1} versus 3×10^6 M^{-1}) (Carrasco and Batista, 2006a; Natkanski et al., 2013). We also decreased the strength of the interaction between the antigen and lipid bilayer by conjugating peptides containing a six histidine tag to the NIP-Qdots and anchoring the Qdots to the PLB via nickel salt-containing lipid, instead of using biotinylated lipids and streptavidin (Reznik et al., 1998). However, in both circumstances the same phenotype was seen as in Figure 6B and C.

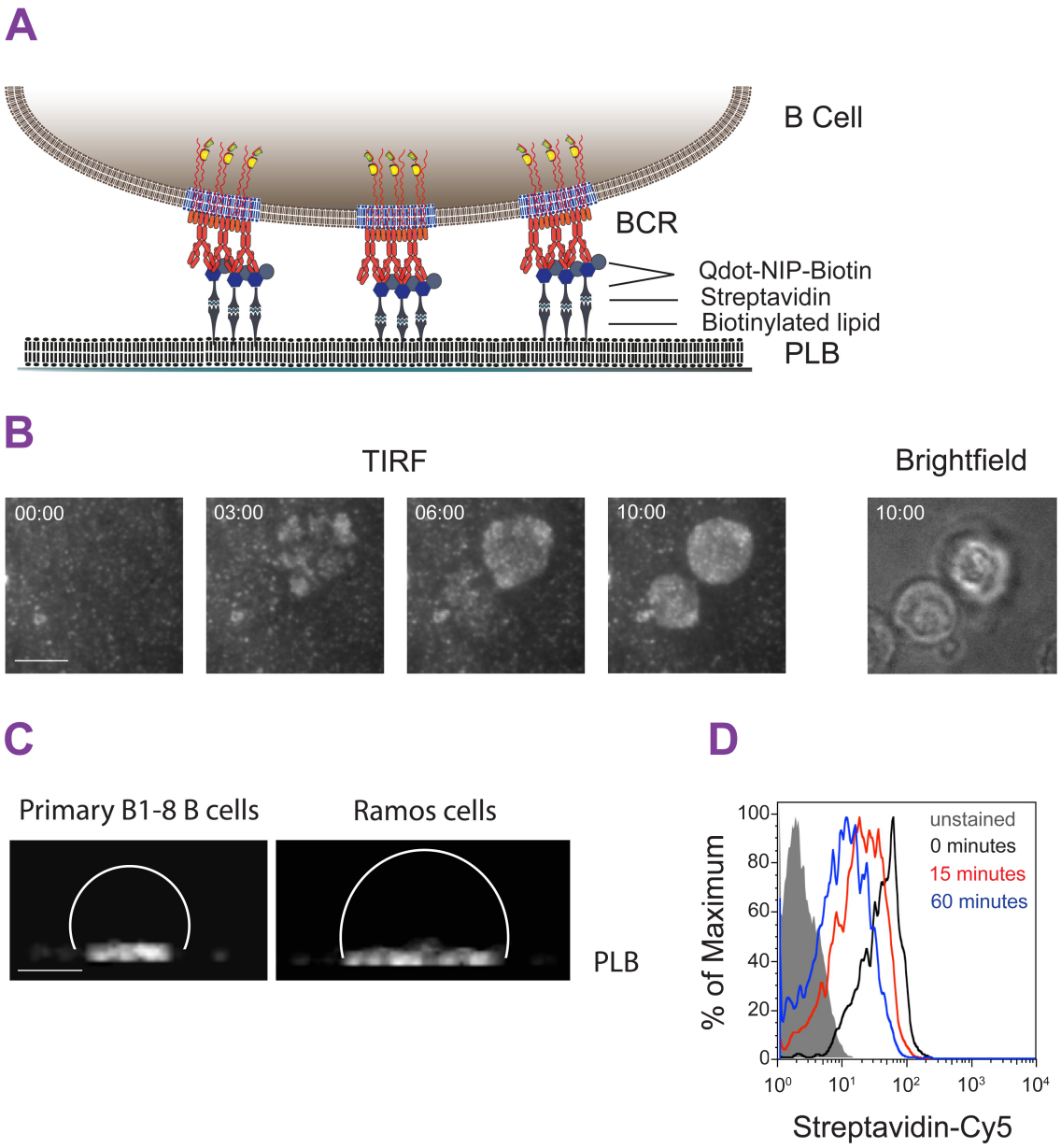

Figure 6: B cells cannot internalise antigen when presented on PLB

A) Diagram of PLB. PLB were formed following the rupture of unilamellar vesicles on glass coverslips. NIP-Qdots were attached to biotinylated lipids using a streptavidin linker

B) TIRF timelapse images showing microcluster and synapse formation between B1-8 B cells and PLB loaded with antigen (NIP-Qdot) (white). Timelapse was done at 37°C. B1-8 B cells were unlabelled. Brightfield image shows the position of B1-8 B cells. Elapsed time following the addition of B1-8 B cells to the PMS is shown in minutes and seconds. Scale bar = 5 μm

C) Side view reconstruction from epifluorescent z-stack images showing synapse formation between NIP-Qdot antigen and B1-8 B cells (left) or αIgM-Qdot antigen and Ramos cells (right). B cells were incubated for 20 minutes at 37°C with antigen-loaded PLB and then fixed before images were taken. White outline shows B cell orientation. Outline was derived from brightfield images. Scale bar = 5 μm

D) Flow cytometry plot showing decreasing surface streptavidin-Cy5 fluorescence as an indication of antigen (NIP-Qdot) internalisation. B1-8 B cells were incubated with antigen on ice for 30 minutes and then the unbound antigen was washed off. B1-8 B cells were then incubated at 37°C for the indicated time points to stimulate antigen internalisation. Following this, B1-8 B cells were fixed and stained with streptavidin-Cy5 to highlight any antigen remaining on the cell surface

3.2.2 B cells are able to internalise antigen from plasma membrane sheets

To visualise internalisation of membrane-bound antigen by B cells, we developed a new surrogate for APCs from the plasma membranes of adherent cells. These plasma membrane sheets (PMS) were formed following the sonication of HEK293A cells, which had been cultured on glass coverslips and then sonicated leaving only the adherent membrane. We anchored antigen, specific for the light chain of the BCR from Bl6 mice (αIgκ), to phosphotidylserine in the exposed inner leaflet of the PMS using an annexin-biotin-streptavidin linkage (Figure 7A). Scanning atomic force microscopy (AFM) revealed that the PMS was suspended approximately 10 nm above the coverslip consistent with the presence of transmembrane proteins or membrane ruffling holding up the PMS (Figure 7B). TIRF images of Bl6 B cells interacting with the antigen-loaded PMS showed B cell spreading and contraction leading to synapse formation as with the PLB (Figure 6B, 7C and Movie 2). However, in contrast to the PLB, the fluorescent antigen signal rapidly disappeared from the TIRF plane indicating internalisation of antigen from PMS (Figure 7C, Movie 2).

A

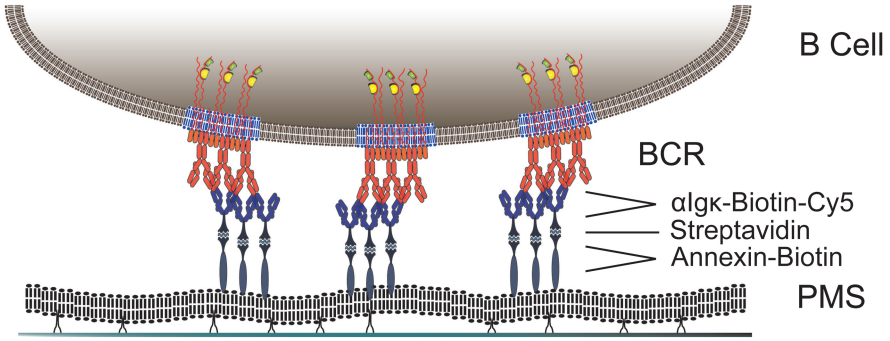
B Cell
BCR
αIgκ-Biotin-Cy5
Streptavidin
Annexin-Biotin
PMS

B

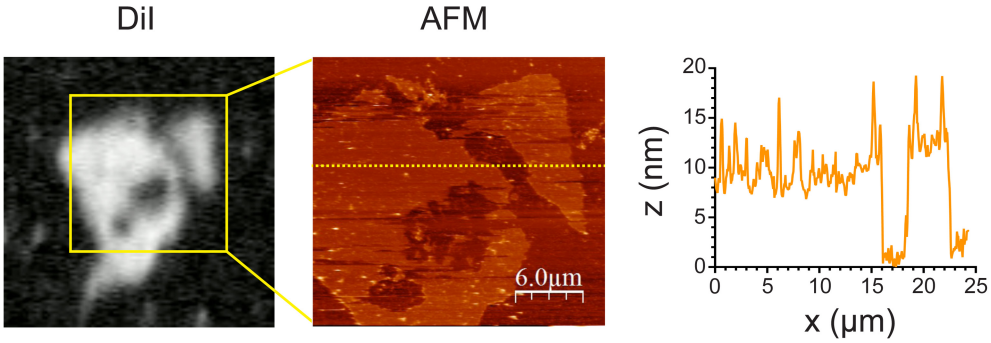
DiI
AFM
6.0μm
z (nm)
x (μm)
0
5
10
15
20
25

C

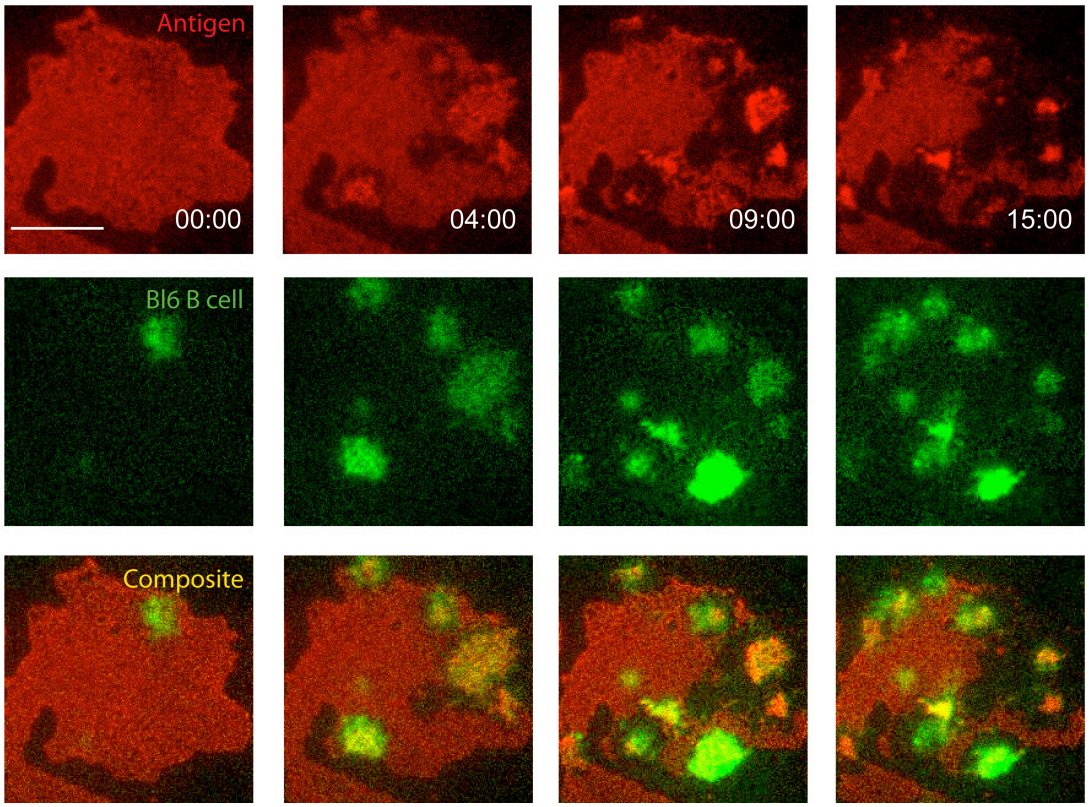
Antigen
00:00
04:00
09:00
15:00
Bl6 B cell
Composite

Figure 7: Bl6 B cells can internalise antigen presented by PMS

A) Diagram of PMS. PMS were formed following sonication of adherent HEK293A cells cultured on glass coverslips. Antigen (αIgκ) was attached to the exposed phosphatidylserine in the inner leaflet of the remaining HEK293A plasma membrane using an annexin-biotin-streptavidin linker

B) Scanning AFM of PMS. Left, fluorescent image of PMS. PMS lipids were labelled with the hydrophobic carbocyanine dye, DiI. Middle, the area shown by the yellow rectangle scanned by AFM. Different colour intensities indicate different heights of the PMS above the coverslip. Right, vertical profile of the dotted line indicated in AFM scan. Experiment done by Pavel Tolar

C) TIRF timelapse images showing microcluster and synapse formation between Bl6 B cells and antigen (αIgκ)-loaded PMS. The BCRs on Bl6 B cells were stained with αIgM Fab for 5 minutes before addition to the imaging chamber. Timelapse was done at 37°C. Disappearance of antigen from the TIRF view indicates internalisation. Elapsed time following the addition of Bl6 B cells to the imaging chamber is shown in minutes and seconds. Scale bar = 10 μm

Antigen internalisation was confirmed by side view reconstructions of epifluorescent z-stack images taken throughout the Bl6 B cell following interaction with antigen-loaded PMS or PLB. These images demonstrated the presence of antigen inside the Bl6 B cells when incubated with PMS but not with PLB (Figure 8A and B). The difference in internalisation from the different substrates was not due to the additional components found in the PMS, as PLB produced from the plasma membranes of HEK293A cells (PMPLB) did not support internalisation either (Figure 8B).

To visualise the fate of membranes in the different substrates during BCR-antigen internalisation, we labelled the lipids in the PMS and PLB using the hydrophobic carbocyanine dye, DiI. This revealed that during antigen internalisation, Bl6 B cells also internalised portions of the antigen-presenting membrane (Figure 8A and C). Imaging of B1-8 B cells acquiring NIP-antigens along with portions of the cell membrane from matured DCs suggested this process is likely to also happen during antigen acquisition from APCs *in vivo* (Figure 8C and D).

In addition, fluorescence recovery after photobleaching (FRAP) experiments confirmed there was no qualitative difference in the fluidity of the lipids or diffusion of the antigen in any of the substrates. The lipid was stained with DiI,

and was seen to be mobile in all substrates shown by the recovery of lipid fluorescence to the bleached spot (Figure 9A), whereas the antigen was seen to be immobile in all substrates (Figure 9B). The immobility of the antigen is likely due to the multivalent nature of the biotin-streptavidin linkage and the oligomerisation of annexin anchoring the antigen to the substrate.

Collectively these studies support the use of PMS instead of PLB as a surrogate for APCs when studying BCR-antigen internalisation. We show that B cells internalise antigen with portions of the presenting membrane from PMS and APCs but not from PLB, and this difference is not due to the composition of the PMS or due to its fluidity.

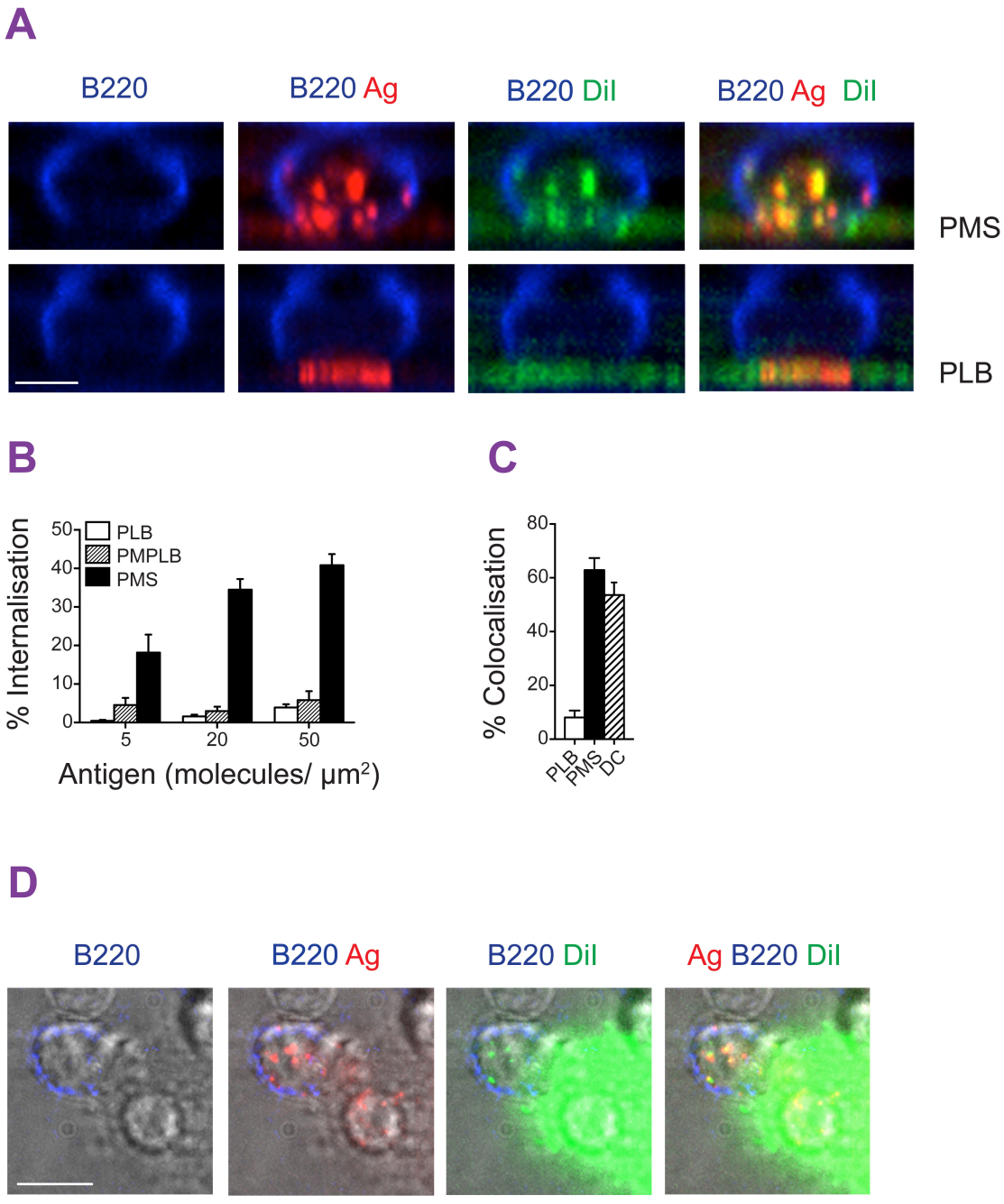

Figure 8: Primary B cells internalise antigen with portions of the presenting membrane from PMS and DC, but not from PLB

A) Side view reconstruction from epifluorescent images of synapses between Bl6 B cells and PMS or PLB loaded with antigen (αIgκ) (Ag) as shown in Figure 7A. Lipids in the different substrates were stained with DiI. Bl6 B cells were incubated with the indicated substrates for 20 minutes at 37°C and then fixed before z-stack images were taken. Bl6 B cell surface was stained after fixing using αB220-FITC. Scale bar = 2 µm

B) Image quantification of Bl6 B cell internalisation of antigen from PLB, PMS or PMPLB (means±SEM, n=23-60 cells). Membrane vesicles used to produce PMPLB were isolated and purified by Wing-Liu Lee

C) Image quantification of colocalisation of antigen with DiI-labelled lipid in primary B cells after internalisation from the substrates (Means±SEM, n=12-21 cells)

D) Epifluorescent image of a B1-8 B cell interacting with a DC loaded with NIP antigen (Ag). The plasma membrane of the DC was labelled with DiI. B1-8 B cells were incubated with the DCs for 20 minutes at 37°C and then fixed before images were taken. B1-8 B cell surface was labelled after fixing with αB220-FITC. Scale bar = 5 μm

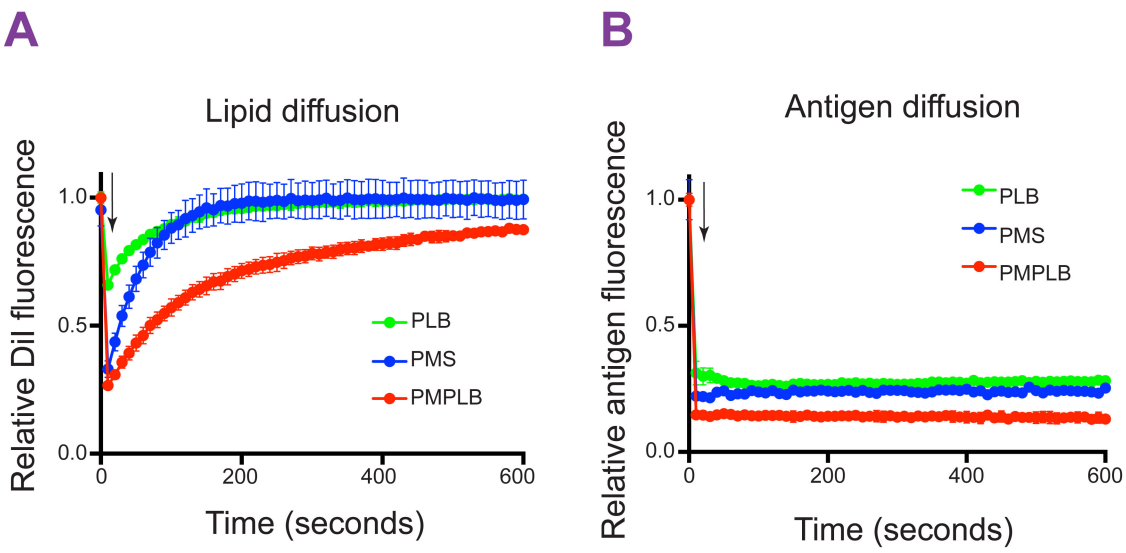

Figure 9: PMS are similar in their fluidity compared to PLB and PMPLB as shown by FRAP

A) Lipids of the substrates were stained with DiI and then bleached for 1 minute. Arrow shows point of bleaching. Recovery of DiI fluorescence to the bleached spot was measured for 10 minutes at 37°C

B) Antigen (αIgκ) was loaded onto substrates and then bleached for 1 minute. Arrow shows point of bleaching. Recovery of antigen fluorescence to the bleached spot was measured for 10 minutes at 37°C

Membrane vesicles used to produce PMPLB were isolated and purified by Wing-Liu Lee

3.2.3 Plasma membrane sheets are similar in their viscoelastic properties to antigen-presenting cells

Since we have shown that B cells can internalise antigen from PMS but not PLB, we wondered whether the 10 nm gap between the lipids of the PMS and coverslip allowed the substrate to be more flexible, and whether lack of this space, and therefore flexibility, was the reason B cells couldn't internalise antigen

from PLB. To test this hypothesis we used AFM force spectroscopy. We labelled the cantiliever tip with streptavidin and lowered it onto the surface of the antigen-loaded PMS, PLB, PMPLB, or live DCs, and then retracted it. During tip retraction, the forces between the tip and substrate were measured until the bond ruptured. In this setting, these measurements can indicate the elasticity and flexibility of the substrates. For example, the forces during tip retraction on PLB and PMPLB increased rapidly to 30-40 pN and produced single-step bond ruptures just a few nanometers from the surface of the substrate (Figure 10A left hand panels and B). The requirement for large forces to pull the PLB up and away from the coverslip, and the fact that following generation of these forces the PLB snapped quickly back down onto the coverslip, indicates a high level of stiffness. However, on both PMS and DCs, forces only increased to 20 pN and then plateaued with the bonds between the tip and substrate rupturing hundreds of nanometers away from the substrate's surface (Figure 10A right hand panels and B). These force profiles show that less force is needed to pull the PMS or DC membrane further away from the coverslip compared with the PLB, and suggest PMS and DCs have a much higher level of elasticity and flexibility. Therefore these results show that PMS are similar in their viscoelastic properties as APCs, and support the hypothesis that B cells require this flexibility in order to internalise antigens.

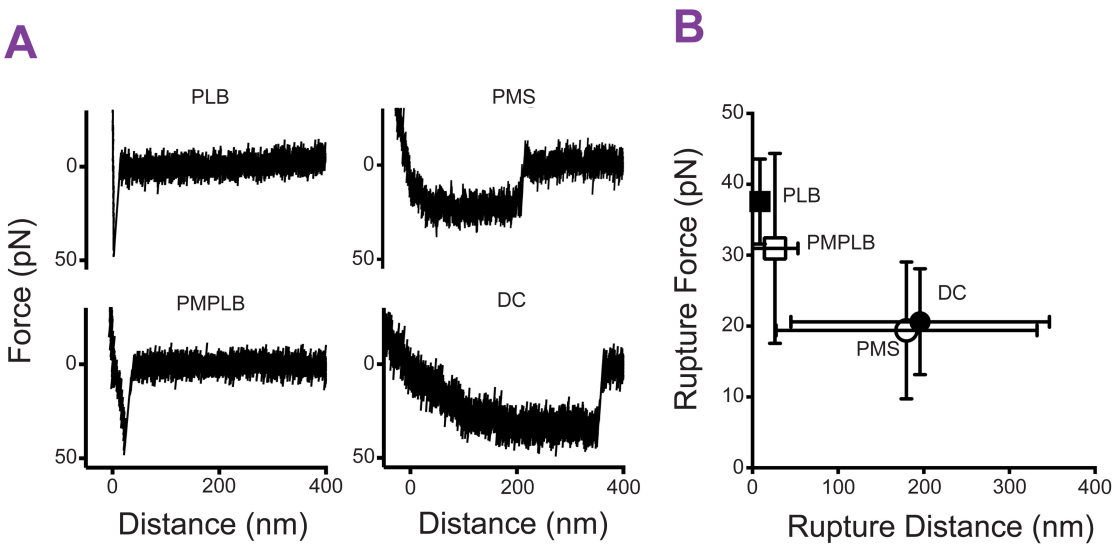

Figure 10: PMS are flexible and similar in their viscoelastic properties to APCs

A) AFM force retraction curves. Curves show the force generated between the streptavidin-coated AFM tip and antigens, during tip retraction. Antigens were αIgκ for PLB, PMPLB and PMS, and NIP for DCs. Speed of retraction was 0.1 μm/second

B) AFM average retraction curves. Data points show the force generated by cantilever retraction from the substrates and the subsequent distance the substrate was pulled up and away from the coverslip until bond rupture (Means±SD, n=31-109 retraction curves).

Experiment done by Pavel Tolar. Membrane vesicles used to produce PMPLB were isolated and purified by Wing-Liu Lee

3.2.4 B cells pull on and invaginate the presenting membrane during antigen internalisation

To visualise the effect of antigen internalisation on the presenting membrane, we imaged the PMS labelled with DiI during B cell antigen extraction. TIRF timelapses of live Bl6 B cells showed that a few seconds after B cell spreading, numerous spots of increased DiI fluorescence appeared in the synapse. Tracking of these lipid spots showed they continued to appear and disappear dynamically during B cell interaction with the antigen-loaded PMS (Figure 11A). The majority of them lasted only 5 seconds, however some lasted over 30 seconds (Figure 11B). These spots of increased DiI fluorescence happened at sites of BCR-antigen internalisation at both the synapse level (Figure 11C and Movie 3) and at the level of the individual antigen microcluster (Figure 11D).

To assess whether the spots of increased DiI-labelled lipid were indeed associated with the upward movement of antigen, we used high-resolution 3D colocalisation of antigen and DiI spots. In this set of experiments lipid was stained with DiI, and the majority of antigen had no fluorescent label apart from a small percentage labelled with Qdots to allow single particle imaging. Insertion of a cylindrical lens into the optical path of the microscope allowed us to determine the vertical position of the Qdot by the change in its shape. For example, when the antigen-Qdot was tethered to the PMS and in focus, it was round. However, when the antigen-Qdot moved upwards away from the PMS, i.e. during internalisation, the round image was distorted into an ellipse (Figure 12A). Through calibration using vertical steps of the microscope stage, the change in shape could be converted to a vertical position. We observed that the brightness

of the DiI spots correlated with the upward movement of antigen-Qdots (Figure 12B). Therefore, these studies demonstrated that the increase in DiI fluorescence in the B cell synapse was due to the B cell pulling up and invaginating the PMS during antigen internalisation.

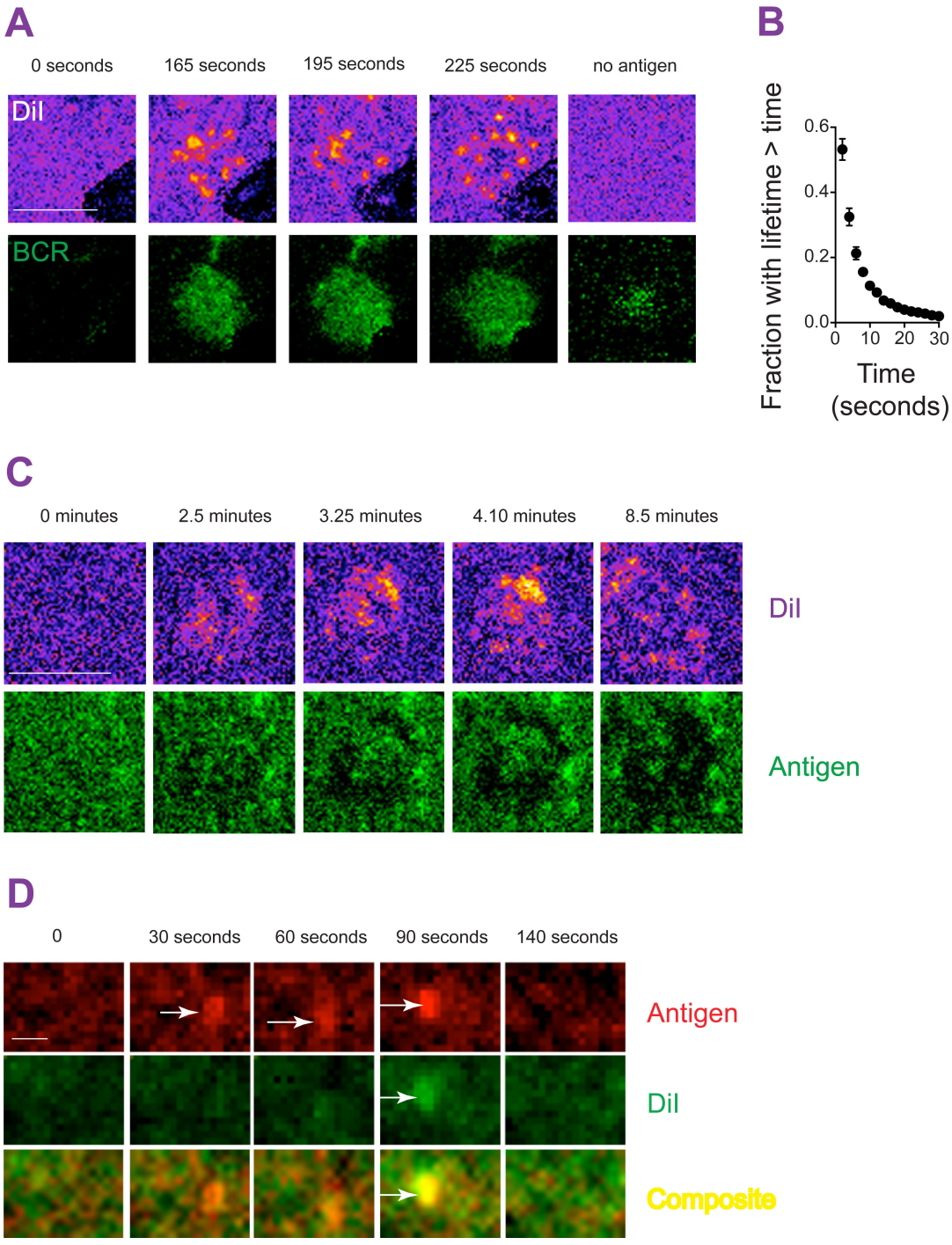

Figure 11: Bl6 B cells pull on and invaginate the PMS during antigen internalisation

A) TIRF timelapse images showing dynamic changes in DiI fluorescence (firescale, top panels) during Bl6 B cell interaction with antigen (αIgκ, no fluorescent label)-loaded PMS. The BCRs on Bl6 B cells were stained with αIgM Fab (green, bottom panels) for 5 minutes before addition to the imaging chamber. Timelapse was done at 37°C. Far right panels show no Bl6 B cell interaction with the PMS when antigen is absent. Scale bar = 5 μm

B) Proportions of DiI-labelled invaginations of different lifetimes produced during Bl6 B cell interaction with antigen (αIgκ, no fluorescent label)-loaded PMS. Data was derived from tracked invaginations in 20 minute TIRF timelapses at 37°C (mean±SEM, n=7 cells)

C) TIRF timelapse images showing dynamic changes in DiI fluorescence (firescale, top panels) during Bl6 B cell interaction with antigen (αIgκ)-loaded PMS (green, bottom panels). Timelapse was done at 37°C. B cells were unlabelled. Scale bar = 5 μm

D) TIRF timelapse images of a single antigen microcluster and corresponding spot of increased DiI fluorescence during Bl6 B cell interaction with antigen (αIgκ)-loaded PMS. Timelapse was done at 37°C. Scale bar = 100 nm

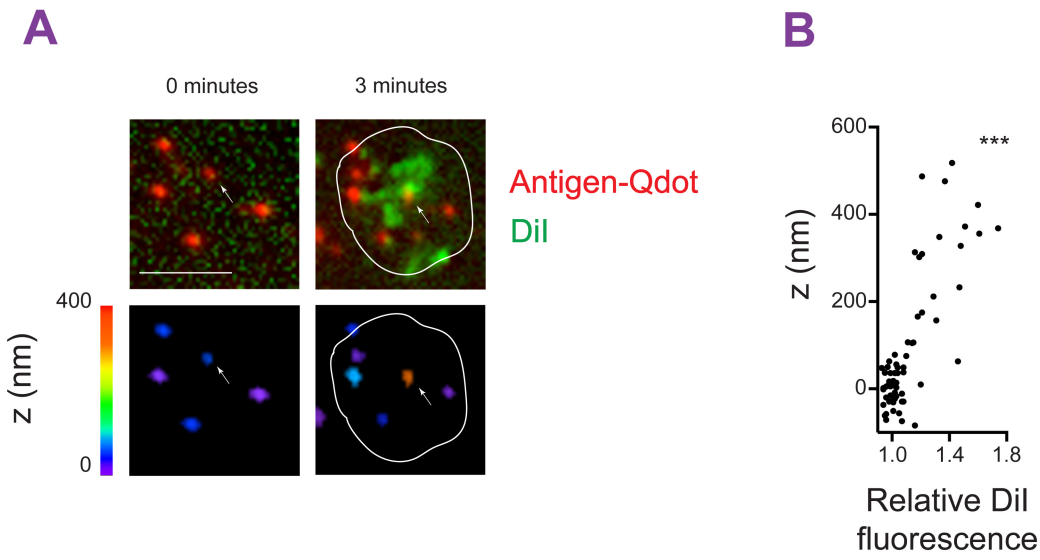

Figure 12: Increased spots of DiI fluorescence are associated with the upward movement of antigen during antigen internalisation

A) High-resolution 3D localisation of antigen-Qdots (αIgκ) in Bl6 B cell synapses. Lipids were labelled with DiI. Epifluorescent images were taken before (top, left) and after (top, right) Bl6 B cell spreading. A cylindrical lense inserted into the optical path of the microscope, caused distortion of the Qdot image seen when moved above the PMS (round to elipse in shape) i.e. when it is being internalised by the Bl6 B cell. Bottom panels show the antigen-Qdots colour-coded for their shape. Arrow shows a Qdot which has changed its shape after addition of Bl6 B cells

B) Vertical position of antigen-Qdots plotted against the colocalised DiI fluorescence following Bl6 B cell spreading (n=10 cells) ***,p<0.001 for Pearson correlation test.
Experiment done by Pavel Tolar

3.2.5 Antigen internalisation occurs only at sites of long-lived invagination formation

Characterisation studies of individual invaginations revealed that short-lived invaginations colocalised with background levels of antigen and terminated abruptly suggesting physical rupture (Figure 13A, left hand panel). However, long-lived invaginations started at points of high antigen fluorescence, indicative of an antigen microcluster, and both fluorescent traces disappeared from the TIRF field together, suggesting internalisation (Figure 13A, right hand panel). By grouping the invaginations by their lifetimes, we saw that the level of antigen fluorescence at the start of the invagination, corresponded to the subsequent invagination lifetime. We also confirmed that there was a significant drop of antigen fluorescence at the end of all invaginations lasting over 20 seconds, which was not seen with short-lived invaginations (Figure 13B).

These results show that B cells pulled on and invaginated the presenting membrane during BCR-antigen internalisation. The sites of invagination contained variable amounts of antigen, but only those with a lifetime longer than 20 seconds ended with productive internalisation, and the lifetime of the invaginations, depended on prior formation of antigen microclusters.

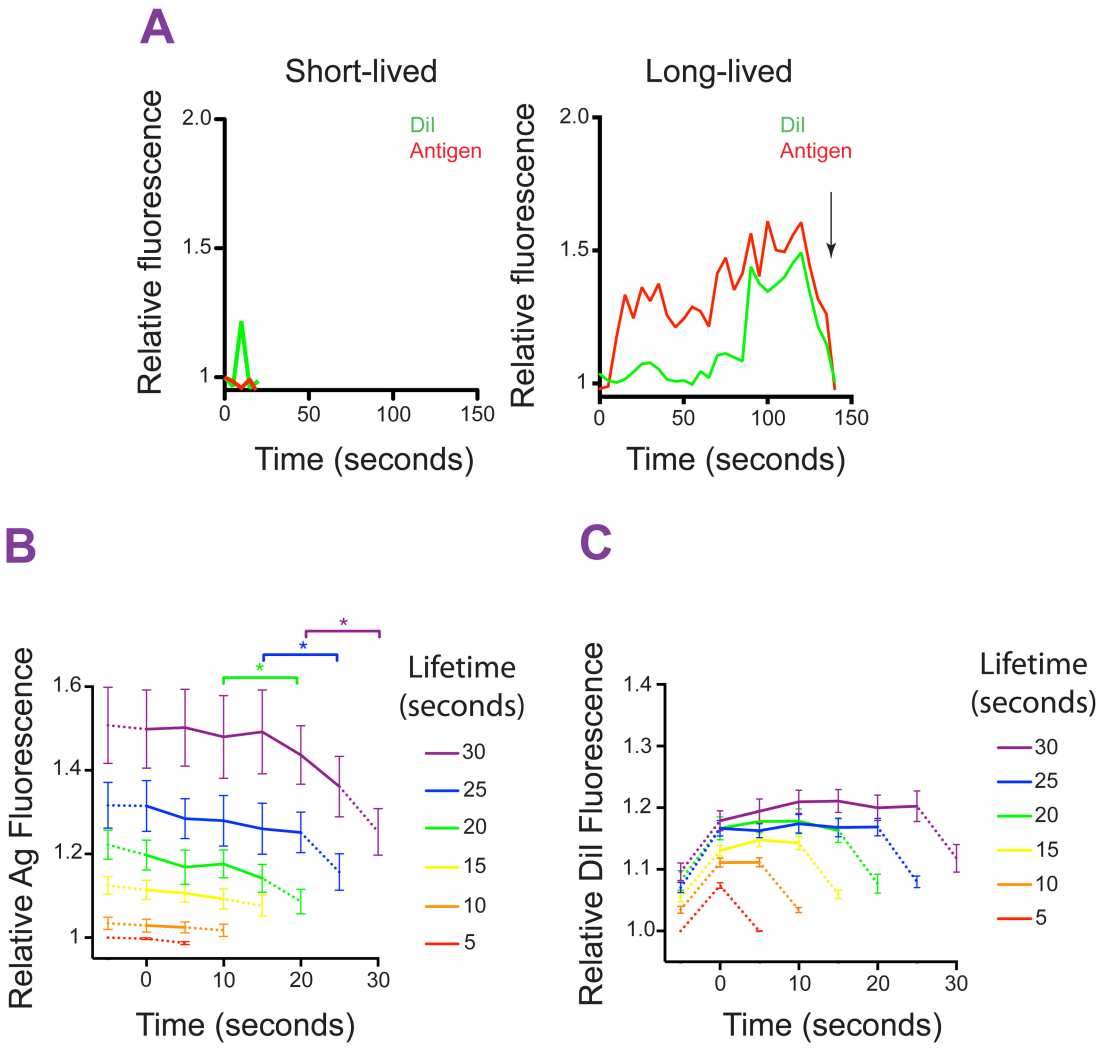

Figure 13: Invaginations produced by Bl6 B cells are dynamic and have varying lifetimes. Long-lived invaginations begin at sites of antigen microclustering and lead to antigen internalisation

A) Antigen (αIgκ) and DiI fluorescence in a single short-lived invagination (left) or a long-lived invagination (right). Arrow indicates internalisation

B) Antigen (αIgκ) (Ag) fluorescence associated with tracked DiI-labelled invaginations grouped by their lifetime. Data was derived from 20 minute TIRF timelapses of Bl6 B cells interacting with antigen-loaded PMS at 37°C. The associated antigen fluorescence was analysed 5 seconds before (dotted lines), during the lifetime (solid lines), and 5 seconds after the disappearance of the invagination (dotted lines) (mean±SEM, n=10 cells). *, $P<0.01$ in paired t-tests between the penultimate time point of the invagination, and the time point 5 seconds after invagination disappearance. Matlab analysis was done by Pavel Tolar

C) DiI fluorescence in tracked invaginations of the indicated lifetimes from the same dataset as in B). Matlab analysis done by Pavel Tolar

3.3 Discussion

We initially attempted to study BCR internalisation of membrane-bound antigen using PLB as surrogates for APCs. Our observations of the interaction between B cells and antigen-loaded PLB match the synapse formation previously reported (Fleire et al., 2006). However, we observed that B cells were inhibited in their ability to internalise antigen from these synapses, therefore, we developed a new antigen-presenting substrate using immobilised plasma membranes from adherent cells.

PLB are very flat surfaces (Attwood et al., 2013; Sackmann, 1996), which have made them ideal substrates for high-resolution TIRF microscopy of the initial molecular events involved in BCR recognition of membrane-bound antigen. In order to expand these studies we originally intended to use these same techniques to study the next step in the B cell activation process: BCR-antigen internalisation. However, the inability of B cells to internalise antigen from PLB was shown both by the formation of stable synapses and absence of antigen detected in the B cells following synapse formation.

We initially thought this was because the biotin-streptavidin-biotin linkage was anchoring the antigen too strongly to the PLB. In an attempt to overcome this limitation, we then used B cells from MuMT-MD4 mice, which have a very high affinity for the HEL antigen, but we still did not observe any internalisation. This experimental set up has been used in previous studies, which reported successful antigen internalisation and presentation by B cells through activation of co-cultured cognate T cell hybridomas (Fleire et al., 2006). The internalisation of antigen described in these studies could be due to the release of small amounts of antigen from the PLB during the long incubation times with B cells and cognate T cells, before assessing T cell activation. If small amounts of antigen were released by the PLB, and internalised and presented by B cells, it is possible that this was enough to activate antigen-specific T cell hybridomas, which are very sensitive to peptide-MHC Class II molecules. This internalisation could also be explained by other recent studies showing that when B cells come

into contact with immobilised antigen, they secrete lysosomes releasing hydrolases and acidifying the synapse, which causes antigen liberation from the presenting surface and facilities internalisation (Yuseff et al., 2011). As PLB completely cover the surface of the coverslip with only a 1 nm space between the bilayer and the glass (Sackmann, 1996), we hypothesised that this surface could be very inflexible and so this release of lysosomes may occur as a consequence of B cells being unable to generate big enough forces to extract the antigen. Therefore, we set out to develop a new more flexible antigen-presenting surface.

Here we show the development of PMS, a new APC surrogate for microscopy studies into B cell antigen acquisition from antigen-presenting surfaces. PMS have been recently used to investigate the formation of clathrin coated pits after reconstitution with cytoplasmic components (Wu et al., 2010). The observed production of endocytic vesicles in these studies indicated a level of flexibility within the PMS, and as predicted, following antigen tethering, B cells were able to internalise antigen from this substrate.

We used AFM force spectroscopy to assess the differences in flexibility between the PLB and PMS, and compared them to the viscoelastic properties of APCs. These studies demonstrated B cells would need to overcome forces of 20 pN to extract antigens from the PMS or DCs, which supports the values required to pull out nanotubes from plasma membranes previously reported (Krieg et al., 2008). However, in order to extract antigen from PLB the B cells would need to generate forces over 40 pN. This supports our hypothesis that PLB are inflexible substrates and suggests that the antigen-presenting surface needs to have a certain level of flexibility to reduce the force required by B cells to facilitate BCR-antigen internalisation.

Scanning AFM revealed that PMS were suspended approximately 10 nm above the coverslip. This 10 nm space is consistent with the presence of transmembrane proteins or ruffling of the adherent cell membranes, which are the source of PMS, and could account for the increased flexibility seen when comparing PMS with PLB. This is also the only primary difference between the

PMS and PMPLB further supporting flexibility in the antigen-presenting surface as an essential factor in antigen internalisation.

To visualise any changes in the topology of the presenting membrane during BCR-antigen internalisation, we used the hydrophobic carbocyanine dye, DiI, which incorporates into the lipid bilayer and acts as a reporter for changes in membrane shape (Sund et al., 1999). TIRF studies showed B cells actively pulled on and invaginated the PMS during BCR-antigen internalisation. The number of invaginations was more frequent and dynamic compared to detectable antigen microclusters, with only long-lived invaginations resulting in internalisation. The high number of non-productive short-lived invaginations suggests a mechanism whereby B cells continually screen the antigen-presenting surface, and only when they bind to pre-formed microclusters and overcome a force of 20pN, can they produce a long-lived invagination and internalise the antigen. This could explain how B cells acquire APC membrane proteins during BCR-antigen internalisation *in vivo* (Suzuki et al., 2009).

PMS do not fully resemble APCs as they lack any adhesion and co-stimulatory molecules found on APCs *in vivo*, which could further regulate BCR-antigen internalisation (Carrasco and Batista, 2006a; Carrasco et al., 2004; Suzuki et al., 2009), however, they do resemble APCs in their viscoelastic properties and are closer in their membrane structure than the historically used PLB. In addition, the use of PMS has allowed us to visualise antigen internalisation previously unseen at the molecular level.

Therefore, although, in the future it will be important to continually optimise this technique to more closely resemble APCs, or use APCs themselves, to confirm the findings shown here, the PMS can be considered a reasonable surrogate for APCs, and used for the identification of molecular components and mechanisms involved in BCR-antigen internalisation.

Chapter 4 B cells use myosin IIA contractility combined with clathrin-mediated endocytosis to internalise membrane-bound antigen

4.1 Introduction

Antigen binding stimulates BCR-antigen internalisation from either a cap of BCR-antigen complexes in response to soluble antigen, (Ma et al., 2001; Salisbury, 1980) or from a synapse when encountered with an antigen tethered to an APC (Batista et al., 2001).

The process of BCR-antigen internalisation is thought to begin with BCR-antigen microclustering and translocation to lipid rafts (Cheng et al., 1999; Sohn, 2006; Sohn et al., 2008; Tolar et al., 2005). Once associated with the lipid rafts BCRs are exposed to the Src family tyrosine kinase Lyn (Cheng et al., 1999; 2001) and a BCR signalling cascade is initiated resulting in BCR-antigen internalisation.

Studies using soluble antigen to stimulate B cells have identified many BCR signalling molecules as regulators of antigen internalisation. These proteins include Lyn itself (Ma et al., 2001; Stoddart et al., 2002), the adaptor proteins Bam32 and WASp (Becker-Herman et al., 2011; Niiro et al., 2004), the guanine exchange factors Vav 1 and 3, and the GTPase Rac (Malhotra et al., 2009a; 2009b). These signalling proteins have also been linked to the control of the actin cytoskeleton, therefore also strongly indicating a requirement for actin activity in BCR-antigen internalisation. In addition, these studies have identified clathrin as the primary endocytic mediator in this process (Salisbury, 1980; Stoddart et al., 2002). However, the precise contribution clathrin, actin and BCR signalling make towards BCR-antigen internalisation is still being discussed.

More recently, attention has been turned to mechanisms, by which B cells extract antigen from APCs (Batista and Harwood, 2009; Batista et al., 2001). To model antigen acquisition from APCs, high-resolution live-cell imaging of B cells

interacting with antigen-loaded PLB have been done. These studies have revealed some signalling molecules involved in B cell spreading and antigen gathering in response to membrane-bound antigen (Arana et al., 2008; Carrasco and Batista, 2006a; Carrasco et al., 2004; Depoil et al., 2007; Fleire et al., 2006; Mattila et al., 2013; Schnyder et al., 2011; Tolar et al., 2009b; Treanor et al., 2011; Weber et al., 2008). However, as these B cells are inhibited in their ability to internalise antigen from the PLB (Chapter 3), it is unknown how gathering of antigen in the B cell-APC synapse leads to internalisation.

Therefore, while these data have identified components involved in BCR-antigen internalisation and the mechanisms of synapse formation, it is still unknown how the signalling cascade initiated by BCR-antigen binding is activating and recruiting the endocytic mediators. We also do not know whether the mechanism of BCR-antigen internalisation changes depending on the context of antigen encounter.

For this chapter our aim was to begin to delineate the mechanisms of antigen internalisation by using PMS as surrogates for APCs. PMS allow live-cell imaging of membrane-bound antigen internalisation, which has not been previously possible in the studies using soluble antigen or PLB. We hoped to identify novel components involved in BCR-antigen internalisation using a customised genetic screen and small-molecule inhibition, and visualise their spatial and temporal activity in real-time with high-resolution TIRF microscopy.

4.2 Results

4.2.1 SiRNA is not a reliable method of protein knockdown for the genetic screen

To identify novel components involved in BCR-antigen internalisation we planned to set up a customised genetic screen. This screen would allow us to systematically test a large number of protein candidates for a role in BCR-antigen internalisation and could allow the unbiased identification of new signalling pathways involved in this process.

We initially attempted to set up this technique using a siRNA-mediated protein knockdown approach. Although B cells are thought to be highly resistant to non-viral methods of siRNA-mediated knockdown (Goffinet and Keppler, 2006; Gresch, 2004), a new amaxa nucleofection technique has been recently shown to increase the transfection efficiency and cell viability following siRNA transfection, and has proved useful in studying the effect of gene knockdowns in T lymphocytes (Goffinet and Keppler, 2006; Gresch, 2004; Mantei et al., 2008; Stallwood et al., 2006).

Initial attempts to optimise siRNA nucleofection in B cells were successful. Approximately 50% reduction of CD19 in Bl6 B cells, and GAPDH in Ramos cells, was seen following siRNA nucleofection of their specific, but not control, oligonucleotides (Figure 14A and B). We then tested this technique using oligonucleotides specific for clathrin, dynamin2, or AP2. These proteins are known to be involved in endocytosis and BCR-antigen internalisation, and therefore would act as positive controls in the genetic screen (Collinet et al., 2010; Stoddart et al., 2005; Taylor et al., 2011). However, no reduction in protein levels was observed (Figure 14C). Its unlikely the absence of knockdown was due to high stability of the proteins, as other studies reported 90% reduction of clathrin under a tetracycline-sensitive promoter, in the same time frame as our knockdown studies, in a B cell line following doxycycline treatment (Stoddart et al., 2005). The unsuccessful knockdown could be because these particular oligonucleotides were not efficiently reducing mRNA levels. However, because of the high rate of failure and also high levels of cell toxicity observed, we decided to abandon siRNA as a method of protein knockdown and use lentiviral delivery of shRNA instead. This process is labour intensive compared to siRNA nucleofection, however the resulting transduction is reported to be higher than nonviral methods and successful knockdown of proteins in B cells has been previously reported (Gresch, 2004; Pavri et al., 2010).

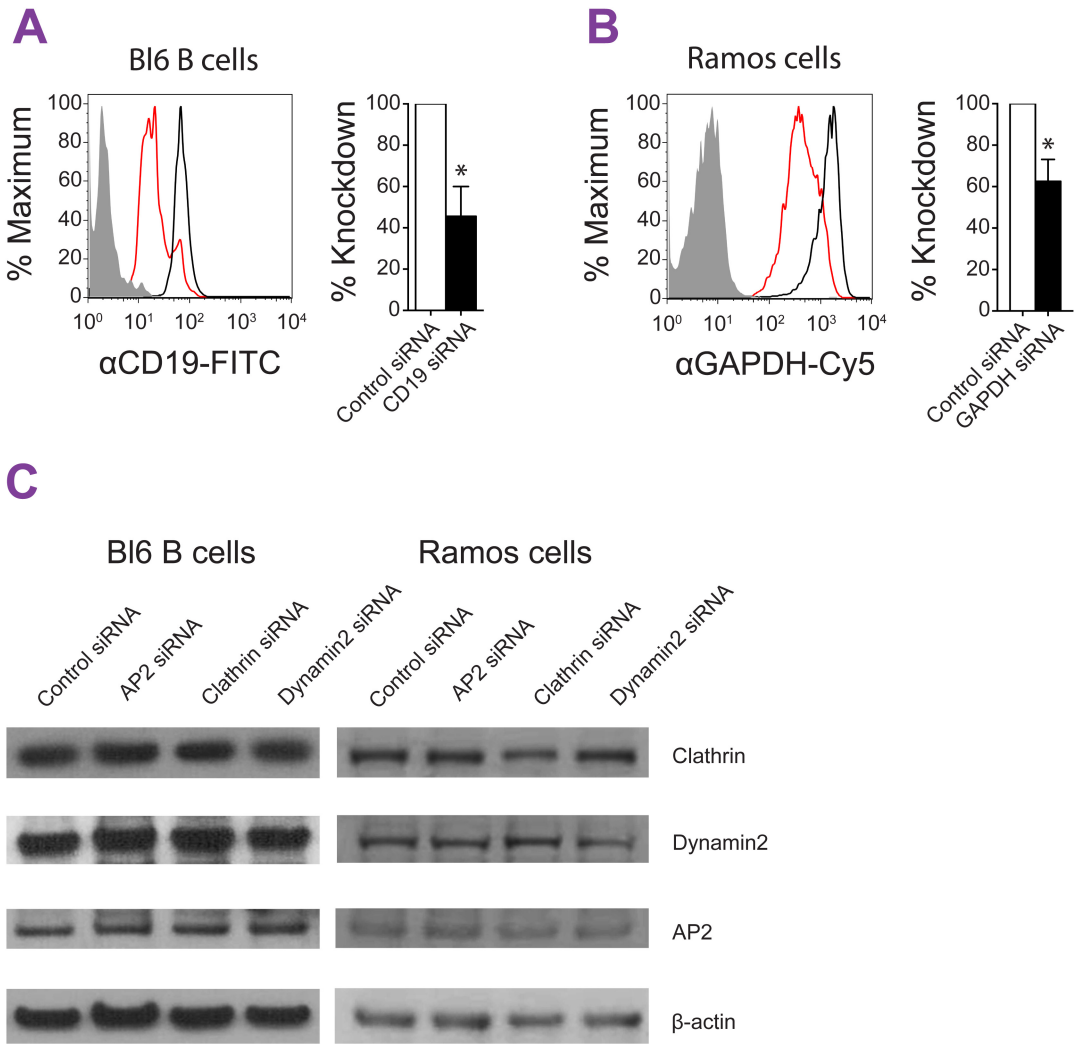

Figure 14: Nucleofection of siRNA produces a modest protein knockdown in B cells

A) Flow cytometry plots (left) and quantification (right) showing CD19 protein levels following siRNA-mediated knockdown. Protein levels were assessed using αCD19-FITC 4 days following siRNA nucleofection. Grey = unstained, black = control siRNA, red = CD19 siRNA (mean±SEM, n=3 independent expeirments) *,p<0.05 in Mann-Whitney test compared to Control siRNA

B) Same as A but with Ramos cells and siRNA-mediated knockdown of GAPDH

C) Western blot showing protein levels 4 days after siRNA-mediated knockdown of indicated proteins

4.2.2 Lentiviral delivery of shRNA mediates protein knockdown of endocytic mediators in B cells

To produce shRNA-lentiviral particles, we transfected the pLKO.1 lentiviral vectors from The RNAi Consortium (Moffat et al., 2006; Root et al., 2006) which contain shRNA constructs specific for our proteins of interest, into HEK293FT

cells. Viral supernatants were collected 3 days later and used to infect Ramos cells.

To ensure infectious particles were being produced, Ramos cells were infected with a control lentivirus containing a GFP construct. An increase in GFP fluorescence provided evidence of successful viral production and infection (Figure 15A). To check if infection of shRNA-lentivirus could mediate protein knockdown, Ramos cells were infected with dynamin2 shRNA-lentivirus. 4 days following infection, knockdown of dynamin2 protein levels was observed in both Bl6 B cells and Ramos cells (Figure 15B and C). Better knockdown efficiency was seen in Ramos cells compared to primary Bl6 B cells. This may be due to a reduced susceptibility of primary B cells to lentiviral infection compared to retroviral infection, which has been described anecdotally (Pavri et al., 2010). For this reason, we chose to use Ramos cells for the continual development of the genetic screen.

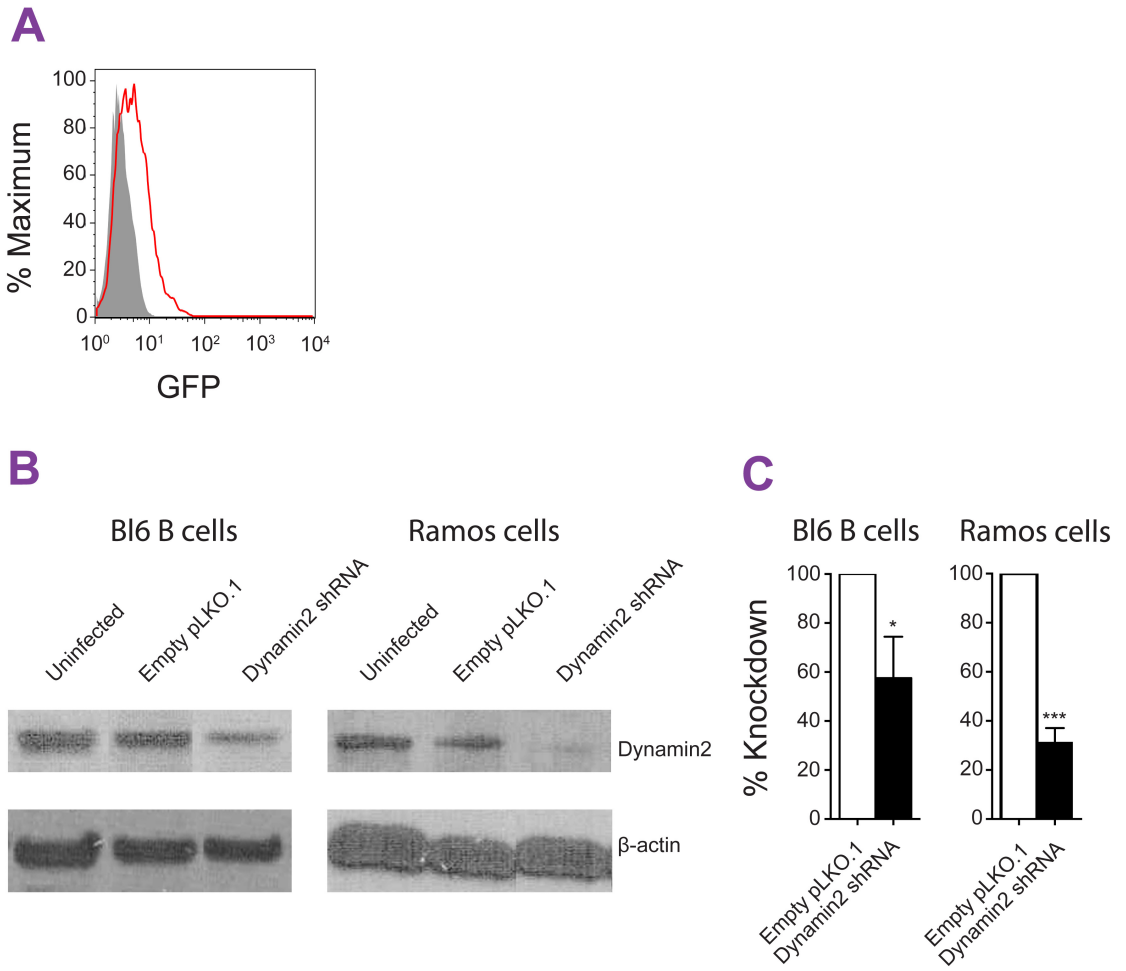

Figure 15: Infection of lentivirus-containing shRNA can mediate protein knockdown in Ramos cells and BI6 B cells

A) Flow cytometry plot showing GFP fluorescence in Ramos cells 1 day following infection of cells with pLKO.1-GFP lentivirus (red) or uninfected controls (grey)

B) Western blot showing dynamin2 protein levels 4 days after infection with lentivirus-containing dynamin2-shRNA

C) Quantification of B (mean±SEM, n=3 independent experiments) *, $p<0.05$, ***,$p<0.001$ in Mann-Whitney test compared to Empty pLKO.1

4.2.3 Inhibition of internalisation following protein knockdown can be assessed by flow cytometry or microscopy

To understand whether the dynamin2 knockdown mediated by shRNA-lentivirus transduction caused a decrease in BCR-antigen internalisation, we stimulated the infected cells to internalise soluble antigen at 37°C. Control cells were left on ice. The cells were then fixed and stained with fluorescent streptavidin to visualise any antigen remaining on the cell surface. While the streptavidin signal decreased after 37°C incubation of the mock-infected samples, which is indicative of fewer antigens on the cell surface due to internalisation, dynamin2 knockdown prevented this decrease indicating antigen retention on the cell surface, and therefore a decrease in BCR-antigen internalisation (Figure 16A and B). This was further confirmed by microscopy, which revealed little colocalisation between antigen and streptavidin in mock infected samples, as the majority of the antigen was inside the B cell and protected from the streptavidin binding. However, in the dynamin2 knockdown cells, antigen was retained on the cell surface resulting in a high level of antigen colocalisation with streptavidin (Figure 16C and D). These results support both the previous studies showing reduced BCR-antigen internalisation following dynamin2 inhibition (Chaturvedi et al., 2011; Malhotra et al., 2009b), as well as the use of this technique in the identification of proteins involved in BCR-antigen internalisation.

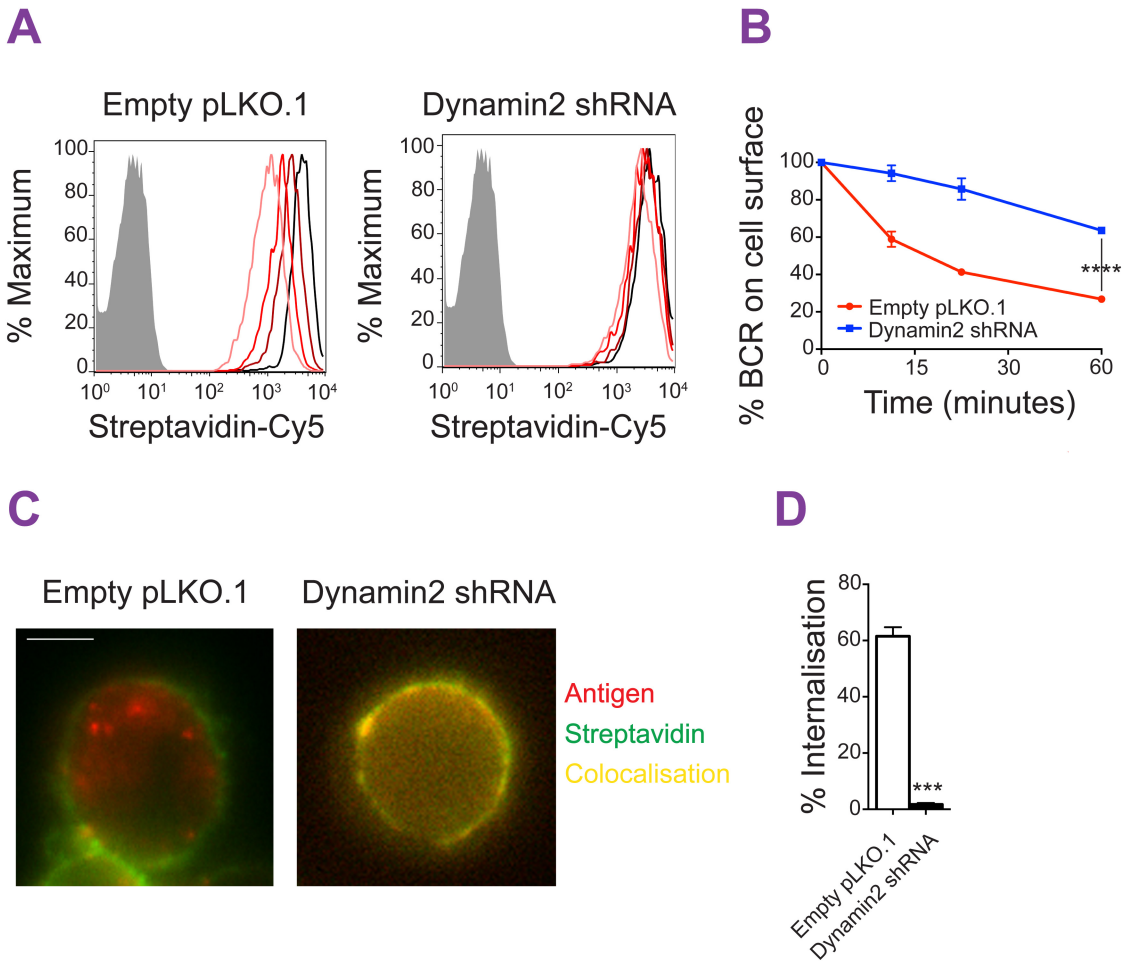

Figure 16: Soluble antigen internalisation is inhibited following dynamin2 knockdown by shRNA-containing lentivirus

A) Flow cytometry plot showing streptavidin-Cy5 fluorescence as an indicator of surface antigen (αIgM, no fluorescent label) levels. Ramos cells were infected with lentivirus containing dynamin2-shRNA (right) or empty pLKO.1 controls (left). Ramos cells were incubated with antigen on ice for 30 min and then the unbound antigen was washed off. Ramos cells were incubated at 37°C for 0 minutes (black), 15 minutes (maroon), 30 minutes (red), or 60 minutes (pink) to stimulate antigen internalisation. Ramos cells were then fixed and stained with streptavidin-Cy5 to highlight any antigen remaining on the cell surface or were left unstained (grey). Flow cytometry plots are representative of 2 independent experiments

B) Quantification of A (mean±SEM, n=2 independent experiments) ****, p< 0.0001 in two-way ANOVA test between lentiviral treatments

C) Epifluorescent images of Ramos cells following treatment as in A) for 20 minutes. Scale bar = 4 μm

D) Quantification of C (mean±SEM, n=4 fields of view per sample, approximately 20 cells for each lentiviral treatment) ***,p<0.001 in Mann-Whitney test compared to Empty pLKO.1

4.2.4 BCR-antigen internalisation is reduced in Ramos cells following shRNA mediated knockdown of myosin IIA and clathrin

20 genes were chosen for a pilot run of the genetic screen. The genes chosen included known and predicted endocytic mediators that are expressed highly in murine primary B cells. 4 days following lentiviral infection, Ramos cells were incubated with antigen-loaded PMS and the extent of internalisation was analysed. If 3 out of 4 clones used for each gene showed a difference in internalisation by 2 standard deviations from the normalised Z score, the gene was counted as a positive hit. Normalised z scores demonstrated that knockdown of dynamin2 (an enzyme required for the pinching off of clathrin-coated vesicles), Ap2 (AP2M1, an essential clathrin adapter protein), myosin IIA (MYH9, a motor protein involved in the actomyosin cytoskeleton), and Rock1 (a myosin IIA activator) all caused significant decreases in BCR-antigen internalisation (Figure 17). This inhibition was validated by subsequent repetitions (Figure 18A) showing that the clathrin pathway (dynamin2 and Ap2) as well as the myosin IIA pathway (myosin IIA and Rock1) are important in mediating membrane-bound antigen internalisation in Ramos cells.

The ability of Ramos cells to pull on and invaginate the PMS during antigen-internalisation was analysed by tracking changes in DiI fluorescence in DiI-stained antigen-loaded PMS (Chapter 3). Interestingly the number of invaginations decreased only if myosin IIA or Rock1 were knocked-down and were unaffected by Ap2 or dynamin2 knockdown (Figure 18B). These results indicate B cells require myosin IIA contractility to invaginate the PMS before internalising antigen in a clathrin-dependent manner.

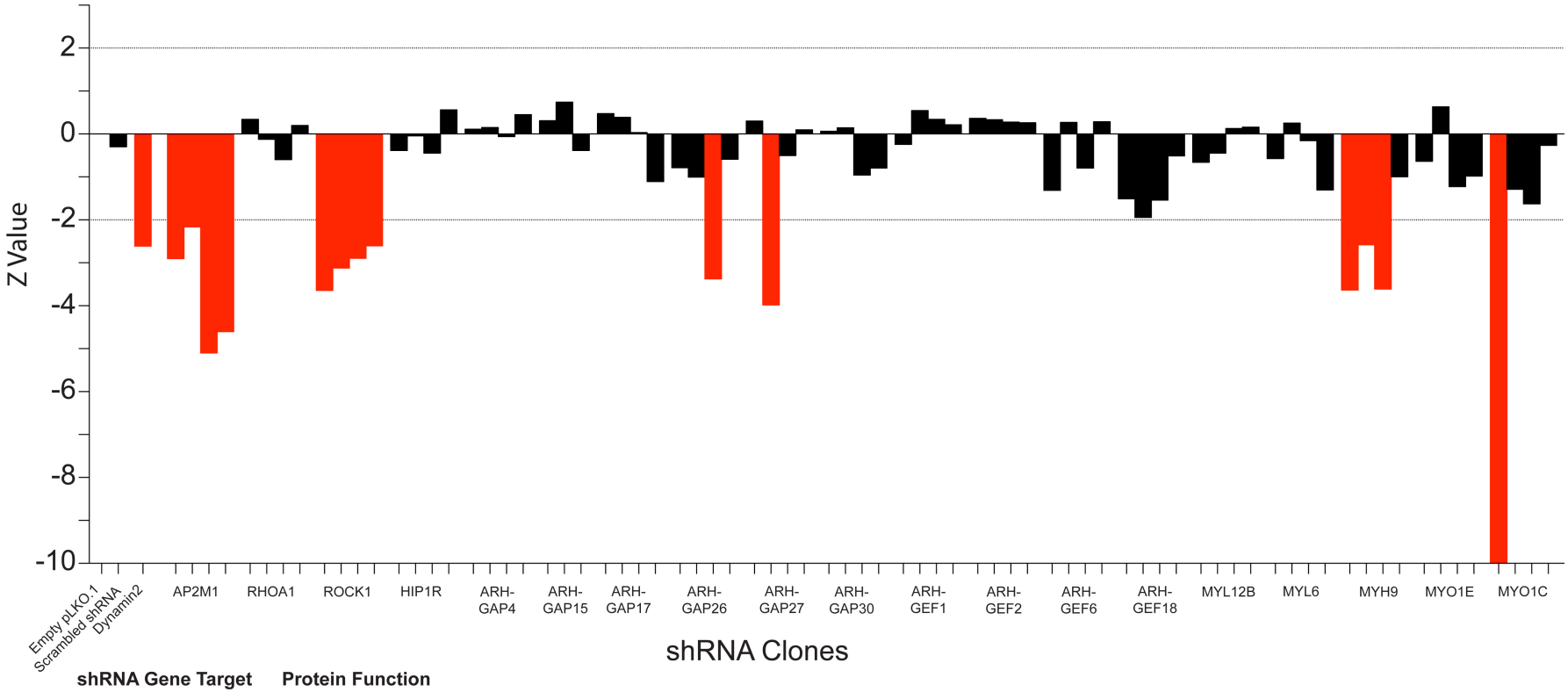

shRNA Gene Target	Protein Function
Dynamin2	GTPase required for pinching off endocytosed vesicles
AP2	Essential clathrin adapter protein required to link clathrin to the endocytic cargo
RHOA	RhoGTPase involved in regulating the cytoskeleton through Rock1 and Diaph1 activation
ROCK1	Protein involved in cytoskeleton regulation
HIPR1	Protein which regulates the interaction between the actin cytoskeleton and clathrin
ARHGAP	RhoGTPase-activating proteins involved in regulating the cytoskeleton
ARHGEF	RhoGTPase-guanine nucleotide exchange factors involved in regulating the cytoskeleton
MYL12B	Myosin II light chain whose phosphorylation regulates myosin IIA activity
MYL6	Myosin light chain
MYH9	Myosin IIA heavy chain component of the myosin IIA actin-based molecular motor
MYO1E	Myosin 1E actin-based molecular motor
MYO1C	Myosin 1C actin-based molecular motor

Figure 17: A pilot customised genetic screen was used to identify components involved in antigen internalisation from the PMS

Ramos cells were infected with shRNA-lentivirus and 4 days later were incubated with antigen (αIgM)-loaded PMS for 20 minutes at 37°C. Cells were then fixed before internalisation was analysed. Each gene was targeted by 4 separate shRNA sequences. Red bars indicate Z values 2 standard deviations or more away from the mean (n=>20 cells, n=1 experiment for each gene)

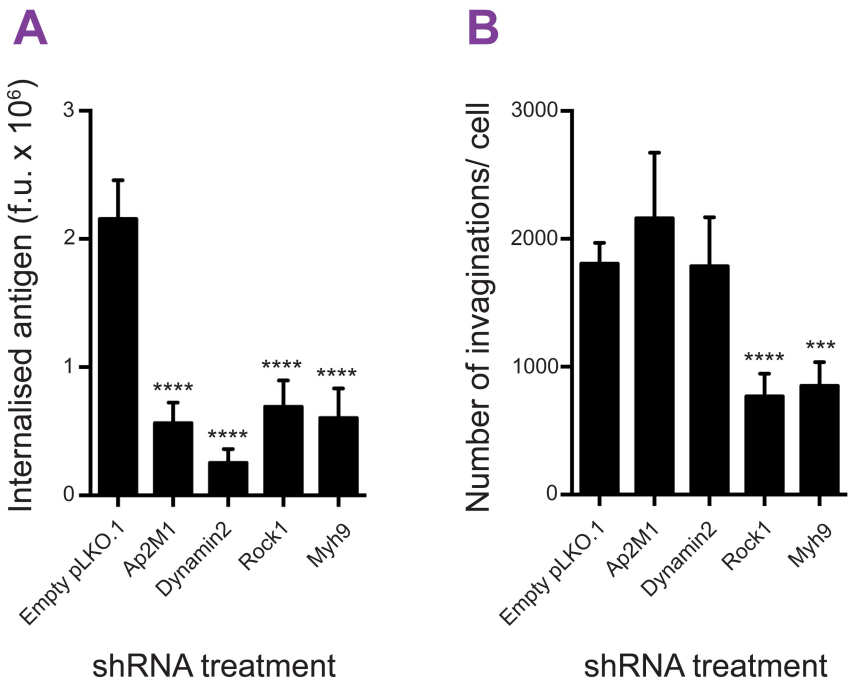

Figure 18: Ramos cells need to invaginate the PMS using myosin IIA contraction before internalising the antigen in a clathrin-dependent manner

A) Repetition of positive hits shown in Figure 17. Antigen (αIgM) internalisation from PMS by Ramos B cells expressing shRNA against AP2, dynamin2, Rock1, or myosin IIA. Ramos cells were incubated with PMS for 20 minutes at 37°C and then fixed before internalisation was analysed. Values shown are pooled results from all 4 shRNA clones (mean±SEM n=>60 cells over 3 independent experiments). f.u., fluorescent units, ****, p<0.0001 in Mann-Whitney test compared to Empty pLKO.1

B) Number of tracked DiI-labelled invaginations pulled from the PMS by Ramos B cells expressing shRNA against AP2, dynamin2, Rock1, or myosin IIA. Tracks were taken from a 20 minute timelapse of Ramos cells interacting with antigen (αIgM)-loaded PMS at 37°C. (mean±SEM n=>20 cells over 2 independent experiments). ****, p<0.0001, ***, p<0.001 in Mann-Whitney test compared to Empty pLKO.1

4.2.5 BCR-antigen internalisation is reduced in Bl6 B cells following pharmacological inhibition of myosin IIA and clathrin

To confirm the results of the pilot screen in Ramos cells independently, we ran another pilot screen using Bl6 B cells and small molecule inhibitors against known and possible endocytic mediators, as well as BCR signalling molecules. Inhibition of Rock1 as well as myosin IIA itself, supported the requirement of the myosin IIA pathway in BCR-antigen internalisation and PMS invagination, and dynamin2 inhibition supported the need for clathrin-mediated endocytosis (Figure 19A). Lyn and formin inhibitors confirmed previous reports showing BCR signalling and the actin cytoskeleton are also needed in BCR-antigen internalisation (Brown and Song, 2001; Fleire et al., 2006; Ma et al., 2001; Stoddart et al., 2005), whereas PKC and Rac1 were seen to be dispensable (Arana et al., 2008; Weber et al., 2008). Erk1/2 signalling was also seen to be important in BCR-antigen internalisation, which supports recent findings suggesting BCR signalling continues following BCR-antigen internalisation (Chaturvedi et al., 2011).

Comparing internalisation of soluble or membrane-bound antigen by Bl6 B cells supported the idea that clathrin and myosin IIA have independent roles in BCR-antigen internalisation. Dynamin2 inhibition (mediated by dynasore) prevented internalisation of antigen whether in solution or tethered to the PMS (Figure 19B). However, it did not stop the B cell from invaginating the PMS (Figure 19C) or BCR signalling, as Bl6 B cells inhibited by dynasore, were able to spread over the PMS, form microclusters and contract bringing them into a central synapse (Figure 20). This suggests clathrin acts as the endoytic mediator in this process but is not required for BCR signalling or PMS invagination prior to internalisation.

In contrast, internalisation following a reduction in the activity of the myosin IIA pathway (mediated by blebbistatin and Y-27632) was only decreased when the antigen was membrane-bound, and antigen internalisation from solution was unaffected (Figure 19B). These inhibited cells were also unable to invaginate the PMS (Figure 19C) or contract in response to membrane-bound antigen shown by an increase in synapse size (Figure 20). These results suggest myosin IIA is the

component responsible for producing the force needed for membrane invagination prior to membrane-bound antigen internalisation (Chapter 3), but as less force is required for soluble antigen internalisation, its activity is dispensable when antigen is in solution.

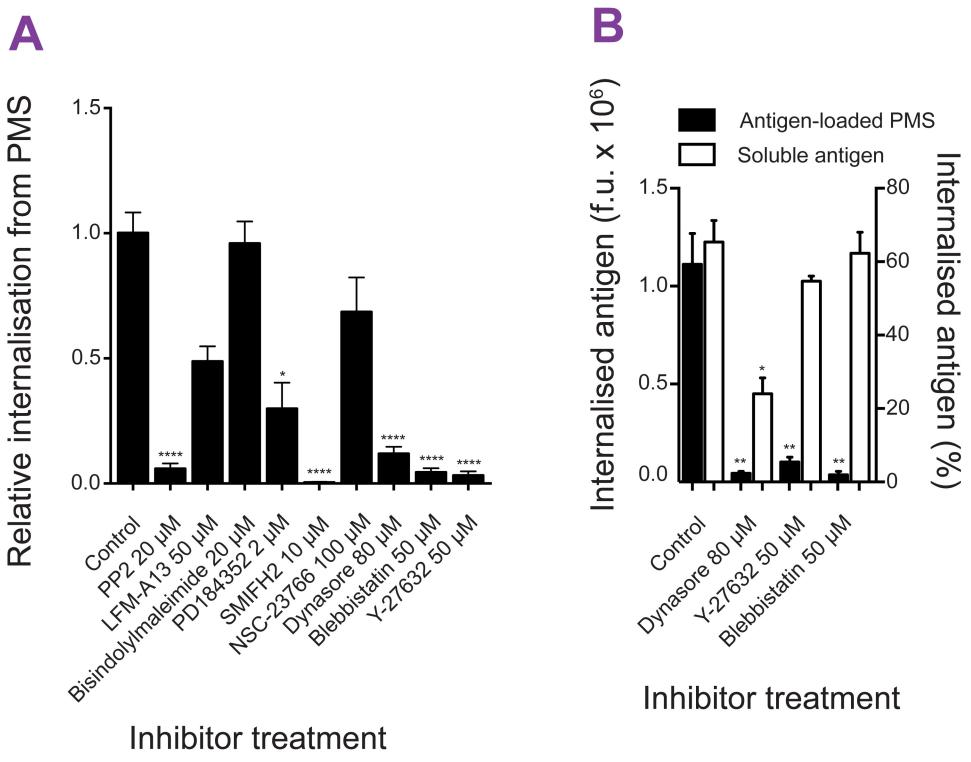

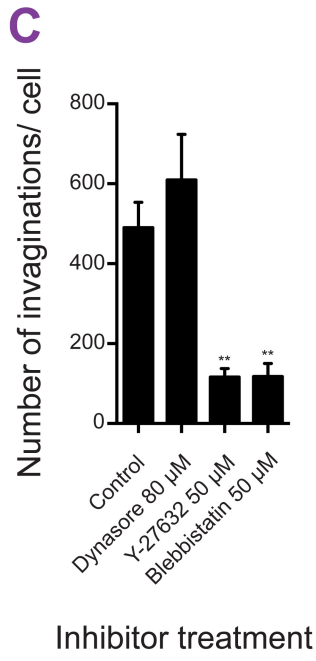

Inhibitor	Target
PP2	Lyn
LFM-A13	Btk
Bisindolylmaleimide	PKC
PD184352	Erk 1/2
SMIFH2	Formins
NSC-23766	Rac1
Dynasore	Dynamin2
Blebbistatin	Myosin IIA
Y-27632	Rock1

Figure 19: Bl6 B cells invaginate the PMS using myosin IIA contraction before internalising the antigen in a clathrin-dependent manner

A) Small molecule inhibitor screen. Relative antigen (αIgκ) internalisation from PMS following protein inhibition in Bl6 B cells. Bl6 B cells were pre-incubated with indicated inhibitor for 15 minutes before addition to the PMS. Bl6 B cells were then incubated with PMS and inhibitor for a further 20 minutes at 37°C and fixed before internalisation was analysed. (mean±SEM, n=>30 cells, n=1 experiment for each inhibitor). ****, p<0.0001, *, p<0.05 in Mann-Whitney test compared to solvent controls

B) Comparison of antigen (αIgκ) internalisation from PMS (solid bars, left y axies) or solution (empty bars, right y axies) by Bl6 B cells incubated with inhibitors against dynamin2 (dynasore), Rock1 (Y-27632), or Myosin IIA (blebbistatin). Bl6 B cells were fixed before internalisation was analysed. (mean±SEM n=>60 cells over 3 independent experiments). f.u., fluorescent units, ****, p<0.0001 in Mann-Whitney test compared to solvent controls

C) Number of tracked DiI-labelled invaginations from a 20 minute timelapse of Bl6 B cells treated with indicated inhibitors interacting with antigen (αIgκ)-loaded PMS at 37°C. (mean±SEM n=>20 cells over 2 independent experiments). ****, p<0.0001, ***, p<0.001 in Mann-Whitney test compared to solvent control

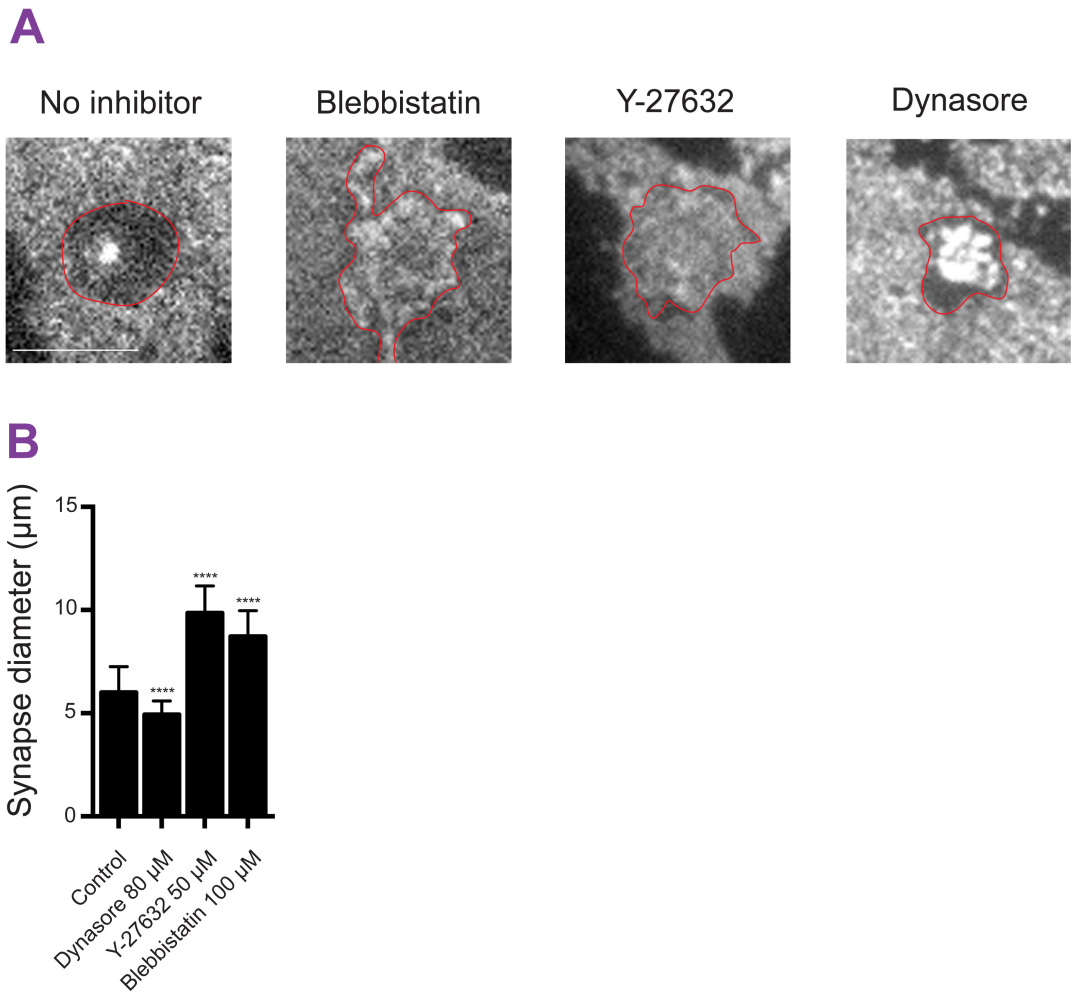

Figure 20: Inhibition of myosin IIA, Rock1 or dynamin2 affects the extent of Bl6 B cell spreading on the PMS

A) TIRF images showing difference in synapse sizes (red) made by Bl6 B cells on antigen (αIgκ)-loaded PMS. B cells were unlabelled. Bl6 B cells were incubated with PMS and inhibitor for 20 minutes at 37°C and then fixed before images were captured. Red outlines represent edges of B cell spreading and were derived from brightfield images

B) Quantification of D. (mean±SEM, n=30-50 cells over 2 independent experiments) ****,p<0.0001 in Mann-Whitney test compared to solvent control

4.2.6 Clathrin is recruited to the synapse at the point of antigen internalisation

To visualise clathrin, myosin IIA and actin activity during BCR-antigen internalisation from the PMS, we infected stimulated Bl6 B cells with retrovirus containing GFP-labelled clathrin light chain, GFP-labelled myosin IIA regulatory light chain (RLC), or the F-actin specific fluorescent probe LifeAct (Riedl et al.,

2008), respectively. Successful infection of Bl6 B cells by retrovirus was shown by increased GFP fluorescence using flow cytometry compared to uninfected controls (Figure 21A).

TIRF images of Bl6 B cells infected with clathrin light chain-GFP on antigen-loaded PMS showed an increase in the number and brightness of clathrin-coated structures (CCS) in the synapse during B cell spreading and antigen-internalisation (Figure 21B and C, Movie 4). Tracking of invaginations allowed us to analyse the colocalisation of invaginations with CCSs, and showed us that short-lived invaginations contained little clathrin, but that this colocalisation increased up to 20% with long-lived invaginations, peaking towards the end of the invagination lifetime (Figure 21D and E). Observations of clathrin and antigen activity in two separate long-lived invaginations revealed the sequential formation of antigen microclusters, invagination of the membrane, and recruitment of clathrin (Figure 22A and B). Although comparisons between the 2 invaginations revealed different temporal regulation (possibly due to differences in antigen microcluster size), both followed the same recruitment pattern of antigen, invagination, and clathrin, and in both cases simultaneous disappearance of all three fluorescent traces was observed indicating the point of internalisation. These observations support the hypothesis suggested in Chapter 3, that successful internalisation occurs by sustaining long-lived invaginations at sites of antigen microclustering. If the invagination is sustained long enough, CCSs assemble allowing successful internalisation. In contrast, short-lived invaginations terminate before clathrin is recruited and endocytosis can occur.

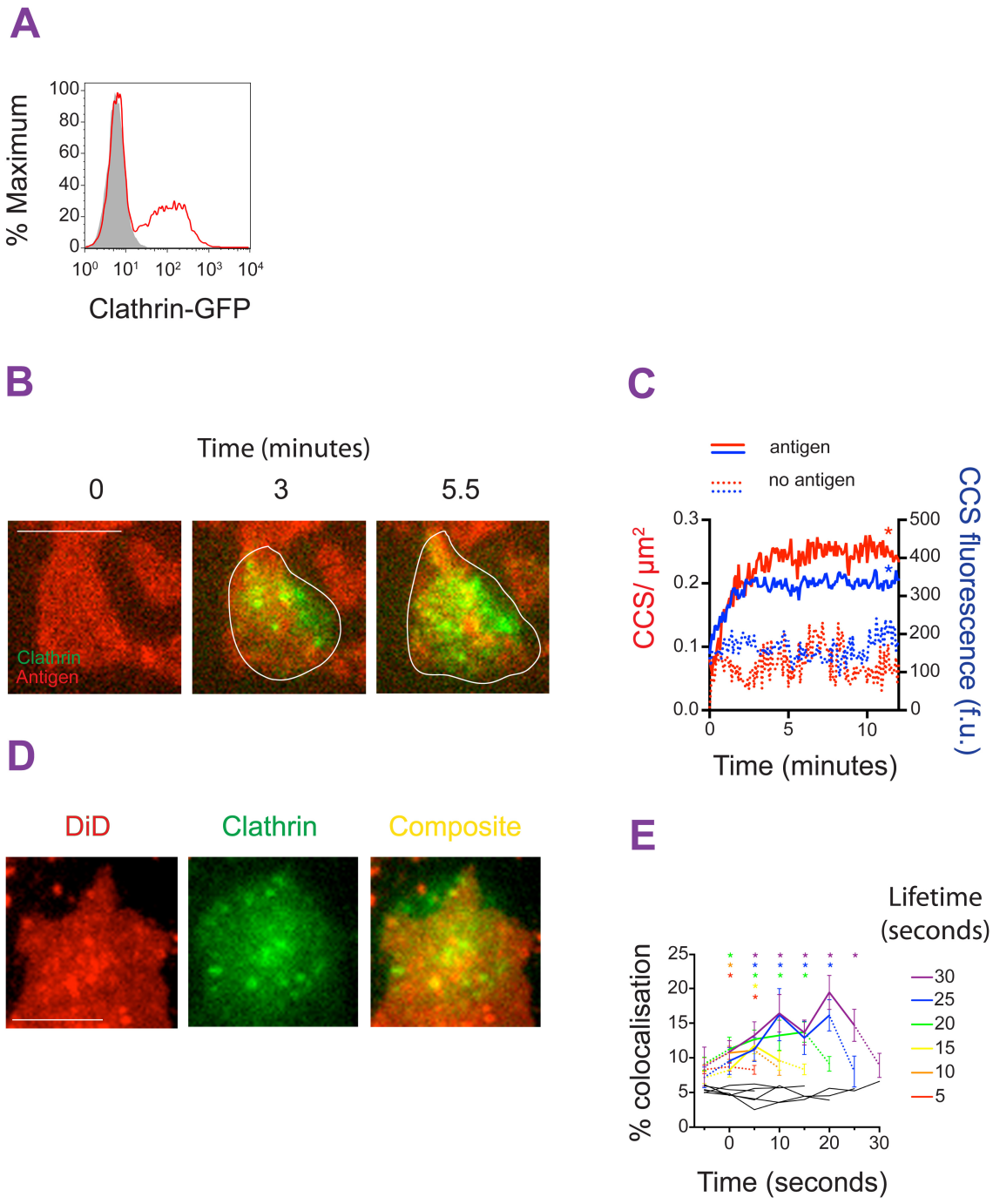

Figure 21: Retroviral infection of clathrin light chain-GFP in Bl6 B cells show clathrin recruitment to Bl6 B cell synapse, and colocalisation of clathrin with long-lived invaginations during antigen internalisation from the PMS

A) Flow cytometry plot showing GFP fluorescence in Bl6 B cells 48 hours following retroviral infection of clathrin light chain-GFP (red) or uninfected controls (grey)

B) Images from a TIRF timelapse showing clathrin recruitment to Bl6 B cell synapse with antigen (αIgκ)- loaded PMS. Bl6 B cells were infected with clathrin light chain-GFP retrovirus and imaged 48 hours later. Timelapse images were taken at 37°C. B cells were unlabelled. White outline represents edges of B cell spreading derived from brightfield images. Scale bars = 5 µm

C) Quantification of the number (red, left hand y axis) and brightness (blue, right hand y axis) of CCSs in Bl6 B cell synapses on antigen (αIgκ)-loaded PMS. CCSs were tracked over a 20 minute TIRF timelapse 48 hours after Bl6 B cells were infected with clathrin light chain-GFP (mean±SEM, n=15-21 cells). *, $p<0.05$ in Mann-Whitney tests for time>1 minute against no-antigen controls

D) Images from a TIRF timelapse showing colocalisation of CCSs in a Bl6 B cell synapse with DiD-labelled invaginations on an antigen (αIgκ, no fluorescent label)- loaded PMS. Bl6 B cells were infected with clathrin light chain-GFP retrovirus and imaged 48 hours later. Timelapse images were taken at 37°C. Image shown was taken 13 minutes after Bl6 B cells were added to the PMS. Scale bars = 5 µm

E) Percentage of CCS fluorescence associated with tracked DiD-labelled invaginations grouped by their lifetime. Data was derived from 20 minute TIRF timelapses of clathrin light chain-GFP expressing Bl6 B cells, interacting with antigen (Igκ, no fluorescent label)-loaded PMS at 37°C. The associated clathrin light chain-GFP fluorescence was analysed 5 seconds before (dotted lines), during the lifetime (solid lines), and 5 seconds after the disappearance of the invagination (dotted lines) (mean±SEM, n=12 cells). Black lines, colocalisation of CCSs with randomly scrambled controls. *, $p<0.01$ in Mann-Whitney tests against scrambled controls. Matlab analysis was done by Pavel Tolar.

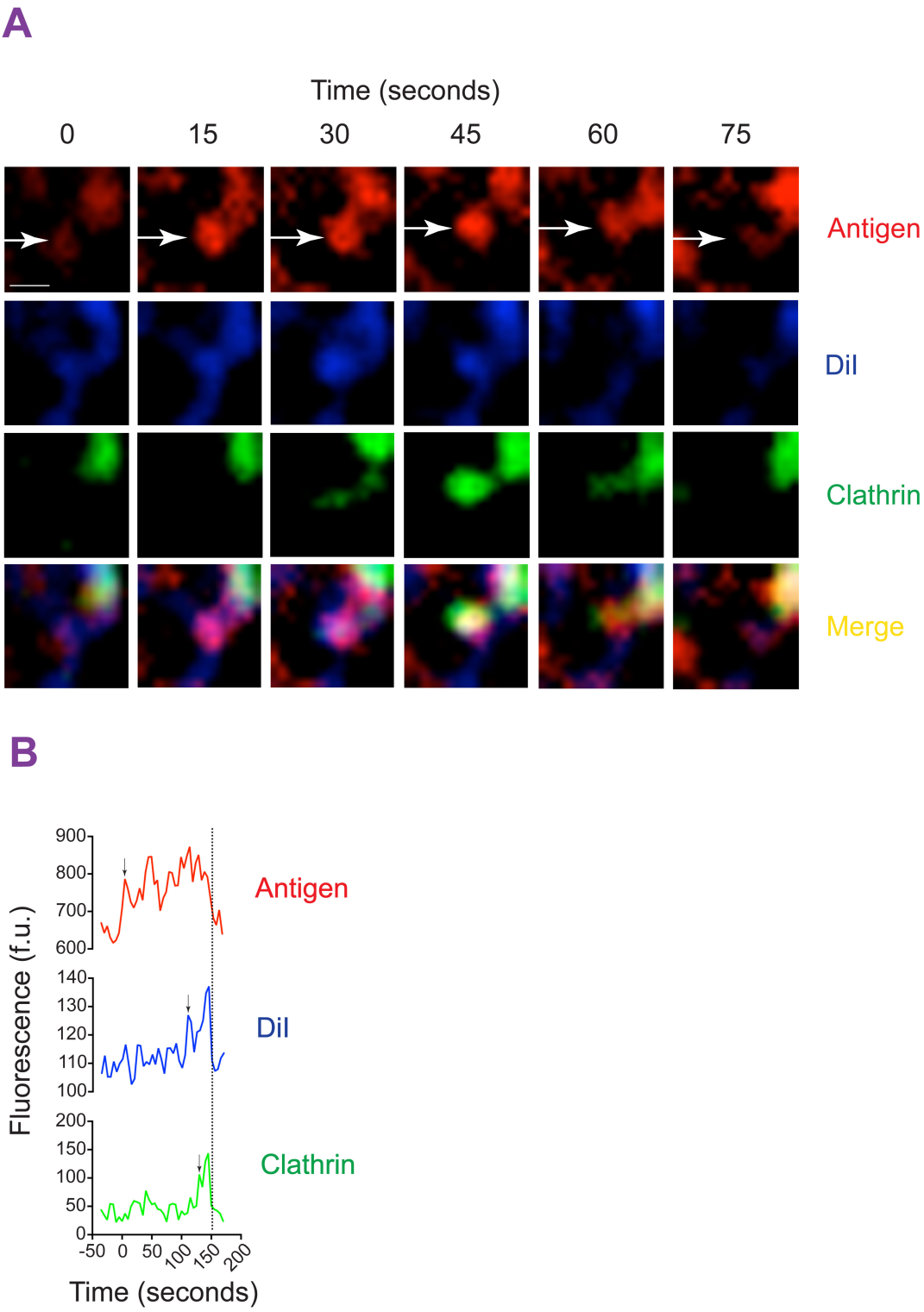

Figure 22: BI6 B cells internalise antigen from the PMS following the sequential formation of antigen microclusters, long-lived invaginations and CCSs

A) Formation of a single antigen (αIgκ) microcluster (arrows, top panels), followed by invagination of DiI-labelled PMS (second row panels), and recruitment of clathrin (third row panels). All three fluorescent images disappear at the same time indicating internalisation.

Images were taken from a 20 minute TIRF timelapse of Bl6 B cell expressing clathrin-GFP on antigen (αIgκ)-loaded and DiI-stained PMS at 37°C. Scale bar = 100 nm

B) Fluorescent traces of a separate antigen microcluster showing same sequential formation of antigen microcluster, DiI invagination, and CCS as above. Arrows show point of recruitment/ formation, and dotted line shows point of internalisation

4.2.7 Myosin IIA is recruited to the synapse immediately before invagination formation

TIRF timelapse images of myosin IIA RLC-GFP and LifeAct activity also support myosin IIA and actin involvement in BCR-antigen internalisation as both showed specific patterns of localisation in the B cell synapse (Figure 23A, 24A, Movie 5 and Movie 6). Analysis of myosin IIA colocalisation with membrane invaginations revealed that myosin IIA recruitment peaked just before the onset of all invaginations irrelevant of their lifetime, in agreement with the idea that the force required for invagination formation is myosin IIA-dependent (Figure 23B and C). In contrast actin was recruited in a biphasic manner, firstly at the onset of the invagination, and then secondly at the end of the invagination if it lasted 20 seconds or longer (Figure 24B and C). The first wave of recruitment supports the involvement of actomyosin cytoskeleton in invagination formation and the second wave supports previous studies showing actin assists in clathrin-mediated endocytosis when force is required to extract the cargo (Boulant et al., 2011; Cureton et al., 2010).

Collectively these results suggest that following membrane-bound antigen encounter, B cells use forces generated by the actomyosin cytoskeleton to pull on and invaginate the presenting membrane. The invagination lifetime depends on the prior formation of antigen microclusters and if the invagination persists long enough, CCS are recruited, and antigen internalisation occurs in a clathrin- and actin-dependent manner.

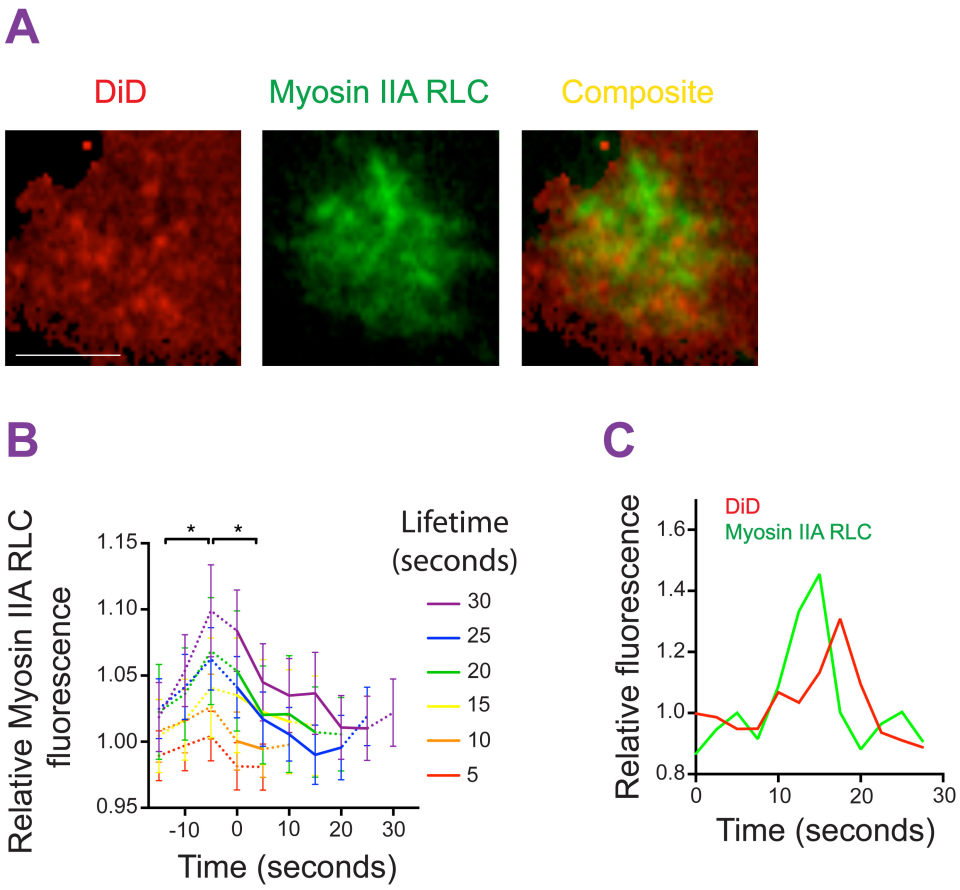

Figure 23: Myosin IIA is recruited to the Bl6 B cell synapse at the onset of invagination formation

A) Images from a TIRF timelapse showing myosin IIA recruitment to the Bl6 B cell synapse with antigen (αIgκ, no fluorescent label)- loaded DiD-stained, PMS. Bl6 B cells were infected with myosin IIA RLC-GFP retrovirus and imaged 48 hours later. Timelapse images were taken at 37°C. Image shown was taken 3 minutes after Bl6 B cells were added to the PMS. Scale bars = 5 μm

B) Myosin IIA RLC-GFP fluorescence associated with tracked DiD-labelled invaginations grouped by their lifetime. Data was derived from 20 minute TIRF timelapses of myosin IIA RLC-GFP expressing Bl6 B cells, interacting with antigen (αIgκ, no fluorescent label)-loaded PMS at 37°C. The associated myosin IIA RLC-GFP fluorescence was analysed 15 seconds before (dotted lines), during the lifetime (solid lines), and 5 seconds after the disappearance of the invagination (dotted lines) (mean±SEM, n=15 cells). *, $p<0.01$ in paired t-tests between myosin IIA RLC-GFP fluorescence values 15 seconds and 5 seconds before invagination onset, and between 5 seconds before invagination onset and 5 seconds after invagination onset. Matlab analysis was done by Pavel Tolar

C) Myosin IIA RLC-GFP and DiD fluorescence in a single long-lived invagination. Fluorescent trace shows peak of myosin IIA recruitment to the synapse just before onset of invagination

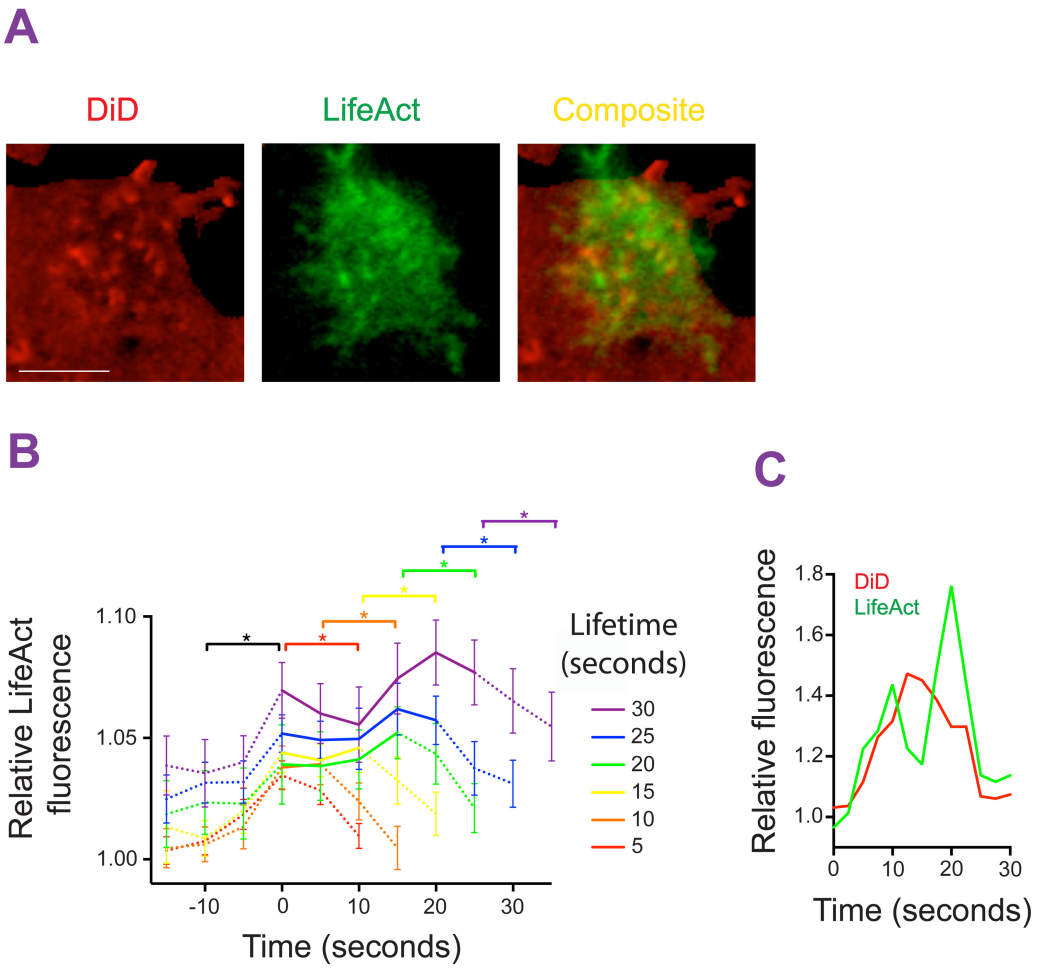

Figure 24: F-actin is recruited to the Bl6 B cells synapse in a biphasic manner

A) Images from a TIRF timelapse showing LifeAct (a fluorescent probe which binds to F-actin) recruitment to the Bl6 B cell synapse with antigen (αIgκ, no fluorescent label)- loaded DiD-stained, PMS. Bl6 B cells were infected with LifeAct retrovirus and imaged 48 hours later. Timelapse images were taken at 37°C. Image shown was taken 5 minutes after Bl6 B cells were added to the PMS. Scale bars = 5 μm

B) LifeAct fluorescence associated with tracked DiD-labelled invaginations grouped by their lifetime. Data was derived from 20 minute TIRF timelapses of LifeAct expressing Bl6 B cells, interacting with antigen (αIgκ, no fluorescent label)-loaded PMS at 37°C. The associated LifeAct fluorescence was analysed 15 sec before (dotted lines), during the lifetime (solid lines), and 10 seconds after the disappearance of the invagination (dotted lines) (mean±SEM, n=13 cells). *, $p<0.015$ in paired t-tests between LifeAct fluorescence values before invagination onset and 10 seconds prior to invagination onset (black bracket) and between values at invagination termination and 10 seconds after invagination termination (colour brackets). Matlab analysis was done by Pavel Tolar

C) LifeAct-GFP and DiD fluorescence in a single long-lived invagination. Fluorescent trace shows two peaks of actin recruitment to the synapse; the first with invagination onset and the second as the invagination is terminated

4.3 Discussion

Using both shRNA-mediated knockdown and protein inhibition we have been able to identify molecular components involved in membrane-bound antigen internalisation for the first time. Live cell imaging of B cells interacting with the PMS allowed us to visualise the temporal and spatial regulation of these identified proteins and therefore understand their distinct roles in BCR-antigen internalisation. These molecular components were shown to be important for antigen internalisation in both primary mouse cells and a human cell line indicating conservation of this mechanism across different species.

Internalisation of both soluble antigen and antigen tethered to the PMS were reduced following inhibition of the components of CCSs; dynamin2 and AP2 (Figures 16, 17, 18 and 19). These results confirmed previous studies identifying clathrin as the main endocytic mediator in soluble antigen internalisation (Salisbury, 1980; Stoddart et al., 2002; 2005), and also indicated a previously unknown role for clathrin in membrane-bound antigen internalisation. Although we demonstrated clathrin was involved in both types of antigen internalisation, it is unlikely that both types of endocytosis occur in the same way. Recent studies suggest that the mode of clathrin-mediated endocytosis can alter depending on the force required for internalisation (Kirchhausen, 2009). For instance, endocytosis of small soluble cargo from plasma membranes with low surface tension, occurs using canonical clathrin coated pits (CCPs) (Boulant et al., 2011; Kirchhausen, 2009) which are restricted in their size (approximately 30-100 nm (Cureton et al., 2010; 2009)) and generally take approximately 30 seconds to form and endocytose (Kirchhausen, 2009). In contrast, endocytosis of very large cargo (over 120 nm) (Cureton et al., 2009; 2010) require much bigger CCSs, which can persist for minutes, and are dependent on force generation (Merrifield et al., 2002; 2005; Taylor et al., 2011). CCSs are also required to internalise cargo from membranes under high surface tension (Boettner et al., 2011; Boulant et al., 2011). This force generation is thought to be actin dependent and examples of interactions between clathrin and actin during endocytosis have been shown (Boulant et al., 2011; Calabia-Linares et al., 2011; Kirchhausen,

2009; Merrifield et al., 2002; 2005). Considering all studies of soluble antigen internalisation to date have been done using small protein antigens, together with the assumption that little or no force is required for internalisation from solution, it is likely that soluble BCR-antigen internalisation happens independently of force generation, and through canonical CCPs. In this case, actin polymerisation is needed only to overcome the tension of B cell plasma membrane and could explain the modest reduction in soluble antigen internalisation reported following actin inhibition (Stoddart et al., 2005). In contrast, since BCR-antigen internalisation from the PMS requires force generation to extract the antigen from the opposing membrane (Chapter 3), it is likely this method of clathrin-mediated endocytosis happens in a non-canonical way using CCSs, which is reminiscent of maturation and disassembly of focal adhesions (Ezratty et al., 2009; Levayer et al., 2011).

The requirement for actin-dependent non-canonical CCS involvement in BCR-antigen internalisation is supported by our live-cell imaging of clathrin light chain-GFP. In these studies we observed the recruitment and development of CCSs, a few of which lasted 30 seconds or more, and the internalisation of antigen microclusters which may have been too big to fit into a CCP (Figure 16C and Movie 4). Independently we also noted that inhibition of some actin polymerisation proteins (formins) inhibited BCR internalisation of membrane-bound antigen, and visualisation of actin through LifeAct showed the second wave of actin assembly (after the membrane invagination) coincided with clathrin recruitment (Figure 19B, 22B and 24C). However, we were not able to analyse internalisation from the PMS following complete inhibition of actin polymerisation because this treatment severely reduces the ability of B cells to spread and attach to the PMS.

Although our studies strongly indicate clathrin is the primary endocytic mediator of BCR-antigen internalisation, we still do not know the mechanics behind this process. For instance, knockdown and inhibition of dynamin2 and AP2 demonstrate clathrin involvement, as these are universally required for clathrin-mediated endocytosis (Boucrot et al., 2010; McMahon and Boucrot, 2011; Merrifield et al., 2002), but it remains unclear whether AP2 binds directly to the

BCR or whether other adaptors are involved (Boucrot et al., 2010; Hou et al., 2006; McMahon and Boucrot, 2011). These studies also do not shed light on whether BCR signalling recruits and initiates clathrin assembly, which has been seen in response to some cargo (Cureton et al., 2009), or whether BCR engagement of antigen merely stabilises CCSs which initiate randomly (Ehrlich et al., 2004). In addition, our live-cell TIRF imaging of clathrin light chain-GFP activity does not discriminate between endosomal clathrin close to the cell surface and clathrin involved in endocytosis. It has been suggested that endosomal clathrin in T lymphocytes has a separate role to the clathrin mediating endocytosis (Calabia-Linares et al., 2011) and therefore it would be important in the future to discriminate between endosomal and plasma membrane forms of clathrin in B cells to fully understand the dynamins of clathrin during BCR-antigen internalisation.

In addition to clathrin, we also observed that myosin IIA activity was vital in BCR-antigen internalisation from the PMS. Nonmuscle myosin IIA is a motor protein highly expressed in B cells and through its actin binding properties can control the cytoskeleton. Myosin IIA activity has been linked with a broad range of cellular processes such as cell migration, cytokinesis and adhesion, and in each of these roles myosin IIA contraction during interaction with actin provides the force needed for these processes to occur (Conti and Adelstein, 2008; Lecuit et al., 2011; Vicente-Manzanares et al., 2009). Therefore, it is likely myosin IIA contraction is the force generator needed for antigen extraction from the PMS. This idea is supported firstly by the fact that soluble antigen internalisation, which does not require high levels of force, is not affected by myosin IIA inhibition (Figure 19B), and secondly by the live-cell imaging of myosin IIA RLC-GFP in B cells interacting with the PMS where we observed the peak in myosin IIA recruitment occurring just before invagination onset. This leads us to hypothesise that myosin IIA organises actin to form a contractile ring at the site of force generation, then myosin IIA contracts the bound-actin leading to invagination of the membrane. Myosin IIA has also been seen to increase its contractility strength under increasing reverse loads (Kovács et al., 2007), which could explain how B cells are able to withstand the opposing tension of the PMS long enough for sufficient clathrin recruitment and productive antigen internalisation.

How myosin IIA activity and localisation are controlled at the B cell synapse is unknown. One possibility is that, as in the maintenance of epithelial cell junctions, B cell adhesion to the PMS stimulates actin adaptor protein recruitment and actin polymerisation, this in turn stimulates myosin IIA activity, which provides the required contractile force (Lecuit et al., 2011). We have also identified the activator of myosin IIA, Rock1 (Pellegrin and Mellor, 2007) as an important protein in the regulation of BCR-antigen internalisation. Rock1 controls myosin IIA activity by the phosphorylation of myosin IIA regulatory light chains and is activated by RhoA, which is stimulated following BCR binding to antigen (Dal Porto et al., 2004; Vicente-Manzanares et al., 2009). Reports have also suggested that myosin IIA can be controlled through phosphorylation of its heavy chain, however one of the proteins known to mediate this phosphorylation; PKC (Figure 19A) was seen to be dispensable for BCR-antigen internalisation in our studies (Vicente-Manzanares et al., 2009). Therefore, further investigations into other components that are able to phosphorylate the myosin IIA heavy chains will allow better understanding of whether this type of myosin IIA regulation plays a prominent role in BCR-antigen internalisation.

Interestingly B cells were able to spread and form large synapses independently of myosin IIA activity. This supports other reports suggesting that B cell spreading is an actin-dependent process (Fleire et al., 2006) and suggests that myosin IIA contractility is required after initial synapse formation for invagination of BCR-antigen microclusters. The biphasic recruitment of actin observed during BCR-antigen internalisation, and its ability to interact with both myosin IIA and clathrin pathways, indicates different roles for the cytoskeleton depending on which point of the internalisation process is under investigation. However as LifeAct binds to all filamentous actin we cannot decipher between these roles in these experiments.

Taken together it is clear that the force generated by myosin IIA is a vital component involved in BCR-antigen internalisation. However, the molecular mechanisms controlling and regulating myosin IIA in this system will require further study.

ShRNA-mediated knockdown experiments are limited in their use, as successful knockdown following transduction of shRNA constructs cannot be guaranteed. In addition, if knockdown is achieved, another protein may compensate for the initial protein loss. Off targets effects are also possible, which could lead to the identification of false positive hits. For example, our shRNA studies did not pick up RhoA even though it is a well-known activator of Rock1 and therefore myosin IIA. Despite these limitations, continuing the shRNA screen by using 4 clones per gene, and by targeting many genes per pathway, should reduce the chance of mis-identifying protein hits.

Whilst the myosin IIA, clathrin and actin pathways identified are involved in a large array of different cellular processes, their situation-specific function depends on the adaptor proteins and signalling molecules controlling them in a particular circumstance. Identification of these regulators by continuing the screen, and subsequent visualisation by using live-cell microscopy, will allow us to delineate the precise roles by which actin polymerisation, myosin IIA contraction, and clathrin recruitment can orchestrate endocytosis of membrane-bound antigen. Ultimately we hope that continuing this genetic screen will allow us to gain a better understanding of how these processes are regulated and linked together, and what translates antigen-stimulated BCR signalling to antigen internalisation, so we can begin to piece together the parts of this complex molecular puzzle.

Collectively these results support a mechanism which links contractility to endocytosis in BCR-antigen internalisation (Levayer et al., 2011). Here we show that following antigen recognition, myosin IIA is activated to pull on the BCR-antigen microclusters causing invagination of the PMS. If the invagination is sustained for over 20 seconds, successful assembly of the CCS can occur and endocytosis of antigen follows. Interestingly, as shown in Chapter 3, the majority of invaginations are short-lived (approximately 5 seconds), occur at sites of minimal antigen clustering, and do not end with a productive internalisation. This suggests BCR-antigen bonds found in small microclusters (low avidity) rupture under the high force generated by myosin IIA before clathrin can be assembled,

and only microclusters with enough BCR-antigen bonds (high avidity) can maintain the invagination and stimulate productive internalisation.

However, *In vivo*, B cells not only need to discriminate between antigens of different avidities, but also between antigens of different affinities, to ensure the selection of high affinity B cell clones. The size of the BCR-antigen microcluster has been shown to depend on the BCR affinity for the antigen (Liu et al., 2010), therefore, we can assume that BCR-antigen bonds of low affinities will produce smaller microclusters that will rupture under the myosin IIA contractility, whereas BCR-antigen complexes of high affinity will produce bigger microclusters that are able to withstand the contractile forces and become internalised. This leads us to hypothesise that this mechanical testing immediately before internalisation could provide a possible proofreading mechanism for affinity discrimination *in vivo*.

Chapter 5 Myosin IIA contractility enables B cells to discriminate between antigen affinities

5.1 Introduction

The development of an effective immune response depends on the selective expansion of high affinity B cell clones to produce high affinity antibodies in response to infection.

In vitro studies have shown that B cells with high affinity BCRs are seen to have increased levels of signalling (Kouskoff et al., 1998), antigen accumulation (Liu et al., 2010), and antigen internalisation and presentation (Batista et al., 2001) compared to B cells with low affinity BCRs. This shows BCRs have the intrinsic ability to discriminate between antigen affinities. However, *in vivo* both high and low affinity BCRs can elicit comparable antibody responses, and only when competition between BCRs of different affinities are introduced, is affinity discrimination shown by a selective expansion of high affinity B cells (Schwickert et al., 2011; Shih et al., 2002a; 2002b).

This shows that affinity discrimination *in vivo* also requires a competition-based B cell extrinsic mechanism. Studies have suggested that this results from limiting T cell help to B cells presenting the highest level of antigen either at the B-T cell boarder or within the germinal centre (Schwickert et al., 2011; Victora et al., 2010). Therefore, taken together, these studies indicate that the increased levels of signalling through high affinity BCRs leads to more antigen internalisation and monopolisation of T cell help, demonstrating a link between affinity-dependent antigen internalisation and affinity discrimination.

In this set of studies we investigated whether myosin IIA contraction and invagination of PMS during BCR internalisation of membrane-bound antigen shown in Chapter 3 and 4, could contribute to the affinity-dependent internalisation and therefore affinity discrimination shown *in vivo*. We hypothesised that the interaction between BCR and high-affinity antigen would be

able to withstand the myosin IIA contractility, and internalise antigen, more successfully compared to low affinity antigen.

5.2 Results

5.2.1 B cells internalise antigen presented by plasma membrane sheets in an affinity-dependent manner

To test the ability of B cells to discriminate between antigen affinities presented on the PMS we used B1-8 B cells which are specific for the low affinity NP, and the high affinity NIP, antigens. These antigens differ approximately 10 times in their monovalent affinity for the Fab fragment of the B1-8 BCR (Natkanski et al., 2013). In solution, B1-8 B cells were able to internalise both antigens to a similar extent (Figure 25A). This could be due to the high avidity nature of NP/ NIP antigens complexed to a protein carrier (goat (Fab')2), which may raise the immunogenicity of the antigens above the $K_a \sim 10^{10} M^{-1}$ threshold, so the B cells would not be able to discriminate between them (Batista and Neuberger, 1998; 2000). However, when they were tethered to the PMS, B1-8 B cells internalised significantly more of the high affinity NIP antigen compared to the low affinity NP (Figure 25B and C).

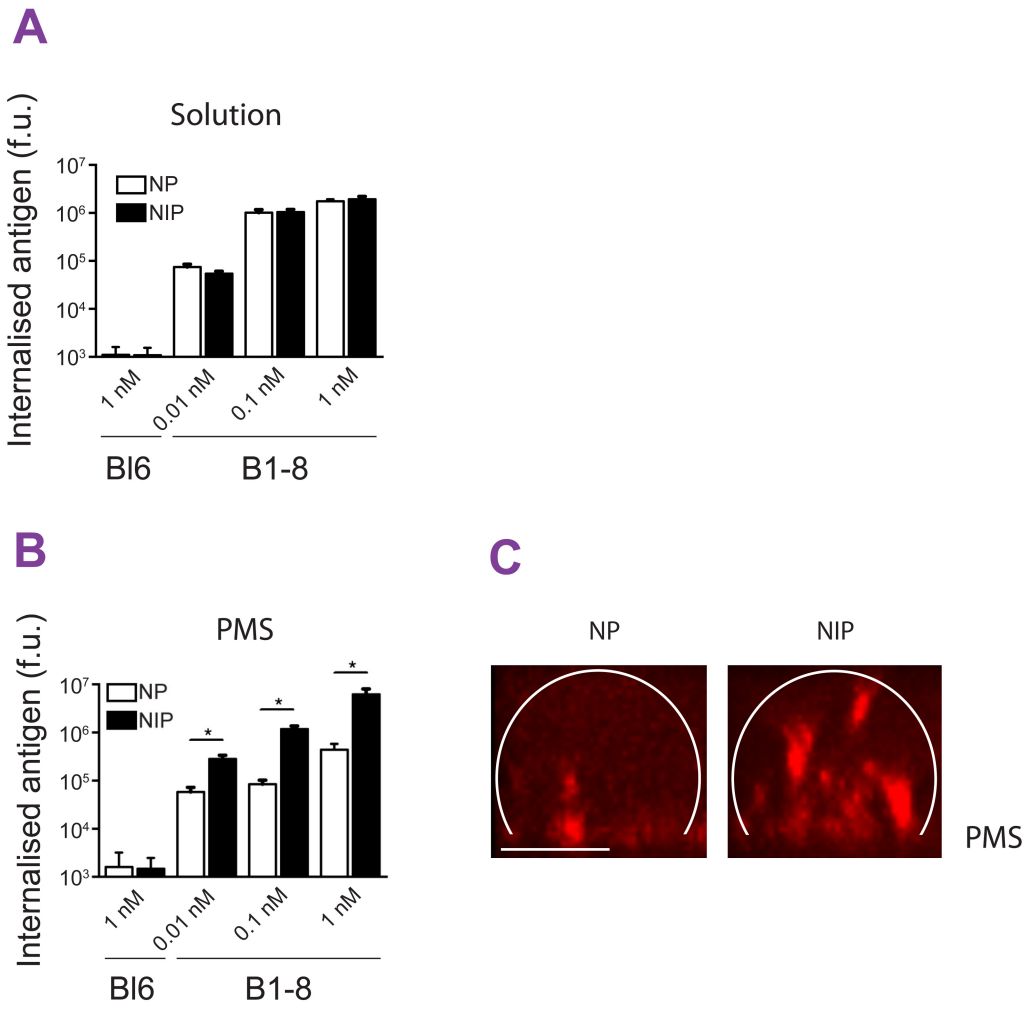

Figure 25: B1-8 B cells can discriminate between antigen affinities when presented on PMS

A) Antigen (NP/NIP) internalisation from solution by Bl6 or B1-8 B cells. B cells were attached to the coverslip and incubated with antigen for 20 minutes at 37°C. B cells were then fixed and any antigen remaining on the cell surface was labelled with streptavidin-Cy3 before analysing the extent of internalisation (mean±SEM, n= 25-118 cells, over >2 individual experiments)

B) Antigen (NP/NIP) internalisation from PMS by Bl6 or B1-8 B cells. B cells were incubated with antigen-loaded PMS for 20 minutes at 37°C. Cells were then fixed before analysing the extent of antigen internalisation (mean±SEM, n= 25-118 cells, over >2 individual experiments). *, $p<0.001$ in Mann-Whitney test between NP and NIP antigens

C) Side view reconstruction from epifluorescent images of synapses between B1-8 B cells and antigen (NP/NIP)-loaded PMS. B1-8 B cells were incubated with PMS for 20 minutes at 37°C, and then fixed before z-stack images were taken. White outline shows B1-8 B cell orientation. Outline was derived from brightfield images. Scale bar = 4 μm

5.2.2 Antigen clustering and invagination lifetime depends on antigen affinity

To assess the differences in synaptic activity between the two antigens we tracked both invaginations and BCR-microclusters produced by B1-8 B cells over 20 minute timelapses. We observed that similar numbers of invaginations were produced in response to both antigens (Figure 26A). However, the NIP antigens stimulated the production of more long-lived invaginations (Figure 26B), greater BCR microcluster formation (Figure 26C), and we observed more NIP antigen associated with the long-lived invaginations than NP antigen (Figure 26D). These results suggest that the reduced levels of BCR microcluster formation in response to NP antigen, together with the already reduced strength of the low-affinity BCR-antigen bond, prevents B1-8 B cells from successful long-lived invagination formation, clathrin assembly and antigen internalisation (Chapter 3 and 4).

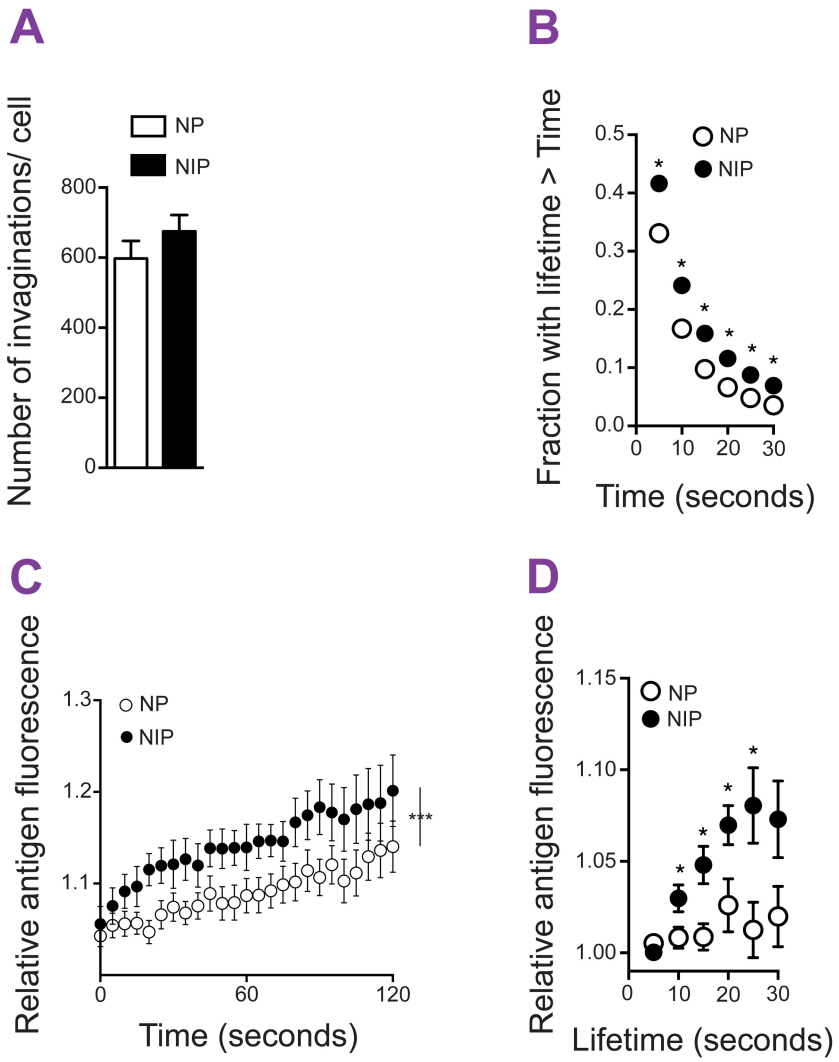

Figure 26: B1-8 B cells produce more long-lived invaginations, produce microclusters faster, and have increased amounts of invagination-associated antigen, when presented with NIP antigen over NP antigen

A) Total number of invaginations tracked from 20 minute TIRF timelapses of B1-8 B cells interacting with NIP- or NP-loaded PMS (mean±SEM, n = 25-118 cells over >2 experiments)

B) Proportion of invaginations with indicated lifetimes tracked from 20 minute TIRF timelapses of B1-8 B cells interacting with NP- or NIP-loaded PMS (mean±SEM, n = 25-118 cells over >2 experiments). *, $p<0.01$ in Mann-Whitney test between NP and NIP antigens

C) Rate of antigen microcluster growth. Antigen microclusters were tracked from 20 minute TIRF timelapses of B1-8 B cells interacting with NP or NIP-loaded PMS (mean±SEM, n=9 cells). ***, $p<0.001$ in Mann-Whitney test between NP and NIP antigens

D) Levels of antigen associated with invaginations of indicated lifetimes. Invaginations were tracked from 20 minute TIRF timelapse images of B1-8 B cells interacting with NP- or NIP-loaded PMS (mean±SEM, n = 25-118 cells over >2 experiments). *, $p<0.05$ in Mann-Whitney test between NP and NIP antigens

B-D Matlab analysis done by Pavel Tolar

5.2.3 Affinity discrimination is mediated by myosin IIA contractility

In Chapter 4 we observed that myosin IIA generated the force required to invaginate the presenting membrane during internalisation of membrane-bound antigen. As we have seen that high and low affinity antigens have different proportions of long-lived invaginations, we wanted to see if myosin IIA modulation affected the ability of B1-8 B cells to discriminate between high and low antigen affinities. To do this we inhibited myosin IIA activity in B1-8 B cells using blebbistatin treatment and analysed the extent of NP or NIP internalisation from the PMS. Interestingly we observed that although the internalisation of both antigens was inhibited at high concentrations of blebbistatin, lower concentrations seemed to improve internalisation levels of the low affinity NP antigen (Figure 27). This suggests that lower concentrations of blebbistatin may reduce the force exerted on the BCR-antigen complexes enough to improve the low affinity binding between the BCR and NP antigen, which would have quickly ruptured under normal myosin IIA activity, thereby increasing the chances of internalisation.

Collectively these results show that presentation of antigen by the PMS allows discrimination between antigens of different affinities that are indistinguishable in solution. High affinity antigen stimulates quicker production of BCR microclusters thereby also improving the antigen avidity. Increased affinity and avidity allow the formation of stronger and more stable BCR-antigen complexes, better resistance against the myosin IIA-generated force and improved internalisation. Therefore, these results provide a possible mechanism for how linking mechanical activity to antigen internalisation can allow the discrimination of membrane-bound antigen.

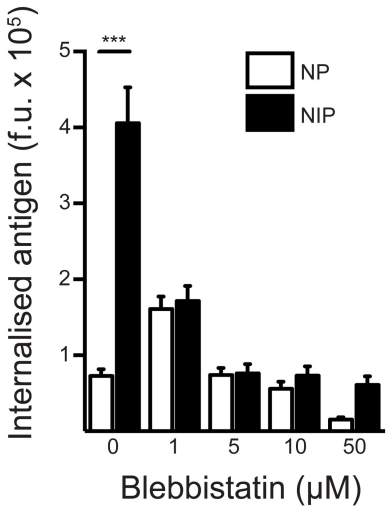

Figure 27: Modulation of myosin IIA activity affects the ability of B1-8 B cells to internalise membrane-bound antigen in an affinity-dependent manner

B1-8 B cells were treated with the indicated concentration of blebbistatin, and then incubated with NP- or NIP- loaded-PMS for 20 minutes at 37°C. B1-8 B cells were fixed before NP/NIP internalisation was analysed (means±SEM, n= 25-118 cells over 3 independent experiments). ***, $p<0.01$ in Mann-Whitney test between NP and NIP antigens

5.2.4 Deletion of myosin IIA in B cells prevents B cell development past the PrePro B cell stage

To begin to understand whether the ability of B cells to discriminate between antigen affinities was also lost following myosin IIA disruption *in vivo*, we generated mice with a B cell specific deletion of the *MyH9* gene. Mice expressing floxed myosin IIA heavy chain ($Myh9^{fl/fl}$) were crossed with mice that expressed Cre recominbase (Cre) under the Mb1 promoter. MyH9 is the only myosin IIA heavy chain expressed in lymphocytes therefore this deletion is expected to prevent any myosin IIA expression, and the *Mb1* gene encodes the Igα subunit of the BCR. Thus, at the point of Igα expression, which occurs at the very early Pro B cell stage in the bone marrow, Cre is expressed, and myosin IIA heavy chain is deleted. Mice need to be heterozygote for MB1-Cre, as homozygote mice have no B cells due to loss of Igα expression (Hobeika et al., 2006).

Before assessing whether or not B cells from these mice ($Cre^{+}MyH9^{fl/fl}$) are impaired in their ability to internalise antigen and discriminate between different

antigen affinities, we wanted to assess whether they had a normal B cell compartment. We isolated immune cells from the bone marrow, peritoneal exudate, inguinal and brachial lymph nodes, and spleen, and identified the B cell subsets in these organs using the cell markers shown in Table 1.

Table 1: B cell markers used to identify different B cell subsets harvested from mice

hi = high levels of expression, lo = low levels of expression, int = intermediate levels of expression.

Organ	B cell subset	B cell markers
Bone marrow	Pre pro B cells	$B220^{hi}$ $CD19^{lo}$
	All B cells	$B220^{hi}$ $CD19^{hi}$
	Pro B cells	$B220^{hi}$ $CD19^{hi}$ $CD2^{lo}$ IgM^{lo}
	Pre B cells	$B220^{hi}$ $CD19^{hi}$ $CD2^{hi}$ IgM^{lo}
	Immature B cells	$B220^{hi}$ $CD19^{hi}$ $CD2^{hi}$ IgM^{hi}
	Mature B cells	$B220^{hi}$ $CD19^{hi}$ $CD2^{hi}$ IgM^{hi} IgD^{hi}
Spleen	Mature B cells	$B220^{hi}$ $CD93^{lo}$
	All transitional B cells	$B220^{hi}$ $CD93^{hi}$
	Transitional B cells subset 1	$B220^{hi}$ $CD93^{hi}$ IgM^{hi} $CD23^{lo}$
	Transitional B cells subset 2	$B220^{hi}$ $CD93^{hi}$ IgM^{hi} $CD23^{hi}$
	Transitional B cells subset 3	$B220^{hi}$ $CD93^{hi}$ IgM^{int} $CD23^{hi}$
	Marginal zone B cells	$B220^{hi}$ $CD93^{lo}$ IgM^{hi} $CD23^{int}$
	Follicular B cells	$B220^{hi}$ $CD93^{lo}$ IgM^{hi} $CD23^{hi}$
Lymph nodes	All B cells	$B220^{hi}$ $TCR\beta^{lo}$
	Mature B cells	$B220^{hi}$ $TCR\beta^{lo}$ IgM^{hi} IgD^{hi}
Peritoneal exudate	All B cells	IgM^{hi} $CD5^{int}$
	B1a B cells	IgM^{hi} $CD5^{hi}$ $CD23^{lo}$
	B1b B cells	IgM^{hi} $CD5^{int}$ $CD23^{lo}$
	B2 B cells	IgM^{hi} $CD5^{int/lo}$ $CD23^{hi}$

In the bone marrow PrePro B cell numbers were found to be normal in $Cre^{+}MyH9^{fl/fl}$ mice but surprisingly Pro B cells were severely reduced (Figure 28A) and all subsets of B cells following Pro B cells in the bone marrow, spleen, lymph nodes and peritoneal exudate were also reduced by at least 90% compared to wild type B cells. This indicates that as soon as $Cre^{+}MyH9^{fl/fl}$ B cells express Igα and begin to loose myosin IIA, they can no longer survive and/or develop revealing a non-redundant function for myosin IIA at the Pro B cell stage (Figure 28). T cell numbers were unaffected in the lymph nodes suggesting that the myosin IIA defect was restricted to B cells as expected (Figure 28C).

However, T cell numbers were slightly reduced in the spleen (Figure 28B), which is likely due to the reduction in spleen size (Figure 29).

Because of the severe reduction in peripheral B cells from $Cre^{+}MyH9^{fl/fl}$ mice, we were unable to determine whether any surviving cells had deleted myosin IIA, and if they had, whether they were inhibited in their ability to internalise antigen and discriminate between antigen affinities, as seen following myosin IIA inhibition *in vitro*. However, we did observe that any $Cre^{+}MyH9^{fl/fl}$ B cells, which developed past the PrePro stage were consistently bigger in their size through all subsequent developmental stages, suggesting they were physiologically different to the wild type B cells and therefore possibly had deleted Myosin IIA (Figure 30). To fully assess the role of myosin IIA in antigen extraction and affinity discrimination, an inducible deletion in mature B cells will be necessary.

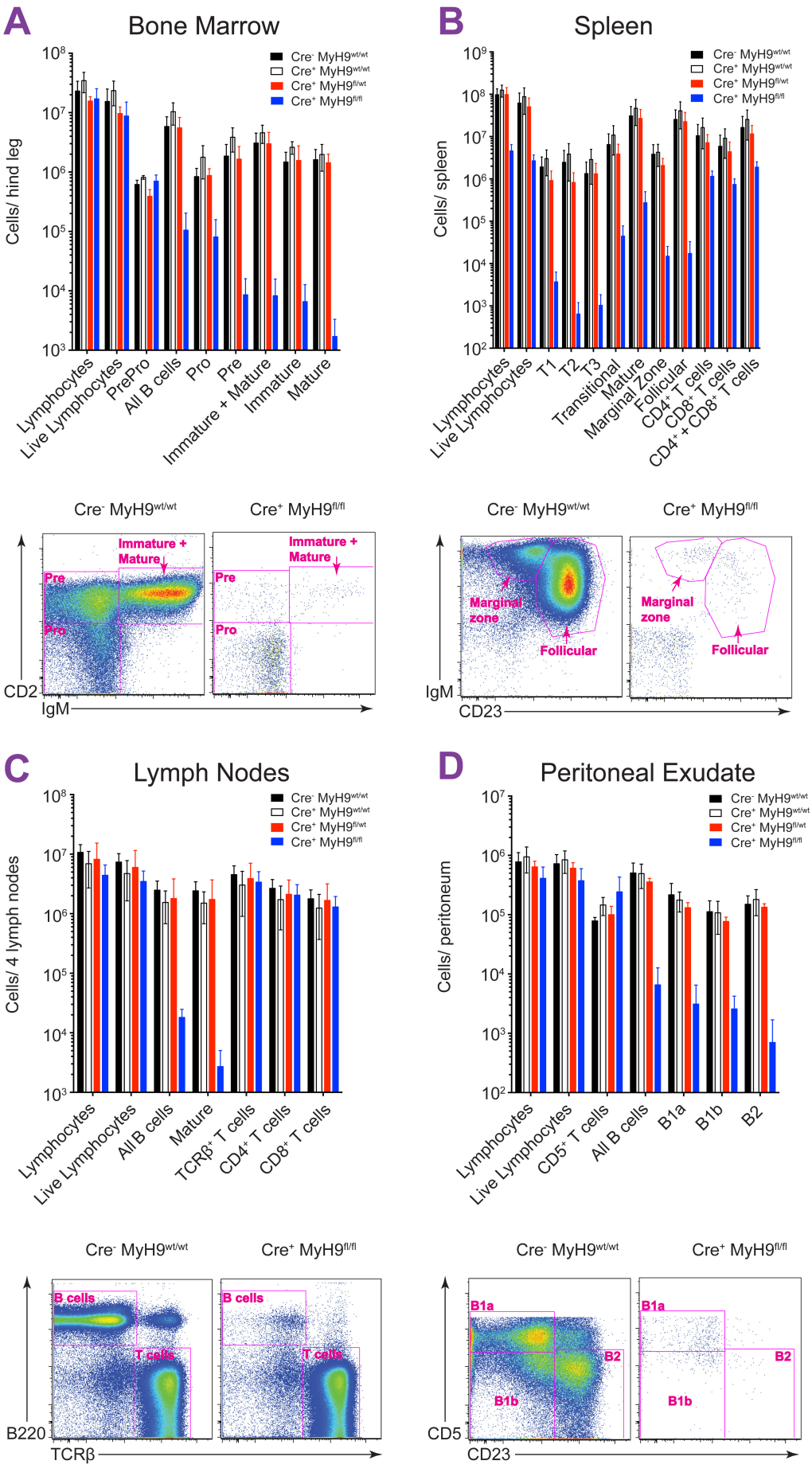
A
Bone Marrow
Cre- MyH9wt/wt
Cre+ MyH9wt/wt
Cre+ MyH9fl/wt
Cre+ MyH9fl/fl
Cells/ hind leg
Lymphocytes
Live Lymphocytes
PrePro
All B cells
Pro
Pre
Immature + Mature
Immature
Mature
B
Spleen
Cells/ spleen
Lymphocytes
Live Lymphocytes
T1
T2
T3
Transitional
Mature
Marginal Zone
Follicular
CD4+ T cells
CD8+ T cells
CD4+ +CD8+ T cells
Cre- MyH9wt/wt
Cre+ MyH9fl/fl
Immature + Mature
Pre
Pro
CD2
IgM
Marginal zone
Follicular
CD23
C
Lymph Nodes
Cells/ 4 lymph nodes
Lymphocytes
Live Lymphocytes
All B cells
Mature
TCRβ+ T cells
CD4+ T cells
CD8+ T cells
B cells
T cells
B220
TCRβ
D
Peritoneal Exudate
Cells/ peritoneum
Lymphocytes
Live Lymphocytes
CD5+ T cells
All B cells
B1a
B1b
B2
CD5
CD23

Figure 28: Cre^{+}MyH9$^{fl/fl}$ mice have a block in B cell development

A) Top panel: Absolute B cell numbers flushed from femur and tibia of rear left leg. Cells were stained for cell markers for 20 minutes on ice and absolute numbers were analysed using FlowJo. Bottom: Representative dot plot showing absence of B cells following the PrePro developmental stage. Cells shown were gated on B220^{hi}CD19^{hi} population

B) Top panel: Absolute B cell numbers and T cell numbers harvested from mashed spleen. Cells were stained for cell markers for 20 minutes on ice and absolute numbers were analysed using FlowJo. Bottom: Representative dot plot showing absence of follicular and marginal zone B cells. Cells shown were gated on B220^{hi}CD93^{lo} population

C) Top panel: Absolute B cell and T cell numbers harvested from mashed brachial and inguinal lymph nodes. Cells were stained for cell markers for 20 minutes on ice and absolute numbers were analysed using FlowJo. Bottom: Representative dot plot showing absence of B cells but an intact T cell compartment

D) Top panel: Absolute B cell numbers flushed from the peritoneal cavity. Cells were stained for cell markers for 20 minutes on ice and absolute numbers were analysed using FlowJo. Bottom: Representative dot plot showing absence of B1 and B2 cells. Cells shown were gated on IgM^{hi}CD5^{int} population

In all panels live B cells were identified as negative for the Live/Dead stain and then B cell subsets were identified using the cell markers described in Table 1 (mean±SEM, n= 3-4 mice for each genotype). Mice were used at 7-9 weeks of age

These experiments were done in collaboration with Harold Hartweger.

Figure 29: Cre^{+}MyH9$^{fl/fl}$ mice have smaller spleens compared to controls

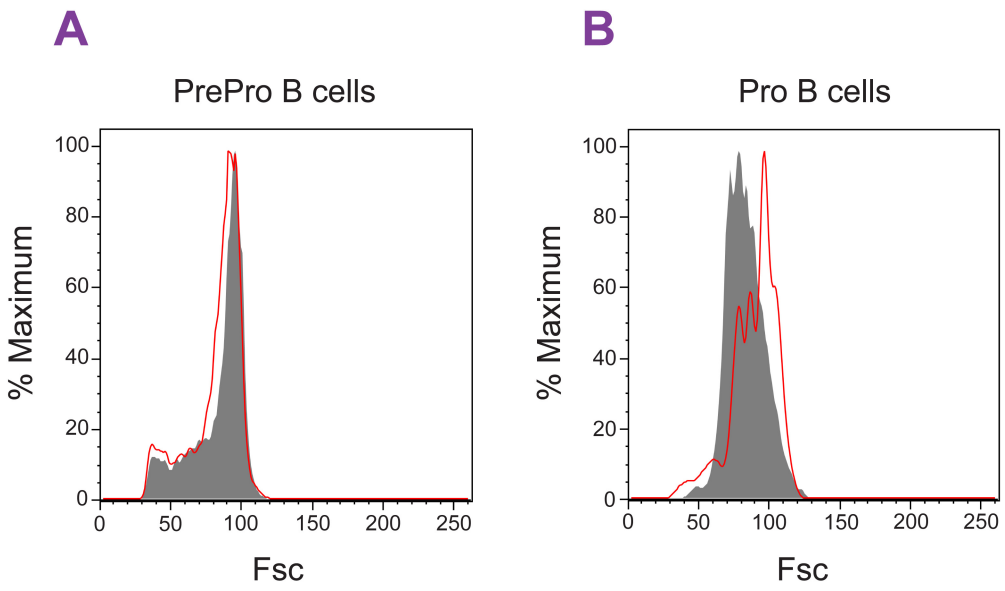

Figure 30: Cre^{+}MyH9$^{fl/fl}$ B cells which develop past the PrePro stage in the bone marrow are larger

A) Cre^{+}MyH9$^{fl/fl}$ (red) and wild type (grey) PrePro B cells. Cells shown were gated on B220^{hi}CD19^{lo}

B) Cre^{+}MyH9$^{fl/fl}$ (red) and wild type (grey) Pro B cells. Cells shown were gated on B220^{hi}CD19^{hi}CD2^{lo}IgM^{lo}

Representative plots from 1 of 3 experiments shown in Figure 28

5.3 Discussion

By using PMS as surrogates for APCs, we have demonstrated that B cells internalise membrane-bound antigen depending on their affinity.

The antigens used in this study consist of 15 NP or NIP haptens complexed with a protein carrier. These antigens have much higher avidity than monomeric antigen, therefore, the subtle differences in affinity were masked when exposed to B cells in solution (Batista and Neuberger, 2000). However, when these same antigens were tethered to the PMS, B cells were able to discriminate between their affinities and they internalised the higher affinity antigen to a greater extent. By tracking the invaginations and BCR microclusters formed in the B1-8 B cell synapse, we saw that B1-8 B cells sustained more long-lived invaginations, produced BCR-antigen microclusters faster, and had more antigen associated with the long-lived invaginations. These studies support other investigations

using PLB as a surrogate for APCs, which show that BCRs have increased spreading and signalling in response to higher affinity antigen and suggest that affinity discrimination is an intrinsic function of the BCR (Fleire et al., 2006; Liu et al., 2010; Wan et al., 2013).

B cells can discriminate between a large range of antigen affinities. Due to the bivalency of the BCR and the high avidity nature of most physiologically relevant antigens, it is possible that the half-lives of BCR-antigen complexes could reach many hours (Batista and Neuberger, 1998). We found that by inhibiting myosin IIA contractility and decreasing the mechanical pressure exerted on the BCR-antigen bonds, the internalisation rate of the low affinity antigens was improved. This suggests that under normal conditions, myosin IIA contractility shortens the lifetime of the BCR-antigen bonds thereby ensuring affinity discrimination occurs over seconds rather than hours and acts as a checkpoint so that only antigens of high enough affinity are internalised. Therefore this mechanism could be important in preventing the internalisation of lower affinity antigens, which could lead to inappropriate B cell activation.

Collectively, these results suggest a model whereby BCRs with a higher affinity for the antigens, produce bigger BCR microclusters faster, this together with the increased strength of the individual high-affinity BCR-antigen bonds, better resists the myosin IIA-generated force, and the invaginations last long enough to allow the full assembly of the CCSs and internalisation. In contrast, low affinity antigens produce BCR microclusters more slowly, which combined with the weaker BCR-antigen interactions, cannot withstand the myosin IIA contractility and the bonds rupture, aborting internalisation. This mechanism provides a possible link for how the increased B cell signalling in response to high-affinity membrane-bound antigen leads to increased antigen internalisation and presentation, required for higher levels of T cell help and B cell proliferation to ensure a competitive advantage over low affinity antigens *in vivo* (Khalil et al., 2012; Schwickert et al., 2011; Shih et al., 2002a; 2002b; Victora et al., 2010).

In vivo, when B cells come into contact with APC-tethered antigen they will also see many other signals such as integrin ligands, complement, and other co-

stimulatory molecules, which may fine tune the B cell response (Carrasco and Batista, 2006a; Carrasco et al., 2004; Chan and Brink, 2012; Suzuki et al., 2009; Wan et al., 2013). In addition, active forces generated by APCs may also influence this process. Therefore, future studies will be necessary to understand how various APCs can further regulate antigen extraction and B cell affinity discrimination *in vivo*.

To assess the role of myosin IIA in BCR-antigen internalisation *in vivo* we produced mice with B cell specific deletion of the *MyH9* gene and therefore myosin IIA ($Cre^{+}MyH9^{fl/fl}$). However, analysis of B cell responses was not possible, as these mice had very few peripheral B cells. The loss of B cells during development was observed at the Pro B cell stage in the bone marrow, exactly when the Mb1-controlled Cre recombinase is expressed (Hobeika et al., 2006). This was not due to loss of Igα, as Igα deficient B cells are arrested at the later Pro B cell to Pre B cell transition (Pelanda et al., 2002), therefore supporting the finding that the loss of B cells was due to myosin IIA deletion by the Cre recombinase.

The loss of B cells in $Cre^{+}MyH9^{fl/fl}$ mice before signalling from the Pre-BCR, which occurs at the Pre B cell stage (Figure 4) (Mårtensson et al., 2010; Wang and Clark, 2003), indicates a role for myosin IIA in B cell development that is separate from its role in BCR-antigen internalisation. Given the important roles myosin IIA has in cell biology, there are many possibilities for why loss of myosin IIA is incompatible with the survival or differentiation of B cell progenitors. In our study we observed that the few $Cre^{+}MyH9^{fl/fl}$ B cells, which made it past the PrePro stage, were consistently larger than wild type B cells. This could suggest that myosin IIA may be required for cytokinesis during B cell division (Matsumura, 2005), which would prevent B cells from completing mitosis needed during B cell development. However, it is generally thought that B cells do not proliferate until exiting the Pro B cell stage and entering the Pre B cell stage, therefore this is unlikely to be the sole cause of the defect seen in our studies (Hardy et al., 1991). This could be resolved by staining the DNA in these cells to understand if they have been arrested at the telophase stage of mitosis. Alternatively, the

enlarged B cells could be explained by loss of cortical tension, which may stimulate cell death due to loss of internal cellular structure and organisation.

Another possible reason for loss of B cells at the Pro B cell stage could be due to lack of survival signals. Myosin IIA activity has been shown to be important for cell migration and adhesion (Vicente-Manzanares et al., 2009). If $Cre^{+}MyH9^{fl/fl}$ B cells were unable to migrate across, or interact with, the stromal cells in the bone marrow during development, this could lead to developmental arrest. For instance, B cells have been shown to migrate between CXCL12-producing stromal cells and IL-7-producing cells during development to receive differentiation and survival components (Nagasawa, 2006). So, if the B cells are unable to migrate across these stromal cells they may die due to lack of appropriate stimulation. It would be interesting in the future to investigate downstream signalling in these myosin IIA deficient B cells to understand whether they are able to respond to survival signals such as IL-7. Therefore, the exact cause for $Cre^{+}MyH9^{fl/fl}$ B cell loss during development will have to be addressed by further study.

Independently, to address the question of whether myosin IIA contractility is involved in antigen internalisation and affinity discrimination *in vivo*, $MyH9^{fl/fl}$ mice will need to be crossed with mice expressing Cre recombinase under a promoter which becomes active only in mature B cells, such as the promoter for CD23, or is induced by drug treatment, such as doxycycline. We will then be able to take mature B cells from these mice and observe their internalisation and affinity discrimination on antigen-loaded PMS *in vitro*, as well as stimulating B cells *in vivo* to see whether loss of myosin IIA inhibits the ability of B cells to respond to antigen in the lymph node.

In conclusion, here we have demonstrated an important role for myosin IIA-generated force in affinity-dependent antigen internalisation *in vitro*. The understanding of whether this mechanism is still relevant *in vivo* is still to be elucidated and is actively being investigated in the lab.

Chapter 6 Conclusions

The aim of this thesis was to investigate and identify novel components and mechanisms involved in BCR-antigen internalisation, particularly focusing on acquisition of antigen from APCs. Antigen internalisation from APCs has been previously shown at the cellular level by intravital imaging. These studies demonstrated that in response to immunisation, cognate B cells interact with APCs over several minutes, during which they become activated and extract the antigen (Carrasco and Batista, 2007; Phan et al., 2007; Qi et al., 2006; Suzuki et al., 2009). This antigen extraction and subsequent internalisation is critical for the production of T cell-dependent B cell responses. However the molecular mechanisms controlling antigen internalisation from APCs are unknown.

To investigate the mechanisms of membrane-bound antigen acquisition, we developed a new antigen-presenting substrate from adherent HEK293A cells, PMS. These PMS were able to support membrane-bound antigen internalisation by B cells in an in an *in vitro* setting. Live-cell imaging of B cell interaction with antigen-loaded PMS revealed that B cells spread over the antigen forming BCR-antigen microclusters. This spreading was followed by B cell invagination of the PMS membrane. The lifetime of these invaginations depended on antigen affinity for the BCR and the extent of BCR-antigen microclustering. BCR-antigen complexes with sufficient affinity and avidity were able to withstand the ~20 pN force exerted by the B cells during invagination formation long enough for internalisation to occur.

To identify the pathways controlling this process we used 2 approaches. The first was shRNA-mediated knockdown of target proteins in Ramos B cells, and the second was inhibition of these proteins using small molecule inhibitors in primary Bl6 B cells. Both strategies identified a sequential role for myosin IIA and clathrin in antigen extraction and endocytosis.

We then used live-cell TIRF microscopy to visualise the activity of these proteins during the internalisation process. These experiments showed that myosin IIA

activity peaked immediately before the onset of membrane invagination, whereas clathrin was only recruited during the termination of long-lived invaginations.

Comparisons of the internalisation process between antigens of low and high affinity revealed that B cells internalised antigen from the PMS in an affinity-dependent manner. High affinity antigens stimulated faster BCR-antigen microcluster formation, more long-lived invaginations, and higher levels of invagination-associated antigen, which led to a greater amount of antigen internalisation.

Taking these results together we present a model by which, after initial antigen binding, B cells spread over the antigen-presenting surface forming BCR-antigen microclusters and invaginating the presenting surface in a myosin IIA-dependent manner. If an invagination is initiated on a big enough BCR-microcluster with a sufficient level of affinity within the BCR-antigen complex, the BCR is able to withstand the force generated by myosin IIA and the invagination persists long enough for clathrin recruitment and BCR-antigen internalisation (Figure 31).

Figure 31: BCR internalisation of membrane-bound antigen

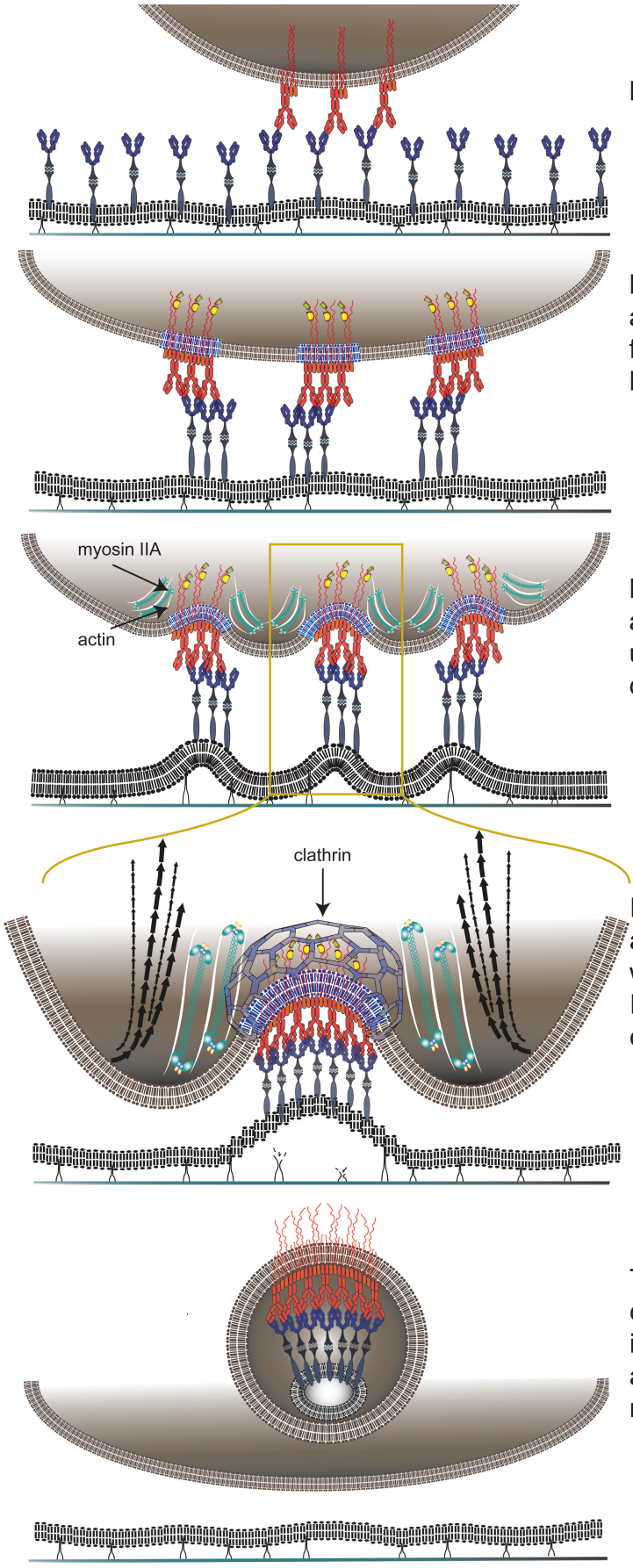

BCRs recognise antigen

B cells spread over the antigen-presenting surface forming signalling-active BCR-antigen microclusters

B cells invaginate the antigen-presenting surface using myosin IIA contractility

If the affinity of the antigen is high enough to withstand the myosin IIA-dependent force, clathrin is recruited

The BCR-antigen complexes are then internalised in a clathrin- and actin-dependent manner

Therefore, we can conclude that coupling myosin IIA contractility to endocytosis permits B cells to internalise antigen in an affinity-dependent manner. This is particularly important at the initiation of the immune response in the B cell follicle, and during affinity maturation in the germinal centre, when the selective expansion of B cell clones depends on the relative amount of antigen internalised and presented to cognate T cells (Paus et al., 2006; Schwickert et al., 2011; Victora et al., 2010).

The *in vitro* based studies presented in this thesis of BCR-antigen internalisation, gave us an insight into the components and mechanisms involved in BCR-antigen internalisation in the context of B cell synapses with APCs. However, BCR-antigen internalisation has the potential to be highly flexible, making investigations into this process difficult. This is supported by studies showing that loss of clathrin, actin or lipid rafts, or any other protein identified as mediating internalisation, decreased the level of BCR antigen-internalisation but did not inhibit it completely, suggesting a high level of redundancy within this process (Becker-Herman et al., 2011; Ma et al., 2001; Malhotra et al., 2009a; 2009b; Niiro et al., 2004; Stoddart et al., 2002; 2005). This is likely to have evolved as B cells are required to recognise and internalise many different possible infections such as bacteria, viruses, fungi, and parasites as well as any type of environmental or synthetic chemical they may come across, which would suggest a necessary level of flexibility in antigen internalisation to be able to accommodate a wide variety antigen sizes and shapes (Chan and Brink, 2012).

Different subtypes of B cells themselves may also internalise antigens in different ways. For example, memory B cells are likely to recognise antigen with a much higher affinity than naïve B cells, and the increase in BCR signalling following high affinity antigen binding, may stimulate a different pathway of internalisation (Kouskoff et al., 1998; Liu et al., 2010).

Finally studies have shown that molecules on the surface of APCs can fine tune and alter the B cell response (Allen and Cyster, 2008; Carrasco and Batista, 2006a; Carrasco et al., 2004; Lanoue et al., 2002), but the types of co-stimulatory molecules can differ in their type and expression between different types of APC,

which may also change the way B cells recognise and internalise antigen (Batista and Harwood, 2009).

In nearly all of the BCR-antigen internalisation studies done to date with soluble antigen, or antigen presented on PLB or PMS, protein antigens with either primary naïve B cells or B cell lines have been used. It would be of great interest in the future to build on these studies by completing the genetic screen begun in the course of this thesis, to put together a molecular pathway for how this process occurs in these conditions, and then develop these findings by seeing how the molecular requirements can change depending on B cell type, APC and antigen used. This would give us a clearer indication for how B cells undergo BCR-antigen internalisation and activation *in vivo*.

Ultimately the knowledge gained from studying BCR-antigen internalisation will hopefully contribute to the design and development of immunotherapy and effective vaccine design. BCR-antigen internalisation is an intricately controlled process that initiates the antibody response. Therefore, inhibition or augmentation of this process is an attractive target in the treatment of autoimmunity and cancer, or vaccine design, respectively. For example, studies have shown that antigens targeted to APCs can boost the effectiveness of immunisations (Caminschi and Shortman, 2012), therefore understanding the relevance of membrane-presented antigen is likely going to be highly applicable in rational design of future vaccines. Similarly, as disruptions in internalisation can potentially contribute to the growth of malignant B cells, targeting B cell trafficking may also be of therapeutic potential (Davis et al., 2010; Young and Staudt, 2013).

These studies signify that by increasing our understanding of BCR-antigen internalisation, we can open the door to a range of possible new targets for the treatment or prevention of B cell diseases.

References

Allen, C.D.C., and Cyster, J.G. (2008). Follicular dendritic cell networks of primary follicles and germinal centers: phenotype and function. Seminars in Immunology *20*, 14–25.

Andrian, von, U.H., and Mempel, T.R. (2003). Homing and cellular traffic in lymph nodes. Nature Reviews Immunology *3*, 867–878.

Arana, E., Vehlow, A., Harwood, N.E., Vigorito, E., Henderson, R., Turner, M., Tybulewicz, V.L.J., and Batista, F.D. (2008). Activation of the Small GTPase Rac2 via the B Cell Receptor Regulates B Cell Adhesion and Immunological-Synapse Formation. Immunity *28*, 88–99.

Arnon, T.I., Horton, R.M., Grigorova, I.L., and Cyster, J.G. (2012). Visualization of splenic marginal zone B-cell shuttling and follicular B-cell egress. Nature *493*, 684–688.

Attwood, S., Choi, Y., and Leonenko, Z. (2013). Preparation of DOPC and DPPC Supported Planar Lipid Bilayers for Atomic Force Microscopy and Atomic Force Spectroscopy. International Journal of Molecular Sciences *14*, 3514–3539.

Bajénoff, M., and Germain, R.N. (2009). B-cell follicle development remodels the conduit system and allows soluble antigen delivery to follicular dendritic cells. Blood *114*, 4989–4997.

Balázs, M., Martin, F., Zhou, T., and Kearney, J.F. (2002). Blood Dendritic Cells Interact with Splenic Marginal Zone B Cells to Initiate T-Independent Immune Responses. Cell *17*, 341–352.

Batista, F.D., and Neuberger, M.S. (1998). Affinity Dependence of the B Cell Response to Antigen: A Threshold, a Ceiling, and the Importance of Off-Rate. Cell *8*, 751–759.

Batista, F.D., and Neuberger, M.S. (2000). B cells extract and present immobilized antigen: implications for affinity discrimination. EMBO Journal *19*, 513–520.

Batista, F., and Harwood, N. (2009). The who, how and where of antigen presentation to B cells. Nature Reviews Immunology *9*, 15–27.

Batista, F., Iber, D., and Neuberger, M. (2001). B cells acquire antigen from target cells after synapse formation. Nature *411*, 489–494.

Bauer, S., Kirschning, C.J., Häcker, H., Redecke, V., Hausmann, S., Akira, S., Wagner, H., and Lipford, G.B. (2001). Human TLR9 confers responsiveness to bacterial DNA via species-specific CpG motif recognition. Proceedings of the National Academy of Sciences *98*, 9237–9242.

Becker-Herman, S., Meyer-Bahlburg, A., Schwartz, M.A., Jackson, S.W., Hudkins, K.L., Liu, C., Sather, B.D., Khim, S., Liggitt, D., Song, W., et al. (2011). WASp-deficient B cells play a critical, cell-intrinsic role in triggering autoimmunity. The Journal of Experimental Medicine *208*, 2033–2042.

Bergtold, A., Desai, D.D., Gavhane, A., and Clynes, R. (2005). Cell Surface Recycling of Internalized Antigen Permits Dendritic Cell Priming of B Cells. Cell *23*, 503–514.

Berney, C., Herren, S., Power, C.A., Gordon, S., Martinez-Pomares, L., and Kosco-Vilbois, M.H. (1999). A member of the dendritic cell family that enters B cell follicles and stimulates primary antibody responses identified by a mannose receptor fusion protein. The Journal of Experimental Medicine *190*, 851–860.

Bléry, M., Tze, L., Miosge, L.A., Jun, J.E., and Goodnow, C.C. (2006). Essential role of membrane cholesterol in accelerated BCR internalization and uncoupling from NF-κB in B cell clonal anergy. The Journal of Experimental Medicine *203*, 1773–1783.

Boettner, D.R., Chi, R.J., and Lemmon, S.K. (2011). Lessons from yeast for clathrin-mediated endocytosis. Nature Cell Biology *14*, 2–10.

Bonnerot, C., Lankar, D., Hanau, D., Spehner, D., Davoust, J., Salamero, J., and Fridman, W.H. (1995). Role of B cell receptor Ig alpha and Ig beta subunits in MHC class II-restricted antigen presentation. Immunity *3*, 335–347.

Boucrot, E., Saffarian, S., Zhang, R., and Kirchhausen, T. (2010). Roles of AP-2 in clathrin-mediated endocytosis. PLoS ONE *5*, e10597.

Boulant, S., Kural, C., Zeeh, J.-C., Ubelmann, F., and Kirchhausen, T. (2011). Actin dynamics counteract membrane tension during clathrin-mediated endocytosis. Nature Cell Biology *13*, 1124–1131.

Brown, B.K., and Song, W. (2001). The Actin Cytoskeleton is Required for the Trafficking of the B Cell Antigen Receptor to the Late Endosomes. Traffic *2*, 414–427.

Calabia-Linares, C., Robles-Valero, J., la Fuente, de, H., Perez-Martinez, M., Martín-Cofreces, N., Alfonso-Pérez, M., Gutierrez-Vázquez, C., Mittelbrunn, M., Ibiza, S., Urbano-Olmos, F.R., et al. (2011). Endosomal clathrin drives actin accumulation at the immunological synapse. Journal of Cell Science *124*, 820–830.

Cambier, J.C., Gauld, S.B., Merrell, K.T., and Vilen, B.J. (2007). B-cell anergy: from transgenic models to naturally occurring anergic B cells? Nature Reviews Immunology *7*, 633–643.

Caminschi, I., and Shortman, K. (2012). Boosting antibody responses by targeting antigens to dendritic cells. Trends in Immunology *33*, 71–77.

Carrasco, Y.R., and Batista, F.D. (2006a). B-cell activation by membrane-bound antigens is facilitated by the interaction of VLA-4 with VCAM-1. EMBO Journal

25, 889–899.

Carrasco, Y.R., and Batista, F.D. (2007). B cells acquire particulate antigen in a macrophage-rich area at the boundary between the follicle and the subcapsular sinus of the lymph node. Immunity *27*, 160–171.

Carrasco, Y., and Batista, F. (2006b). B cell recognition of membrane-bound antigen: an exquisite way of sensing ligands. Current Opinion in Immunology *18*, 286–291.

Carrasco, Y., Fleire, S., Cameron, T., Dustin, M., and Batista, F. (2004). LFA-1/ICAM-1 interaction lowers the threshold of B cell activation by facilitating B cell adhesion and synapse formation. Immunity *20*, 589–599.

Carroll, M.C. (1998). The role of complement and complement receptors in induction and regulation of immunity. Annual Review of Immunology *16*, 545–568.

Cassard, S., Salamero, J., Hanau, D., Spehner, D., Davoust, J., Fridman, W.H., and Bonnerot, C. (1998). A tyrosine-based signal present in Ig alpha mediates B cell receptor constitutive internalization. The Journal of Immunology *160*, 1767–1773.

Catron, D.M., Pape, K.A., Fife, B.T., van Rooijen, N., and Jenkins, M.K. (2010). A protease-dependent mechanism for initiating T-dependent B cell responses to large particulate antigens. The Journal of Immunology *184*, 3609–3617.

Chan, T.D., and Brink, R. (2012). Affinity-based selection and the germinal center response. Immunological Reviews *247*, 11–23.

Chan, T.D., Wood, K., Hermes, J.R., Butt, D., Jolly, C.J., Basten, A., and Brink, R. (2012). Elimination of Germinal-Center-Derived Self-Reactive B Cells Is Governed by the Location and Concentration of Self-Antigen. Cell *37*, 893–904.

Chan, V.W.F., Lowell, C.A., and DeFranco, A.L. (1998). Defective negative regulation of antigen receptor signaling in Lyn-deficient B lymphocytes. Current Biology *8*, 545–553.

Chan, V., Meng, F., Soriano, P., DeFranco, A., and Lowell, C. (1997). Characterization of the B lymphocyte populations in Lyn-deficient mice and the role of Lyn in signal initiation and down-regulation. Immunity *7*, 69–81.

Chappell, C.P., Draves, K.E., Giltiay, N.V., and Clark, E.A. (2012). Extrafollicular B cell activation by marginal zone dendritic cells drives T cell-dependent antibody responses. The Journal of Experimental Medicine *209*, 1825–1840.

Chaturvedi, A., Dorward, D., and Pierce, S. (2008). The B cell receptor governs the subcellular location of Toll-like receptor 9 leading to hyperresponses to DNA-containing antigens. Immunity *28*, 799–809.

Chaturvedi, A., Martz, R., Dorward, D., Waisberg, M., and Pierce, S.K. (2011).

Endocytosed BCRs sequentially regulate MAPK and Akt signaling pathways from intracellular compartments. Nature Immunology *12*, 1119–1126.

Chen, C., Radic, M.Z., Erikson, J., Camper, S.A., Litwin, S., Hardy, R.R., and Weigert, M. (1994). Deletion and editing of B cells that express antibodies to DNA. The Journal of Immunology *152*, 1970–1982.

Cheng, P.C., Brown, B.K., Song, W., and Pierce, S.K. (2001). Translocation of the B cell antigen receptor into lipid rafts reveals a novel step in signaling. The Journal of Immunology *166*, 3693–3701.

Cheng, P.C., Dykstra, M.L., Mitchell, R.N., and Pierce, S.K. (1999). A role for lipid rafts in B cell antigen receptor signaling and antigen targeting. The Journal of Experimental Medicine *190*, 1549–1560.

Christensen, S.R. (2005). Toll-like receptor 9 controls anti-DNA autoantibody production in murine lupus. The Journal of Experimental Medicine *202*, 321–331.

Cinamon, G., Zachariah, M., Lam, O., Foss, F., and Cyster, J. (2007). Follicular shuttling of marginal zone B cells facilitates antigen transport. Nature Immunology *9*, 54–62.

Collinet, C., Stöter, M., Bradshaw, C., Samusik, N., Rink, J., Kenski, D., Habermann, B., Buchholz, F., Henschel, R., and Mueller, M. (2010). Systems survey of endocytosis by multiparametric image analysis. Nature *464*, 243–249.

Conti, M.A., and Adelstein, R.S. (2008). Nonmuscle myosin II moves in new directions. Journal of Cell Science *121*, 11–18.

Cureton, D.K., Massol, R.H., Saffarian, S., Kirchhausen, T.L., and Whelan, S.P.J. (2009). Vesicular stomatitis virus enters cells through vesicles incompletely coated with clathrin that depend upon actin for internalization. PLoS Pathogens *5*, e1000394.

Cureton, D.K., Massol, R.H., Whelan, S.P.J., and Kirchhausen, T. (2010). The length of vesicular stomatitis virus particles dictates a need for actin assembly during clathrin-dependent endocytosis. PLoS Pathogens *6*, e1001127.

Cyster, J.G., Ansel, K.M., Reif, K., Ekland, E.H., Hyman, P.L., Tang, H.L., Luther, S.A., and Ngo, V.N. (2000). Follicular stromal cells and lymphocyte homing to follicles. Immunological Reviews *176*, 181–193.

Cyster, J. (2010). B cell follicles and antigen encounters of the third kind. Nature Immunology *11*, 989–996.

Dal Porto, J.M., Haberman, A.M., Shlomchik, M.J., and Kelsoe, G. (1998). Antigen drives very low affinity B cells to become plasmacytes and enter germinal centers. The Journal of Immunology *161*, 5373–5381.

Dal Porto, J.M., Gauld, S.B., Merrell, K.T., Mills, D., Pugh-Bernard, A.E., and Cambier, J. (2004). B cell antigen receptor signaling 101. Molecular

Immunology *41*, 599–613.

Dal Porto, J.M., Haberman, A.M., Kelsoe, G., and Shlomchik, M.J. (2002). Very low affinity B cells form germinal centers, become memory B cells, and participate in secondary immune responses when higher affinity competition is reduced. The Journal of Experimental Medicine *195*, 1215–1221.

Davidson, H.W., Reid, P.A., Lanzavecchia, A., and Watts, C. (1991). Processed antigen binds to newly synthesized MHC class II molecules in antigen-specific B lymphocytes. Cell *67*, 105–116.

Davis, R., Ngo, V., Lenz, G., Tolar, P., Young, R., Romesser, P., Kohlhammer, H., Lamy, L., Zhao, H., and Yang, Y. (2010). Chronic active B-cell-receptor signalling in diffuse large B-cell lymphoma. Nature *463*, 88–92.

Delamarre, L., Pack, M., Chang, H., Mellman, I., and Trombetta, E.S. (2005). Differential lysosomal proteolysis in antigen-presenting cells determines antigen fate. Science *307*, 1630–1634.

Depoil, D., Fleire, S., Treanor, B., Weber, M., Harwood, N., Marchbank, K., Tybulewicz, V., and Batista, F. (2007). CD19 is essential for B cell activation by promoting B cell receptor–antigen microcluster formation in response to membrane-bound ligand. Nature Immunology *9*, 63–72.

Ehrlich, M., Boll, W., Van Oijen, A., Hariharan, R., Chandran, K., Nibert, M.L., and Kirchhausen, T. (2004). Endocytosis by random initiation and stabilization of clathrin-coated pits. Cell *118*, 591–605.

Ezratty, E.J., Bertaux, C., Marcantonio, E.E., and Gundersen, G.G. (2009). Clathrin mediates integrin endocytosis for focal adhesion disassembly in migrating cells. The Journal of Cell Biology *187*, 733–747.

Fang, Y., Xu, C., Fu, Y.X., Holers, V.M., and Molina, H. (1998). Expression of complement receptors 1 and 2 on follicular dendritic cells is necessary for the generation of a strong antigen-specific IgG response. The Journal of Immunology *160*, 5273–5279.

Ferguson, A.R., Youd, M.E., and Corley, R.B. (2004). Marginal zone B cells transport and deposit IgM-containing immune complexes onto follicular dendritic cells. International Immunology *16*, 1411–1422.

Fleire, S.J., Goldman, J.P., Carrasco, Y.R., Weber, M., Bray, D., and Batista, F.D. (2006). B cell ligand discrimination through a spreading and contraction response. Science *312*, 738–741.

Gazumyan, A., Reichlin, A., and Nussenzweig, M.C. (2006). Igβ tyrosine residues contribute to the control of B cell receptor signaling by regulating receptor internalization. The Journal of Experimental Medicine *203*, 1785–1794.

Goffinet, C., and Keppler, O.T. (2006). Efficient nonviral gene delivery into primary lymphocytes from rats and mice. The FASEB Journal *20*, 500–502.

Gong, S., and Nussenzweig, M.C. (1996). Regulation of an early developmental checkpoint in the B cell pathway by Ig beta. Science *272*, 411–414.

Gonzalez, S.F., Degn, S.E., Pitcher, L.A., Woodruff, M., Heesters, B.A., and Carroll, M.C. (2011). Trafficking of B cell antigen in lymph nodes. Annual Review of Immunology *29*, 215–233.

Gonzalez, S.F., Lukacs-Kornek, V., Kuligowski, M.P., Pitcher, L.A., Degn, S.E., Turley, S.J., and Carroll, M.C. (2010a). Complement-dependent transport of antigen into B cell follicles. The Journal of Immunology *185*, 2659–2664.

Gonzalez, S., Kuligowski, M., Pitcher, L., Roozendaal, R., and Carroll, M. (2010b). The Role of Innate Immunity in B Cell Acquisition of Antigen Within LNs. Advances in Immunology *106*, 1–19.

Gonzalez, S., Lukacs-Kornek, V., Kuligowski, M., Pitcher, L., Degn, S., Kim, Y., Cloninger, M., Martinez-Pomares, L., Gordon, S., and Turley, S. (2010c). Capture of influenza by medullary dendritic cells via SIGN-R1 is essential for humoral immunity in draining lymph nodes. Nature Immunology *11*, 427–434.

Goodnow, C.C. (1997). Chance encounters and organized rendezvous. Immunological Reviews *156*, 5–10.

Goodnow, C.C., Crosbie, J., Adelstein, S., Lavoie, T.B., Smith-Gill, S.J., Brink, R.A., Pritchard-Briscoe, H., Wotherspoon, J.S., Loblay, R.H., and Raphael, K. (1988). Altered immunoglobulin expression and functional silencing of self-reactive B lymphocytes in transgenic mice. Nature *334*, 676–682.

Grakoui, A., Bromley, S.K., Sumen, C., Davis, M.M., Shaw, A.S., Allen, P.M., and Dustin, M.L. (1999). The immunological synapse: a molecular machine controlling T cell activation. Science *285*, 221–227.

Gresch, O. (2004). New non-viral method for gene transfer into primary cells. Methods *33*, 151–163.

Gretz, J.E., Norbury, C.C., Anderson, A.O., Proudfoot, A.E., and Shaw, S. (2000). Lymph-borne chemokines and other low molecular weight molecules reach high endothelial venules via specialized conduits while a functional barrier limits access to the lymphocyte microenvironments in lymph node cortex. The Journal of Experimental Medicine *192*, 1425–1440.

Han, S., Hathcock, K., Zheng, B., Kepler, T.B., Hodes, R., and Kelsoe, G. (1995). Cellular interaction in germinal centers. Roles of CD40 ligand and B7-2 in established germinal centers. The Journal of Immunology *155*, 556–567.

Hardy, R.R., and Hayakawa, K. (2001). B cell development pathways. Annual Review of Immunology *19*, 595–621.

Hardy, R.R., Carmack, C.E., Shinton, S.A., Kemp, J.D., and Hayakawa, K. (1991). Resolution and characterization of pro-B and pre-pro-B cell stages in normal mouse bone marrow. The Journal of Experimental Medicine *173*, 1213–1225.

Hartley, S.B., Crosbie, J., Brink, R., Kantor, A.B., Basten, A., and Goodnow, C.C. (1991). Elimination from peripheral lymphoid tissues of self-reactive B lymphocytes recognizing membrane-bound antigens. Nature *353*, 765–769.

Hasler, P., and Zouali, M. (2001). B cell receptor signaling and autoimmunity. The FASEB Journal *15*, 2085–2098.

Heesters, B.A., Chatterjee, P., Kim, Y.-A., Gonzalez, S.F., Kuligowski, M.P., Kirchhausen, T., and Carroll, M.C. (2013). Endocytosis and Recycling of Immune Complexes by Follicular Dendritic Cells Enhances B Cell Antigen Binding and Activation. Cell *38*, 1164–1175.

Heinen, E., Braun, M., Coulie, P.G., Van Snick, J., Moeremans, M., Cormann, N., Kinet-Denoël, C., and Simar, L.J. (1986). Transfer of immune complexes from lymphocytes to follicular dendritic cells. European Journal of Immunology *16*, 167–172.

Hibbs, M.L., Harder, K.W., Armes, J., Kountouri, N., Quilici, C., Casagranda, F., Dunn, A.R., and Tarlinton, D.M. (2002). Sustained Activation of Lyn Tyrosine Kinase In Vivo Leads to Autoimmunity. The Journal of Experimental Medicine *196*, 1593–1604.

Hobeika, E., Thiemann, S., Storch, B., Jumaa, H., Nielsen, P.J., Pelanda, R., and Reth, M. (2006). Testing gene function early in the B cell lineage in mb1-cre mice. Proceedings of the National Academy of Sciences *103*, 13789–13794.

Hombach, J., Tsubata, T., Leclercq, L., Stappert, H., and Reth, M. (1990). Molecular components of the B-cell antigen receptor complex of the IgM class. Nature *343*, 760–762.

Hou, P., Araujo, E., Zhao, T., Zhang, M., Massenburg, D., Veselits, M., Doyle, C., Dinner, A., and Clark, M. (2006). B cell antigen receptor signaling and internalization are mutually exclusive events. PLoS Biology *4*, e200.

Huang, B., Wang, W., Bates, M., and Zhuang, X. (2008). Three-dimensional super-resolution imaging by stochastic optical reconstruction microscopy. Science *319*, 810–813.

Huang, N.-N., Han, S.-B., Hwang, I.-Y., and Kehrl, J.H. (2005). B cells productively engage soluble antigen-pulsed dendritic cells: visualization of live-cell dynamics of B cell-dendritic cell interactions. The Journal of Immunology *175*, 7125–7134.

Isnardi, I., Ng, Y.-S., Srdanovic, I., Motaghedi, R., Rudchenko, S., Bernuth, von, H., Zhang, S.-Y., Puel, A., Jouanguy, E., Picard, C., et al. (2008). IRAK-4- and MyD88-dependent pathways are essential for the removal of developing autoreactive B cells in humans. Immunity *29*, 746–757.

Jacob, J., Kelsoe, G., Rajewsky, K., and Weiss, U. (1991). Intraclonal generation of antibody mutants in germinal centres. Nature *354*, 389–392.

Jacobelli, J., Friedman, R.S., Conti, M.A., Lennon-Duménil, A.-M., Piel, M., Sorensen, C.M., Adelstein, R.S., and Krummel, M.F. (2010). Confinement-optimized three-dimensional T cell amoeboid motility is modulated via myosin IIA–regulated adhesions. Nature Immunology *11*, 953–961.

Jang, C., Machtaler, S., and Matsuuchi, L. (2010). The role of Ig-α/β in B cell antigen receptor internalization. Immunology Letters *134*, 75–82.

Junt, T., Moseman, E.A., Iannacone, M., Massberg, S., Lang, P.A., Boes, M., Fink, K., Henrickson, S.E., Shayakhmetov, D.M., Di Paolo, N.C., et al. (2007). Subcapsular sinus macrophages in lymph nodes clear lymph-borne viruses and present them to antiviral B cells. Nature *450*, 110–114.

Khalil, A.M., Cambier, J.C., and Shlomchik, M.J. (2012). B cell receptor signal transduction in the GC is short-circuited by high phosphatase activity. Science *336*, 1178–1181.

Kirchhausen, T. (2009). Imaging endocytic clathrin structures in living cells. Trends in Cell Biology *19*, 596–605.

Kitamura, D., Roes, J., Kühn, R., and Rajewsky, K. (1991). A B cell-deficient mouse by targeted disruption of the membrane exon of the immunoglobulin mu chain gene. Nature *350*, 423–426.

Kouskoff, V., Famiglietti, S., Lacaud, G., Lang, P., Rider, J.E., Kay, B.K., Cambier, J.C., and Nemazee, D. (1998). Antigens varying in affinity for the B cell receptor induce differential B lymphocyte responses. The Journal of Experimental Medicine *188*, 1453–1464.

Kovács, M., Thirumurugan, K., Knight, P.J., and Sellers, J.R. (2007). Load-dependent mechanism of nonmuscle myosin 2. Proceedings of the National Academy of Sciences *104*, 9994–9999.

Kraus, M., Alimzhanov, M.B., Rajewsky, N., and Rajewsky, K. (2004). Survival of resting mature B lymphocytes depends on BCR signaling via the Igα/β heterodimer. Cell *117*, 787–800.

Krieg, M., Helenius, J., Heisenberg, C.-P., and Müller, D.J. (2008). A Bond for a Lifetime: Employing Membrane Nanotubes from Living Cells to Determine Receptor-Ligand Kinetics. Angewandte Chemie International Edition *47*, 9775–9777.

Kurosaki, T., Shinohara, H., and Baba, Y. (2010). B Cell Signaling and Fate Decision. Annual Review of Immunology *28*, 21–55.

Lam, K.P., Kühn, R., and Rajewsky, K. (1997). In vivo ablation of surface immunoglobulin on mature B cells by inducible gene targeting results in rapid cell death. Cell *90*, 1073–1083.

Lane, P., Traunecker, A., Hubele, S., Inui, S., Lanzavecchia, A., and Gray, D. (1992). Activated human T cells express a ligand for the human B cell-associated antigen CD40 which participates in T cell-dependent activation of B

lymphocytes. European Journal of Immunology *22*, 2573–2578.

Lankar, D., Briken, V., Adler, K., Weiser, P., Cassard, S., Blank, U., Viguier, M., and Bonnerot, C. (1998). Syk tyrosine kinase and B cell antigen receptor (BCR) immunoglobulin-alpha subunit determine BCR-mediated major histocompatibility complex class II-restricted antigen presentation. The Journal of Experimental Medicine *188*, 819–831.

Lanoue, A., Batista, F.D., Stewart, M., and Neuberger, M.S. (2002). Interaction of CD22 with α2,6-linked sialoglycoconjugates: innate recognition of self to dampen B cell autoreactivity? European Journal of Immunology *32*, 348–355.

Lanzavecchia, A. (1985). Antigen-specific interaction between T and B cells. Nature *314*, 537–539.

Lanzavecchia, A. (1987). Antigen Uptake and Accumulation in Antigen-Specific B Cells. Immunological Reviews *99*, 39–51.

Lau, C.M., Broughton, C., Tabor, A.S., Akira, S., Flavell, R.A., Mamula, M.J., Christensen, S.R., Shlomchik, M.J., Viglianti, G.A., Rifkin, I.R., et al. (2005). RNA-associated autoantigens activate B cells by combined B cell antigen receptor/Toll-like receptor 7 engagement. The Journal of Experimental Medicine *202*, 1171–1177.

Leadbetter, E., Rifkin, I., Hohlbaum, A., Beaudette, B., Shlomchik, M., and Marshak-Rothstein, A. (2002). Chromatin–IgG complexes activate B cells by dual engagement of IgM and Toll-like receptors. Nature *416*, 603–607.

Lecuit, T., Lenne, P.-F., and Munro, E. (2011). Force generation, transmission, and integration during cell and tissue morphogenesis. Annual Review of Cell and Developmental Biology *27*, 157–184.

Levayer, R., Pelissier-Monier, A., and Lecuit, T. (2011). Spatial regulation of Dia and Myosin-II by RhoGEF2 controls initiation of E-cadherin endocytosis during epithelial morphogenesis. Nature Cell Biology *13*, 529–540.

Lin, K., Freeman, S., Zabetian, S., Brugger, H., Weber, M., Lei, V., Dang-Lawson, M., Tse, K., Santamaria, R., and Batista, F. (2008). The rap GTPases regulate B cell morphology, immune-synapse formation, and signaling by particulate B cell receptor ligands. Immunity *28*, 75–87.

Liu, C., Miller, H., Orlowski, G., Hang, H., Upadhyaya, A., and Song, W. (2012). Actin reorganization is required for the formation of polarized B cell receptor signalosomes in response to both soluble and membrane-associated antigens. The Journal of Immunology *188*, 3237–3246.

Liu, W., Meckel, T., Tolar, P., Sohn, H.W., and Pierce, S.K. (2010). Antigen affinity discrimination is an intrinsic function of the B cell receptor. The Journal of Experimental Medicine *207*, 1095–1111.

Ma, H., Yankee, T.M., Hu, J., Asai, D.J., Harrison, M.L., and Geahlen, R.L. (2001). Visualization of Syk-antigen receptor interactions using green

fluorescent protein: differential roles for Syk and Lyn in the regulation of receptor capping and internalization. The Journal of Immunology *166*, 1507–1516.

Mackay, F., Figgett, W.A., Saulep, D., Lepage, M., and Hibbs, M.L. (2010). B-cell stage and context-dependent requirements for survival signals from BAFF and the B-cell receptor. Immunological Reviews *237*, 205–225.

Malhotra, S., Kovats, S., Zhang, W., and Coggeshall, K.M. (2009a). Vav and Rac Activation in B Cell Antigen Receptor Endocytosis Involves Vav Recruitment to the Adapter Protein LAB. Journal of Biological Chemistry *284*, 36202–36212.

Malhotra, S., Kovats, S., Zhang, W., and Coggeshall, K.M. (2009b). B cell antigen receptor endocytosis and antigen presentation to T cells require Vav and dynamin. Journal of Biological Chemistry *284*, 24088–24097.

Manolova, V., Flace, A., Bauer, M., Schwarz, K., Saudan, P., and Bachmann, M.F. (2008). Nanoparticles target distinct dendritic cell populations according to their size. European Journal of Immunology *38*, 1404–1413.

Mantei, A., Rutz, S., Janke, M., Kirchhoff, D., Jung, U., Patzel, V., Vogel, U., Rudel, T., Andreou, I., and Weber, M. (2008). siRNA stabilization prolongs gene knockdown in primary T lymphocytes. European Journal of Immunology *38*, 2616–2625.

Matsumura, F. (2005). Regulation of myosin II during cytokinesis in higher eukaryotes. Trends in Cell Biology *15*, 371–377.

Mattila, P.K., Feest, C., Depoil, D., Treanor, B., Montaner, B., Otipoby, K.L., Carter, R., Justement, L.B., Bruckbauer, A., and Batista, F.D. (2013). The Actin and Tetraspanin Networks Organize Receptor Nanoclusters to Regulate B Cell Receptor-Mediated Signaling. Immunity *38*, 1–14.

Mårtensson, I.-L., Almqvist, N., Grimsholm, O., and Bernardi, A.I. (2010). The pre-B cell receptor checkpoint. FEBS Letters *584*, 2572–2579.

McKean, D., Huppi, K., Bell, M., Staudt, L., Gerhard, W., and Weigert, M. (1984). Generation of antibody diversity in the immune response of BALB/c mice to influenza virus hemagglutinin. Proceedings of the National Academy of Sciences *81*, 3180–3184.

McMahon, H.T., and Boucrot, E. (2011). Molecular mechanism and physiological functions of clathrin-mediated endocytosis. Nature Reviews Molecular Cell Biology *12*, 517–533.

Mebius, R.E., and Kraal, G. (2005). Structure and function of the spleen. Nature Reviews Immunology *5*, 606–616.

Merrifield, C., Feldman, M., Wan, L., and Almers, W. (2002). Imaging actin and dynamin recruitment during invagination of single clathrin-coated pits. Nature Cell Biology *4*, 691–698.

Merrifield, C., Perrais, D., and Zenisek, D. (2005). Coupling between clathrin-coated-pit invagination, cortactin recruitment, and membrane scission observed in live cells. Cell *121*, 593–606.

Moffat, J., Grueneberg, D., Yang, X., Kim, S., Kloepfer, A., Hinkle, G., Piqani, B., Eisenhaure, T., Luo, B., and Grenier, J. (2006). A lentiviral RNAi library for human and mouse genes applied to an arrayed viral high-content screen. Cell *124*, 1283–1298.

Morita, S., Kojima, T., and Kitamura, T. (2000). Plat-E: an efficient and stable system for transient packaging of retroviruses. Gene Therapy *7*, 1063–1066.

Moseman, E.A., Iannacone, M., Bosurgi, L., Tonti, E., Chevrier, N., Tumanov, A., Fu, Y.-X., Hacohen, N., and Andrian, von, U.H. (2012). B Cell Maintenance of Subcapsular Sinus Macrophages Protects against a Fatal Viral Infection Independent of Adaptive Immunity. Immunity *36*, 415–426.

Nagasawa, T. (2006). Microenvironmental niches in the bone marrow required for B-cell development. Nature Reviews Immunology *6*, 107–116.

Nagata, K., Nakamura, T., Kitamura, F., Kuramochi, S., Taki, S., Campbell, K.S., and Karasuyama, H. (1997). The Igα/Igβ heterodimer on μ-negative proB cells is competent for transducing signals to induce early B cell differentiation. Immunity *7*, 559–570.

Natkanski, E., Lee, W.Y., Mistry, B., Casal, A., Molloy, J.E., and Tolar, P. (2013). B Cells Use Mechanical Energy to Discriminate Antigen Affinities. Science *340*, 1587–1590.

Niiro, H., Allam, A., Stoddart, A., Brodsky, F.M., Marshall, A.J., and Clark, E.A. (2004). The B lymphocyte adaptor molecule of 32 kilodaltons (Bam32) regulates B cell antigen receptor internalization. The Journal of Immunology *173*, 5601–5609.

Norvell, A., Mandik, L., and Monroe, J.G. (1995). Engagement of the antigen-receptor on immature murine B lymphocytes results in death by apoptosis. The Journal of Immunology *154*, 4404–4413.

Nutt, S.L., Heavey, B., Rolink, A.G., and Busslinger, M. (1999). Commitment to the B-lymphoid lineage depends on the transcription factor Pax5. Nature *401*, 556–562.

O'Keefe, T.L., Williams, G.T., Batista, F.D., and Neuberger, M.S. (1999). Deficiency in CD22, a B Cell-specific Inhibitory Receptor, Is Sufficient to Predispose to Development of High Affinity Autoantibodies. The Journal of Experimental Medicine *189*, 1307–1313.

O'Keefe, T.L., Williams, G.T., Davies, S.L., and Neuberger, M.S. (1996). Hyperresponsive B cells in CD22-deficient mice. Science *274*, 798–801.

O'Neill, S.K., Getahun, A., Gauld, S.B., Merrell, K.T., Tamir, I., Smith, M.J., Dal Porto, J.M., Li, Q.-Z., and Cambier, J.C. (2011). Monophosphorylation of CD79a

and CD79b ITAM Motifs Initiates a SHIP-1 Phosphatase-Mediated Inhibitory Signaling Cascade Required for B Cell Anergy. Immunity *35*, 746–756.

O'Neill, S.K., Veselits, M.L., Zhang, M., Labno, C., Cao, Y., Finnegan, A., Uccellini, M., Alegre, M.-L., Cambier, J.C., and Clark, M.R. (2009). Endocytic sequestration of the B cell antigen receptor and toll-like receptor 9 in anergic cells. Proceedings of the National Academy of Sciences *106*, 6262–6267.

Ohnishi, K., and Melchers, F. (2003). The nonimmunoglobulin portion of λ5 mediates cell-autonomous pre-B cell receptor signaling. Nature Immunology *4*, 849–856.

Okada, T., Miller, M.J., Parker, I., Krummel, M.F., Neighbors, M., Hartley, S.B., O'Garra, A., Cahalan, M.D., and Cyster, J.G. (2005). Antigen-engaged B cells undergo chemotaxis toward the T zone and form motile conjugates with helper T cells. PLoS Biology *3*, e150.

Pape, K., Catron, D., Itano, A., and Jenkins, M. (2007). The humoral immune response is initiated in lymph nodes by B cells that acquire soluble antigen directly in the follicles. Immunity *26*, 491–502.

Parker, D.C. (1993). T cell-dependent B cell activation. Annual Review of Immunology *11*, 331–360.

Patel, K.J., and Neuberger, M.S. (1993). Antigen presentation by the B cell antigen receptor is driven by the alpha/beta sheath and occurs independently of its cytoplasmic tyrosines. Cell *74*, 939–946.

Paus, D., Phan, T.G., Chan, T.D., Gardam, S., Basten, A., and Brink, R. (2006). Antigen recognition strength regulates the choice between extrafollicular plasma cell and germinal center B cell differentiation. The Journal of Experimental Medicine *203*, 1081–1091.

Pavri, R., Gazumyan, A., Jankovic, M., Di Virgilio, M., Klein, I., Ansarah-Sobrinho, C., Resch, W., Yamane, A., Reina San-Martin, B., Barreto, V., et al. (2010). Activation-induced cytidine deaminase targets DNA at sites of RNA polymerase II stalling by interaction with Spt5. Cell *143*, 122–133.

Pelanda, R., Braun, U., Hobeika, E., Nussenzweig, M.C., and Reth, M. (2002). B cell progenitors are arrested in maturation but have intact VDJ recombination in the absence of Ig-alpha and Ig-beta. The Journal of Immunology *169*, 865–872.

Pellegrin, S., and Mellor, H. (2007). Actin stress fibres. Journal of Cell Science *120*, 3491–3499.

Phan, T., Grigorova, I., Okada, T., and Cyster, J. (2007). Subcapsular encounter and complement-dependent transport of immune complexes by lymph node B cells. Nature Immunology *8*, 992–1000.

Pierce, S., and Liu, W. (2010). The tipping points in the initiation of B cell signalling: how small changes make big differences. Nature Reviews

Immunology *10*, 767–777.

Plotz, P.H. (2003). The autoantibody repertoire: searching for order. Nature Reviews Immunology *3*, 73–78.

Pulendran, B., Kannourakis, G., Nouri, S., Smith, K.G., and Nossal, G. (1995). Soluble antigen can cause enhanced apoptosis of germinal-centre B cells. Nature *375*, 331–334.

Putnam, M.A., Moquin, A.E., Merrihew, M., Outcalt, C., Sorge, E., Caballero, A., Gondré-Lewis, T.A., and Drake, J.R. (2003). Lipid raft-independent B cell receptor-mediated antigen internalization and intracellular trafficking. The Journal of Immunology *170*, 905–912.

Qi, H., Egen, J.G., Huang, A.Y., and Germain, R.N. (2006). Extrafollicular activation of lymph node B cells by antigen-bearing dendritic cells. Science *312*, 1672–1676.

Qin, D., Wu, J., Carroll, M.C., Burton, G.F., Szakal, A.K., and Tew, J.G. (1998). Evidence for an important interaction between a complement-derived CD21 ligand on follicular dendritic cells and CD21 on B cells in the initiation of IgG responses. The Journal of Immunology *161*, 4549–4554.

Rajewsky, K. (1996). Clonal selection and learning in the antibody system. Nature *381*, 751–758.

Reth, M., and Wienands, J. (1997). Initiation and processing of signals from the B cell antigen receptor. Annual Review of Immunology *15*, 453–479.

Reznik, G.O., Vajda, S., Sano, T., and Cantor, C.R. (1998). A streptavidin mutant with altered ligand-binding specificity. Proceedings of the National Academy of Sciences *95*, 13525–13530.

Riedl, J., Crevenna, A.H., Kessenbrock, K., Yu, J.H., Neukirchen, D., Bista, M., Bradke, F., Jenne, D., Holak, T.A., Werb, Z., et al. (2008). Lifeact: a versatile marker to visualize F-actin. Nature Chemical Biology *5*, 605–607.

Root, D., Hacohen, N., Hahn, W., Lander, E., and Sabatini, D. (2006). Genome-scale loss-of-function screening with a lentiviral RNAi library. Nature Methods *3*, 715–719.

Roozendaal, R., Mempel, T.R., Pitcher, L.A., Gonzalez, S.F., Verschoor, A., Mebius, R.E., Andrian, von, U.H., and Carroll, M.C. (2009). Conduits Mediate Transport of Low-Molecular-Weight Antigen to Lymph Node Follicles. Cell *30*, 264–276.

Russell, D.M., Dembić, Z., Morahan, G., Miller, J.F., Bürki, K., and Nemazee, D. (1991). Peripheral deletion of self-reactive B cells. Nature *354*, 308–311.

Sackmann, E. (1996). Supported Membranes: Scientific and Practical Applications. Science *271*, 43–48.

Salisbury, J.L. (1980). Role of coated vesicles, microfilaments, and calmodulin in receptor- mediated endocytosis by cultured B lymphoblastoid cells. The Journal of Cell Biology *87*, 132–141.

Schamel, W.W.A., and Reth, M. (2000). Monomeric and Oligomeric Complexes of the B Cell Antigen Receptor. Cell *13*, 5–14.

Schnyder, T., Castello, A., Feest, C., Harwood, N.E., Oellerich, T., Urlaub, H., Engelke, M., Wienands, J., Bruckbauer, A., and Batista, F.D. (2011). B cell receptor-mediated antigen gathering requires ubiquitin ligase Cbl and adaptors Grb2 and Dok-3 to recruit dynein to the signaling microcluster. Immunity *34*, 905–918.

Schweighoffer, E., Vanes, L., Nys, J., Cantrell, D., McCleary, S., Smithers, N., and Tybulewicz, V.L.J. (2013). The BAFF Receptor Transduces Survival Signals by Co-opting the B Cell Receptor Signaling Pathway. Immunity *38*, 475–488.

Schwickert, T.A., Lindquist, R.L., Shakhar, G., Livshits, G., Skokos, D., Kosco-Vilbois, M.H., Dustin, M.L., and Nussenzweig, M.C. (2007). In vivo imaging of germinal centres reveals a dynamic open structure. Nature *446*, 83–87.

Schwickert, T.A., Victora, G.D., Fooksman, D.R., Kamphorst, A.O., Mugnier, M.R., Gitlin, A.D., Dustin, M.L., and Nussenzweig, M.C. (2011). A dynamic T cell-limited checkpoint regulates affinity-dependent B cell entry into the germinal center. The Journal of Experimental Medicine *208*, 1243–1252.

Shih, T.-A.Y., Meffre, E., Roederer, M., and Nussenzweig, M.C. (2002a). Role of BCR affinity in T cell dependent antibody responses in vivo. Nature Immunology *3*, 570–575.

Shih, T.-A.Y., Roederer, M., and Nussenzweig, M.C. (2002b). Role of antigen receptor affinity in T cell-independent antibody responses in vivo. Nature Immunology *3*, 399–406.

Shokat, K.M., and Goodnow, C.C. (1995). Antigen-induced B-cell death and elimination during germinal-centre immune responses. Nature *375*, 334–338.

Sohn, H.W. (2006). Fluorescence resonance energy transfer in living cells reveals dynamic membrane changes in the initiation of B cell signaling. Proceedings of the National Academy of Sciences *103*, 8143–8148.

Sohn, H.W., Tolar, P., and Pierce, S.K. (2008). Membrane heterogeneities in the formation of B cell receptor-Lyn kinase microclusters and the immune synapse. The Journal of Cell Biology *182*, 367–379.

Sonoda, E., Pewzner-Jung, Y., Schwers, S., Taki, S., Jung, S., Eilat, D., and Rajewsky, K. (1997). B cell development under the condition of allelic inclusion. Immunity *6*, 225–233.

Srinivasan, L., Sasaki, Y., Calado, D.P., Zhang, B., Paik, J.H., DePinho, R.A., Kutok, J.L., Kearney, J.F., Otipoby, K.L., and Rajewsky, K. (2009). PI3 kinase

signals BCR-dependent mature B cell survival. Cell *139*, 573–586.

Stallwood, Y., Briend, E., Ray, K.M., Ward, G.A., Smith, B.J., Nye, E., Champion, B.R., and McKenzie, G.J. (2006). Small interfering RNA-mediated knockdown of notch ligands in primary CD4+ T cells and dendritic cells enhances cytokine production. The Journal of Immunology *177*, 885–895.

Stoddart, A., Dykstra, M., Brown, B., Song, W., Pierce, S., and Brodsky, F. (2002). Lipid rafts unite signaling cascades with clathrin to regulate BCR internalization. Immunity *17*, 451–462.

Stoddart, A., Jackson, A.P., and Brodsky, F.M. (2005). Plasticity of B cell receptor internalization upon conditional depletion of clathrin. Molecular Biology of the Cell *16*, 2339–2348.

Sund, S.E., Swanson, J.A., and Axelrod, D. (1999). Cell membrane orientation visualized by polarized total internal reflection fluorescence. Biophysical Journal *77*, 2266–2283.

Suzuki, K., Grigorova, I., Phan, T.G., Kelly, L.M., and Cyster, J.G. (2009). Visualizing B cell capture of cognate antigen from follicular dendritic cells. The Journal of Experimental Medicine *206*, 1485–1493.

Szakal, A.K., Holmes, K.L., and Tew, J.G. (1983). Transport of immune complexes from the subcapsular sinus to lymph node follicles on the surface of nonphagocytic cells, including cells with dendritic morphology. The Journal of Immunology *131*, 1714–1727.

Taylor, J.J., Martinez, R.J., Titcombe, P.J., Barsness, L.O., Thomas, S.R., Zhang, N., Katzman, S.D., Jenkins, M.K., and Mueller, D.L. (2012). Deletion and anergy of polyclonal B cells specific for ubiquitous membrane-bound self-antigen. The Journal of Experimental Medicine *209*, 2065–2077.

Taylor, M.J., Perrais, D., and Merrifield, C.J. (2011). A high precision survey of the molecular dynamics of mammalian clathrin-mediated endocytosis. PLoS Biology *9*, e1000604.

Taylor, P.R., Brown, G.D., Herre, J., Williams, D.L., Willment, J.A., and Gordon, S. (2004). The role of SIGNR1 and the beta-glucan receptor (dectin-1) in the nonopsonic recognition of yeast by specific macrophages. The Journal of Immunology *172*, 1157–1162.

Tolar, P., Sohn, H., and Pierce, S. (2005). The initiation of antigen-induced B cell antigen receptor signaling viewed in living cells by fluorescence resonance energy transfer. Nature Immunology *6*, 1168–1176.

Tolar, P., Sohn, H., Liu, W., and Pierce, S. (2009a). The molecular assembly and organization of signaling active B-cell receptor oligomers. Immunological Reviews *232*, 34–41.

Tolar, P., Hanna, J., Krueger, P.D., and Pierce, S.K. (2009b). The constant region of the membrane immunoglobulin mediates B cell-receptor clustering

and signaling in response to membrane antigens. Immunity *30*, 44–55.

Treanor, B., Depoil, D., Bruckbauer, A., and Batista, F.D. (2011). Dynamic cortical actin remodeling by ERM proteins controls BCR microcluster organization and integrity. The Journal of Experimental Medicine *208*, 1055–1068.

Treanor, B., Depoil, D., Gonzalez-Granja, A., Barral, P., Weber, M., Dushek, O., Bruckbauer, A., and Batista, F.D. (2010). The membrane skeleton controls diffusion dynamics and signaling through the B cell receptor. Immunity *32*, 187–199.

van Ewijk, W., Brekelmans, P.J., Jacobs, R., and Wisse, E. (1988). Lymphoid microenvironments in the thymus and lymph node. Scanning Microscopy *2*, 2129–2140.

Vicente-Manzanares, M., Ma, X., Adelstein, R.S., and Horwitz, A.R. (2009). Non-muscle myosin II takes centre stage in cell adhesion and migration. Nature Reviews Molecular Cell Biology *10*, 778–790.

Victora, G.D., and Nussenzweig, M.C. (2012). Germinal centers. Annual Review of Immunology *30*, 429–457.

Victora, G., Schwickert, T., Fooksman, D., Kamphorst, A., Meyer-Hermann, M., Dustin, M., and Nussenzweig, M. (2010). Germinal Center Dynamics Revealed by Multiphoton Microscopy with a Photoactivatable Fluorescent Reporter. Cell *143*, 592–605.

Viglianti, G., Lau, C., Hanley, T., Miko, B., Shlomchik, M., and Marshak-Rothstein, A. (2003). Activation of autoreactive B cells by CpG dsDNA. Immunity *19*, 837–847.

Vos, Q., Lees, A., Wu, Z.Q., Snapper, C.M., and Mond, J.J. (2000). B-cell activation by T-cell-independent type 2 antigens as an integral part of the humoral immune response to pathogenic microorganisms. Immunological Reviews *176*, 154–170.

Wan, Z., Zhang, S., Fan, Y., Liu, K., Du, F., Davey, A.M., Zhang, H., Han, W., Xiong, C., and Liu, W. (2013). B cell activation is regulated by the stiffness properties of the substrate presenting the antigens. The Journal of Immunology *190*, 4661–4675.

Wang, L.D., and Clark, M.R. (2003). B-cell antigen-receptor signalling in lymphocyte development. Immunology *110*, 411–420.

Wang, X., Cho, B., Suzuki, K., Xu, Y., Green, J.A., An, J., and Cyster, J.G. (2011). Follicular dendritic cells help establish follicle identity and promote B cell retention in germinal centers. The Journal of Experimental Medicine *208*, 2497–2510.

Weber, M., Treanor, B., Depoil, D., Shinohara, H., Harwood, N.E., Hikida, M., Kurosaki, T., and Batista, F.D. (2008). Phospholipase C-gamma2 and Vav

cooperate within signaling microclusters to propagate B cell spreading in response to membrane-bound antigen. The Journal of Experimental Medicine *205*, 853–868.

Wu, M., Huang, B., Graham, M., Raimondi, A., Heuser, J.E., Zhuang, X., and De Camilli, P. (2010). Coupling between clathrin-dependent endocytic budding and F-BAR-dependent tubulation in a cell-free system. Nature Cell Biology *12*, 902–908.

Wu, Y., Sukumar, S., Shikh, El, M.E., Best, A.M., Szakal, A.K., and Tew, J.G. (2008). Immune complex-bearing follicular dendritic cells deliver a late antigenic signal that promotes somatic hypermutation. The Journal of Immunology *180*, 281–290.

Wykes, M., Pombo, A., Jenkins, C., and MacPherson, G.G. (1998). Dendritic cells interact directly with naive B lymphocytes to transfer antigen and initiate class switching in a primary T-dependent response. The Journal of Immunology *161*, 1313–1319.

Xu, Y., Harder, K.W., Huntington, N.D., Hibbs, M.L., and Tarlinton, D.M. (2005). Lyn tyrosine kinase: accentuating the positive and the negative. Immunity *22*, 9–18.

Yang, J., and Reth, M. (2010). Oligomeric organization of the B-cell antigen receptor on resting cells. Nature *467*, 465–469.

Young, R.M., and Staudt, L.M. (2013). Targeting pathological B cell receptor signalling in lymphoid malignancies. Nature Reviews Drug Discovery *12*, 229–243.

Yuseff, M.-I., Reversat, A., Lankar, D., Diaz, J., Fanget, I., Pierobon, P., Randrian, V., Larochette, N., Vascotto, F., Desdouets, C., et al. (2011). Polarized Secretion of Lysosomes at the B Cell Synapse Couples Antigen Extraction to Processing and Presentation. Immunity *35*, 361–374.

Appendix – Movie figure legends

Movie 1. TIRF timelapse showing B1-8 B cells (unlabelled) spreading over the NIP-Qdot (white)-loaded PLB and contracting to form a mature synapse. Elapsed time is shown in minutes and seconds.

Movie 2. TIRF timelapse showing Bl6 B cells labelled with αIgM Fab (green) spreading and extracting antigen (αIgκ, red) from a PMS. Disappearance of antigen from the TIRF view indicates internalisation. Elapsed time is shown in minutes and seconds.

Movie 3. TIRF timelapse showing membrane invaginations and antigen microclustering in a DiI-stained (fire scale, left panel) and antigen (αIgκ)-loaded (green, right panel) PMS, during Bl6 B cell synapse formation. Antigen disappearance indicates internalisation. DiI intensity was normalised to the DiI image before B cell spreading. Bl6 B cell was unlabelled. Elapsed time is shown in minutes and seconds.

Movie 4. TIRF timelapse showing a Bl6 B cell expressing clathrin light chain-GFP (green) during spreading on an antigen (αIgκ)-loaded PMS (red). Elapsed time is shown in minutes and seconds.

Movie 5. TIRF timelapse showing a Bl6 B cell expressing myosin IIA RLC-GFP (green) during spreading on a DiD-labelled PMS (red) loaded with antigen (αIgκ, no fluorescent label). DiD intensity was normalised to the DiD image before B cell spreading. Elapsed time is shown in minutes and seconds.

Movie 6. TIRF timelapse showing a Bl6 B cell expressing LifeAct (green) during spreading on a DiD-labelled PMS (red) loaded with antigen (αIgκ, no fluorescent label). DiD intensity was normalised to the DiD image before B cell spreading. Elapsed time is shown in minutes and seconds.